1972

Applications of the finite element method to beam-column problems, September 1972, Ph.D. dissertation

Negussie Tebedge

OFFICE

OF

RESEARCH

LEHIGH UNIVERSITY

Residual Stresses in Thick Welded Plates

APPLICATIONS OF THE FINITE ELEMENT METHOD TO BEAM-COLUMN PROBLEMS

by
Negussie Tebedge

September, 1972

Fritz Laboratory Report No. 337.32

APPLICATIONS OF THE FINITE ELEMENT METHOD
TO BEAM-COLUMN PROBLEMS

by

Negussie Tebedge

A Dissertation

Presented to the Graduate Committee

of Lehigh University

in Candidacy of the Degree of

Doctor of Philosophy

in

Civil Engineering

Lehigh University

1972

<u>CERTIFICATE OF APPROVAL</u>

Approved and recommended for acceptance as a dissertation in partial fulfillment of the requirements for the degree of Doctor of Philosophy.

11 August 1972
(Date)

Lambert Tall
Professor in Charge

Accepted 7 September 1972
(Date)

Special committee directing the doctoral work of Mr. Negussie Tebedge

George C. Driscoll, Jr.
Professor George C. Driscoll, Jr.
Chairman

Lambert Tall
Professor Lambert Tall

W. F. Chen
Professor Wai-Fah Chen

Robert A. Lucas
Professor Robert A. Lucas

David Allan VanHorn
Professor David A. VanHorn
Ex Officio

ACKNOWLEDGMENTS

The author is deeply indepted to Professor Lambert Tall, Professor in Charge of this dissertation, for his guidance and continuous encouragement in the preparation of this thesis and throughout the author's graduate studies. The guidance of Professors George C. Driscoll (Chairman), Wai-Fah Chen, Robert A. Lucas, and David A. VanHorn, members of the special committee directing the author's doctoral work, is gratefully acknowledged.

Sincere appreciation is expressed to all the author's associates in Fritz Laboratory, in particular Suresh Desai, for fruitful discussions throughout this investigation.

The investigation leading to this dissertation is part of a research project "Residual Stresses in Thick Welded Plates", which is jointly sponsored by the National Science Foundation and the Column Research Council. Dr. L. Tall and Dr. W. F. Chen are the directors of the project.

The author owes a special debt of gratitude to the African-American Institute for their support during the first year of his graduate study.

Acknowledgments are also due to the Computer Center at Lehigh University which provided facilities for the computer work. The assistance of Shirley Matlock in typing the manuscript and of John Gera and his staff for preparing the drawings, is gratefully acknowledged.

LIST OF TABLES

LIST OF FIGURES

TABLE OF CONTENTS

ABSTRACT

This dissertation is concerned with developing a finite element formulation of the analysis of beam-columns, and with demonstrating the applicability of the method to general beam-column problems as a practical tool. The treatment includes linear static, linear stability and non-linear analyses of beam-columns.

In the linear static analysis, a formulation is presented to develop a one-dimensional finite element using variational principles. The formulation is based on a functional consisting of two independent fields: a polynomial approximation of a strain field in the domain, and displacements at the boundary. The beam element has two nodes and seven degrees of freedom at each node.

The linear stability analysis, which reduces to an eigenvalue determination, utilizes a displacement formulation based on a finite element idealization. A systematic procedure is developed to evaluate the geometric stiffness matrices for beam-columns. The matrices derived correspond to large displacements in axial and transverse directions and also in twist. The finite element solutions are compared to analytical solutions and the convergence characteristics are studied for a variety of problems which include: columns with distributed axial loads, tapered columns, columns on elastic foundations, pretwisted columns, space frames and the lateral buckling of beams.

Finally, a finite element formulation of nonlinear analysis is given to study general instability problems of beam-columns. A solution procedure, using a direct incremental approach, is applied to numerical examples to demonstrate the validity of the procedure.

The contributions achieved in this dissertation are:

- A one-dimensional finite element model is developed to analyze general linear static beam-column problems.

- A systematic procedure is presented to evaluate geometric stiffness matrices for beam-columns which are required to perform a finite element analysis of stability problems.

- The geometric stiffness matrices are derived which correspond to large lateral and torsional displacements.

- The advantages of the finite element method are demonstrated in the solution of a few stability problems, such as the buckling of pretwisted columns and the lateral buckling of tapered beams, the analytical solutions of which are not yet available.

1. INTRODUCTION

A beam-column, also known as a rod in classical terms, is defined in this dissertation as a three dimensional body having one dimension significantly greater than the other two. Examples of bodies which may be so regarded are numerous, such as members of framed structures, arches and curved beams. In the case of framed structures, for example, the members are identified further depending on the loading conditions, where columns represent the one limiting case where the bending moments become zero, and beams the case in which the axial force vanishes.

The purpose of a theory of beams is to provide appropriate one-dimensional equations applicable to beam-type bodies. A one-dimensional analysis, referred to as a beam theory, is necessarily approximate and furnishes only partial or limited information. Indeed, the desire for such limited information is the basic motivation for the construction of a one-dimensional theory with the aim of providing a simpler theory for the limited information sought. While the three-dimensional viewpoint is certainly the most fundamental, the possibility of employing a one-dimensional model for beam-type bodies presents itself in a natural way because of the considerable difficulties associated with the derivation of the beam theory from the three-dimensional equations. The model, however, must be capable of supplying a substantial portion of information the three-dimensional theory would furnish. The notion of employing a model for an idealized body is frequently used in classical continuum mechanics, in fact, the continuum itself is a model representing an idealized body in some sense.

An approximate system of equations for beam-type bodies may be developed by converting formally the three-dimensional field relationships to their one-dimensional analogue. Historically, interest in the construction of more elaborate theories of beams arose from the desire to treat wave propagation and vibrations of elastic rods. After the three-dimensional theories were accepted in certain domains of mechanics, Cauchy and Poisson sought to obtain theories by averaging over a cross-section the results from a three-dimensional theory and then letting the cross-sectional area approach zero[1,2,3]. Recently, the use of polynomial approximations has been adopted extensively to develop analytical beam theories. For example, the three-dimensional field relations may be converted to their one dimensional analogues by replacing the field variables by series expansions in products of Legendre polynomials[4,5,6]. In these efforts, the Legendre expansions lead to reducing the governing partial differential equations to either ordinary differential equations, or to more tractable partial differential equations. The exact analysis of beam behavior, when treated in this fashion, will be intrinsically more complex, necessitating the satisfaction of the boundary conditions on numerous planes as compared to one pair of surfaces for plates or shells.

Inasmuch as considerable difficulties remain in the derivation of a system of equations from the three-dimensional theory, the alternative development is to utilize a direct approach if a simplified formulation is sought. The "classical beam theory", for example, is based on a direct approach. In the development of the classical theory, Bernoulli (1705) was the first to make kinematical assumptions to solve flexural problems, and hypotheses regarding the constitution of the material were first given by Euler (1771). Saint-Venant (1855) was the first to remark that six equations are needed to express the equilibruim of rods which are twisted as well as bent, based on special simplifying hypotheses. The general equations were given in principle, but obscurely, by Kirchhoff (1859). The process by which Kirchhoff developed his theory was, to a great extent, kinematical. Clebsch (1862) modified the theory and gave explicit general equations which were confirmed by later writers[1,7].

Recently, it has been established that the Euler-Bernoulli theory of beams was not applicable to thin-walled beams because of the inherent distortion of the cross section that occurs during bending. Wagner (1929) was the first to introduce the concept of "warping" in the analysis of thin-walled beams[8]. Comprehensive reviews on the bending and torsion of open sections including the buckling characteristics were made by Goodier[9] and Timoshenko[10]. A general treatment of beams is fully described in Vlasov's treatise of thin-walled beams[11]. A common feature in these investigations is that each formulation results in the development of the governing differential equations from consideration of equilibrium conditions. Many particular problems based on these general formulations have been solved either exactly or approximately by seeking the analytical solutions of the differential equations or by employing different numerical techniques. A historical review on this subject, particularly on the development and utilization of the various numerical approaches that have been used to solve the governing equations is given in Ref. 12.

More recently, the calculation of complex structural problems by means of the concept of piecewise approximations has received a great impetus. A significant intermediary step in the evolution of modern structural mechanics is the discrete element method. Here, in the context of beam-type bodies, the structural beam is physically replaced as a combination of elastic blocks, rigid bars, torsional springs and flexural springs. This is equivalent to the early works of Hrenikoff[(13)], representing a plane solid as an assembly of discrete systems, which is regarded as a forerunner to the development of general discrete methods of structural mechanics. It has been shown that the discrete element approach is mathematically equivalent to the finite difference method and thus it may be considered as a physical interpretation of the finite difference method[(14)].

During the past decade, great strides have been made on the development and utilization of the finite element method. This method can be considered as the most powerful and versatile technique presently available for the numerical solution of complex structural problems. Moreover, it can be formulated in terms of simple physical concepts without recourse to complex differential equations. The method was developed originally as an application of the standard structural analysis procedure to a physically discretized approximation of the actual system. The concept has been extensively described in Refs. 15 and 16. Study of the mathematical foundations of the method[(16,17)] as well as its application to a wider class of field problems[(15,16)] has clarified the basic requirements for its effective formulation.

Two parallel developments were responsible for the widespread acceptance of the finite element method; the formulation of the matrix transformation theory of structures and the introduction of high-speed digital computers. The use of matrices allows a very efficient, systematic and simplified calculation superior to any other currently available scheme. Once the initial matrices are assembled, the subsequent operations involve merely elementary matrix algebra, which are ideally suitable for automatic computations using the computer.

While the advantages of the finite element method have been widely recognized and its applications extensively demonstrated particularly to a variety of problems in solid mechanics and in structural mechanics, more specifically to plate and shell structures, the application of the method to beam-column analyses has not been explored to an equivalent degree. Analysis of beam-columns, and in particular, beam-columns under general loading and support conditions, is a subject of wide interest in current research. Most of the previous developments in beam-column analysis by finite elements are found in Refs. 18 to 22.

In this study, a direct approach is employed to analyse the beam-column problem where a numerical solution is sought by utilizing the finite element concept and its applications. The beam is fictitiously subdivided by imaginary planes into an assembly of elements and is regarded as a one-dimensional problem. This notion of subdivision, which is mathematical and not physical does not consider the beam to be divided into separate physical elements that are assembled in the analysis procedure. Using this concept, a variational principle is employed in constructing a finite element formulation to evaluate the properties of the elements and finally to solve the complete system. In order to demonstrate the best balance in practical usage, the study takes into consideration factors such as simplicity of formulation, versatility of application, reliability, computational efforts and accuracy of results.

2. FORMULATION FOR THE STIFFNESS MATRIX OF THE BEAM ELEMENT

2.1 INTRODUCTION

The finite element technique may be applied to analyse the beam problem in which the beam can be treated as a three-dimensional body with the use of three-dimensional elements, or as a general plane stress problem when two-dimensional elements are used. Here the sole interest is to construct a one-dimensional model capable of furnishing a substantial portion of the information a three-dimensional theory would furnish. Indeed, the evaluation of the element is one of the most important aspects of the finite element analysis. A fundamental property of finite element models is that typical elements can be isolated from the idealized system and their behavior can be studied independently. The process of connecting the elements to form the final system is mainly a topological one and is independent of the physical nature of the problem.

In evaluating the element properties, either a direct method or a variational method may be used. The direct approach, in which direct consideration is given to the conditions of equilibrium and compatibility, is not used in this study. A thorough treatment of the direct approach is given in Ref. 23.

The formulation presented herein is based on an appropriately constructed functional where variational principles are applied to develop the finite element model. The functional is established based on two independent fields: a polynomial approximation of the strain field in the domain, and displacements at the boundaries. The use of polynomials is advantageous since it permits differentiation and integration with relative ease. The main purpose of the choice of such a formulation is its ability to incorporate the underlying hypotheses given by the beam theories in a rather simple manner. Further discussions and justifications for the choice of the formulation are given in a later section. Of course, in most structural problems, assumption of the displacement field alone usually will furnish good results. This is because the strain field can be derived in a straightforward manner, by using the relationships given by the deformation theory, as the derivatives of the displacement. However, the same logic does not hold true for the case of a one-dimensional analysis of the beam problem due to the complex nature of the problem.

2.2 A VARIATIONAL FORMULATION FOR THE BEAM ELEMENT

A Generalized Variational Principle

The variational principle may be regarded as one of the most important bases for the finite element method[24,25]. It has contributed to the development of structural analysis in leading to finite element formulations. Numerous finite element models may be derived, based on variational principles, by introducing different constraining conditions within the element or at the interelement boundaries. Since the problem usually cannot be solved exactly, the variational method provides an approximate formulation of the problem which yields a solution compatible with the assumed degree of approximation[26].

The variational formulation has several other advantages once the existence of a functional is assured. The functional which is subject to variation may usually be given a physical interpretation (such as strain energy or complementary energy) and is invariant under coordinate transformation. The original problem may be transformed into an equivalent one that can be solved more easily, for example, by applying the method of the Lagrangian multiplier for problems having subsidiary conditions. Another advantageous aspect of the variational principles is that they may lead to establishing upper and lower bounds of the exact solution; also, they may provide convergence proofs[24,26].

The generalized variational principle, often referred to as the Washizu-Hu principle, involves several free and independent fields [26,27]. The general principle is based on three independent fields in the domain, namely, the displacement field u_i, strain field ε_{ij} and stress field σ_{ij}; and two fields on the boundary, the displacement field $\bar{u}_i$ on S_u and boundary traction p_i on S. The generalized functional may be expressed by[*]

(*)Standard tensor notation and the summation convention is used. A comma denotes partial derivation with respect to the variable that follows.

$$\pi_W = \int_V \left\{\frac{1}{2} D_{ijk\ell}\, \epsilon_{ij}\, \epsilon_{k\ell} - \sigma_{ij}\left[\epsilon_{ij} - \frac{1}{2}(u_{i,j} + u_{j,i})\right] - \bar{F}_i\, u_i \quad dV\right.$$

$$- \int_{S_\sigma} \bar{T}_i\, u_i\, dS + \int_{S_u} (\bar{u}_i - u_i)\, p_i\, dS \tag{2.1}$$

In this expression

$D_{ijk\ell}$ = generalized Hookean constant

ϵ_{ij} = strain tensor

σ_{ij} = stress tensor

u_i = displacement

$\bar{F}_i$ = prescribed body force

$\bar{T}_i$ = prescribed traction on boundary S_σ

p_i = prescribed traction on boundary S

$\bar{u}_i$ = prescribed displacement on boundary S_u

S_σ, S_u = portions of boundaries over which $\bar{T}_i$ and $\bar{u}_i$ are prescribed, respectively

$S = S_\sigma + S_u$ = whole surface

There are eighteen independent variables subject to variation in the functional π_W, with no constraining or subsidiary conditions, these are: three displacements u_i, six strains ϵ_{ij}, six stresses σ_{ij} and three boundary tractions P_i. Taking variations with respect to these quantities leads to the following[28]

$$\delta\pi_W = \int_V (D_{ijk\ell}\, \epsilon_{k\ell} - \sigma_{ij})\, \delta\, \epsilon_{ij}\, dV \qquad \text{(constitutive equations)}$$

$$- \int_V \left[\epsilon_{ij} - \frac{1}{2}(u_{j,i} + u_{i,j})\right] \delta\, \sigma_{ij}\, dV \qquad \text{(strain-displacement relations)}$$

$$- \int_V (\sigma_{ij,i} + \bar{F}_j) \, \delta u_j \, dV \qquad \text{(equations of equilibrium)} \tag{2.2}$$

$$- \int_{S_\sigma} (\bar{T}_j - n_i \sigma_{ij}) \, \delta u_j \, dS \qquad \text{(static boundary conditions on } S_\sigma)$$

$$- \int_{S_u} (u_i - \bar{u}_i) \, \delta P_i \, dS \qquad \text{(kinematic boundary conditions on } S_u)$$

$$- \int_{S_u} (P_j - n_i \sigma_{ij}) \, \delta u_j \, dS \qquad \text{(continuity of tractions on } S_u)$$

The vanishing of $\delta\pi_W$ will establish the relations between the fields and impose on them the appropriate field equations, and boundary and continuity conditions as expressed by the following Euler equations

$$\begin{array}{lll}
\text{(i)} & \sigma_{ij} = D_{ijk\ell} \, \epsilon_{k\ell} & \text{in } V \\
\text{(ii)} & \epsilon_{ij} = \frac{1}{2}(u_{j,i} + u_{i,j}) & \text{in } V \\
\text{(iii)} & \sigma_{ij,j} + \bar{F}_i = 0 & \text{in } V \\
\text{(iv)} & \bar{T}_j = n_i \, \sigma_{ij} = T_j & \text{on } S \\
\text{(v)} & u_i = \bar{u}_i & \text{on } S_u \\
\text{(vi)} & P_j = n_i \, \sigma_{ij} = T_j & \text{on } S_u
\end{array} \tag{2.3}$$

Based on the generalized variational principle given by Eq. 2.1, different forms of variational principles may be derived by making a priori assumptions on one or more subsidiary conditions. For example, by stipulating that the stress and the strain fields are related by the constitutive equations, the variational principle will be involved with one less independent field. The functional π_W thus will be reduced to another functional π_R, equivalent to the Hellinger-Reissner principle[29]. Stipulating further that the strain fields are related to the displacement field, and by satisfying the kinematic boundary conditions, the functional π_R reduces to another functional π_P, which is equivalent to the principle of minimum potential energy. Similarly, the principle of minimum complementary energy also can be derived by introducing the appropriate subsidiary conditions[26].

A Variational Principle for a Beam Model

At this stage, a variational principle can be established from the generalized principle to evaluate the properties of the finite element model. The functions that will be assumed in this variational principle are

a) strain fields ϵ_{ij} in the domain V

b) boundary displacement fields $\bar{u}_i$ in S_u.

If, in addition, it is stipulated that the stress and the strain fields are related by the constitutive equations and the static boundary conditions are satisfied, then incorporating these constraint conditions in the functional given by Eq. 2.1, and introducing the Lagrangian multiplier technique, the functional will be reduced to:

$$\begin{aligned} \pi = &\int_V \left(\frac{1}{2} D_{ijk\ell}\, \epsilon_{ij}\, \epsilon_{k\ell} - \bar{F}_i\, u_i\right) dV \\ &- \int_S T_i\, u_i\, dS + \int_{S_u} T_i\, \tilde{u}_i\, dS \end{aligned} \tag{2.4}$$

where $\tilde{u}_i$ is the interelement boundary displacement and is the same for two adjacent elements on their common boundary.

Taking the variations with respect to the independent quantities results in the following,

$$
\begin{aligned}
\delta\pi = & \int_V [(D_{ijk\ell}\, \epsilon_{ij})_{,j} + \bar{F}_i]\, \delta\, u_i\, dV \\
& + \int_V (D_{ijk\ell}\, \epsilon_{k\ell}\, n_j - T_i)\, \delta\, u_i\, dS \\
& + \int_S (\tilde{u}_i - u_i)\, \delta\, T_i\, dS \\
& + \int_{S_u} T_i\, \delta\, \tilde{u}_i\, dS
\end{aligned}
\tag{2.5}
$$

The vanishing of $\delta\pi$ for an arbitrary δu_i in V and an arbitrary $\delta\tilde{u}_i$ on the interelement boundaries S_u, will give the following Euler equations

$$
\begin{aligned}
(D_{ijk\ell}\, \epsilon_{k\ell})_{,j} + \bar{F}_i &= 0 \qquad \text{in } V \\
D_{ijk\ell}\, \epsilon_{k\ell}\, n_j - T_i &= 0 \qquad \text{on } S \\
\tilde{u}_i - u &= 0 \qquad \text{on } S_u
\end{aligned}
\tag{2.6}
$$

A finite element model that satisfies the conditions in Eq. 2.6 is developed in the following section. In the development of this model, the functional given by Eq. 2.4 is applied directly.

A Finite Element Model

In this analysis, the body forces $\bar{F}_i$ are ignored and the matrix notation following Pian's[30] notations is employed. The functions $\{\epsilon\}$ and $\{u\}$ are simply chosen as polynomials with unknown coefficients. The strain field $\{\epsilon\}$ is expressed in terms of polynomial functions of the coordinates $[P]$ and undetermined strain coefficients $\{\beta\}$. The displacements along the interelement boundaries $\{\tilde{u}\}$ are represented by the interpolating functions [L] and the generalized displacements $\{\delta\}$ at the nodes. In matrix form they may be written respectively as

$$\{\epsilon\} = [P]\{\beta\} \tag{2.7}$$

$$\{\tilde{u}\} = [L]\{\delta\} \tag{2.8}$$

$$\{u\} = [P_u]\{\delta\} \tag{2.9}$$

The stress field may be derived from the strain field using the constitutive equations, thus

$$\{\sigma\} = [D][P]\{\beta\} \tag{2.10}$$

The tractions at the boundaries $\{\sigma_b\}$ are expressed in terms of the stress field $\{\sigma\}$ and the undetermined coefficients $\{\beta\}$ as follows

$$\{\sigma_b\} = [R]\{\beta\} \tag{2.11}$$

where [R] contains the coordinates on the surface.

The functional given in Eq. 2.4 when written in matrix form will reduce to

$$\begin{aligned} \pi &= \int_V \frac{1}{2}\{\beta\}^T [P]^T [D][P]\{\beta\}\, dV \\ &- \int_S \{\beta\}^T [R]^T [L]\{\delta\}\, dS \\ &= \frac{1}{2}\{\beta\}^T [H]\{\beta\} - \{\beta\}^T [T]\{\delta\} \end{aligned} \tag{2.12}$$

where

$$[H] = \int_V [P]^T [D][P]\, dV$$

and

$$[T] = \int_S [R]^T [L] \, dS$$

Minimizing the functional π with respect to each $\{\beta\}$, that is $\partial\pi/\partial \beta_i = 0$, yields

$$[H] \{\beta\} - [T] \{\delta\} = 0 \tag{2.13}$$

from which the undetermined coefficients are solved as

$$\{\beta\} = [H]^{-1} [T] \{\delta\} \tag{2.14}$$

Since the functional can be expressed in terms of the element stiffness matrix $[k]$, the generalized force vector $\{f\}$, and the generalized displacements $\{\delta\}$ as

$$\pi = \frac{1}{2} \{\delta\}^T [k] \{\delta\} - \{\delta\}^T \{f\} \tag{2.15}$$

comparison with Eq. 2.12 yields the element stiffness matrix,

$$[k] = [T]^T [H]^{-1} [T] \tag{2.16}$$

and the generalized force vector

$$\{f\} = [T]^T [H^{-1}] [T] \{\delta\} = [k] \{\delta\} \tag{2.17}$$

2.3 EVALUATION OF THE BEAM STIFFNESS MATRIX

Following the outline described above, the stiffness matrix for the beam element is derived. The beam is assumed to be a straight bar of uniform cross section. Among the many possible, and perhaps equally acceptable, ways of representing generalized displacements, the chosen set consists of extensions, bending rotations, transverse displacements, torsional and warping rotations. The corresponding generalized stresses, sometimes referred to as stress resultants, are determined by lumping the integrals of the boundary stresses at the nodes of the element.

In this study, the generalized force system is reduced to smaller uncoupled systems in order to demonstrate the application of the formulation more effectively. This is achieved, without much loss of generality, by making an appropriate selection of the reference axes. The flexural and torsional components, for instance, will be uncoupled by employing as reference axes a right-handed rectangular coordinate (cartesian) system where one of the axes is oriented parallel to the element. Of course, this is true only if the material is linearly elastic. The reference axes system adopted for the beam element is shown in Fig. 2.1, where the x-axis is directed parallel to the element.

It has been indicated earlier in this study, that the major problem associated in formulating the beam problem is in developing a kinematical model from which the strain-displacement relationship can be easily established. The formulation of the beam problem is based on Vlasov's hypothesis of the invariability of the beam cross section(11). The hypothesis implies that distances between points on the normal plane of the beam do not change during deformation. This reduces the strain field to fewer strain components which can be represented directly by using a polynomial expansion. Polynomials are used, as in many other situations, because of their simplicity in manipulation. Based on these approximate fields and utilizing the finite element model described in Section 2.2, the beam problem can then be formulated by treating separately the flexural and torsional problems.

Stiffness Matrix in Extension and Flexure

For a linearly elastic material the flexural problem can be further uncoupled into three systems; two bending components about the two axes and the extension component, provided the axes of the beam element coincide with the centroidal-principal axes of the cross section. However, it is found inexpedient to limit the analysis based on the use of the centroidal-principal axes, therefore, the general flexural problem will be analyzed.

The strain field $\{\epsilon\}$ in the beam element when expressed in terms of polynomial functions of the coordinate $[P]$ and the undetermined coefficients $\{\beta\}$ is rewritten as

$$\{\epsilon\} = [P]\,\{\beta\} \tag{2.18}$$

The assumption that the cross section remains invariant will set the strain components ϵ_{yy}, ϵ_{zz}, ϵ_{yz} zero. For flexural problems, the remaining three strain components may be approximated by taking the linear terms in x, y, and z of a polynomial. Thus, Eq. 2.18 is written as

$$\begin{Bmatrix} \epsilon_{xx} \\ \epsilon_{xy} \\ \epsilon_{xz} \end{Bmatrix} = \begin{bmatrix} 1 & y & xy & z & xz \\ 0 & 0 & \varphi(y,z) & 0 & \chi(y,z) \\ 0 & 0 & \chi(y,z) & 0 & \Psi(y,z) \end{bmatrix} \begin{Bmatrix} \beta_1 \\ \beta_2 \\ \beta_3 \\ \beta_4 \\ \beta_5 \end{Bmatrix} \tag{2.19}$$

It is noted that, when the shear strain functions $\varphi(y,z)$, $\chi(y,z)$ and $\psi(y,z)$ in Eq. 2.19 are set to zero, shear strains are eliminated in the formulation and the strain field will be equivalent to Bernoulli's hypothesis: plane sections remain plane where normals to the reference axis before bending remain normal after bending (elementary beam theory). Similarly, prescribing the functions $\varphi(y,z)$ and $\psi(y,z)$ with constant values introduces shear strains in the formulation, and the resulting strain field will be equivalent to that derived from Timoshenko's kinematical model[31], where points on normals to a reference axis before deformation remain on a straight line after deformation (Timoshenko beam theory). Or, when stated differently, plane sections remain plane but planes normal to a reference axis before deformations do not necessarily remain normal after deformation. In a similar fashion, various forms of kinematical models may be developed by manipulating the shear strain functions. Inclusion of higher order terms of y and z in ϵ_{xx} will also furnish mainfold forms of more sophisticated kinematical models.

In the discussion presented so far, it has been tacitly assumed that the shearing strains ϵ_{xy} and ϵ_{xz} are linearly dependent functions of ϵ_{xx}. It is shown at a later state that this relationship exists as a result of a minimization process. From a different standpoint, the established relationship can be viewed as a result of the overall equilibrium condition of the beam element. The manner in which these relationships are established is now presented.

The stress field corresponding to the strain field given by Eq. 2.19 is obtained by employing the constitutive relationships,

$$\begin{Bmatrix} \sigma_{xx} \\ \sigma_{xy} \\ \sigma_{xz} \end{Bmatrix} = \begin{bmatrix} D_{11} & D_{12} & D_{13} \\ D_{21} & D_{22} & D_{23} \\ D_{31} & D_{32} & D_{33} \end{bmatrix} \begin{bmatrix} 1 & y & xy & z & xz \\ 0 & 0 & \varphi(y,z) & 0 & \chi(y,z) \\ 0 & 0 & \chi(y,z) & 0 & \psi(y,z) \end{bmatrix} \begin{Bmatrix} \beta_1 \\ \beta_2 \\ \beta_3 \\ \beta_4 \\ \beta_5 \end{Bmatrix} \qquad (2.20)$$

For a beam whose material is elastic, isotropic and homogeneous, the Hookean constants are taken as

$$D_{11} = E \qquad \text{(Young's Modulus)}$$

$$D_{22} = D_{33} = G \qquad \text{(Shear Modulus)}$$

$$D_{ij} = 0 \qquad (\text{for } i \neq j)$$

For different situations, as in the case of the inelastic beam or a beam of anisotropic material, the appropriate Hookean constants must be used.

Figure 2.2 shows the stress resultants which are equivalent to the integrals of the boundary stresses lumped at nodes 1 and 2. The stress resultants are,

$$\begin{aligned} P_i &= \int_A \sigma_{xx_i} \, dA \\ V_{y_i} &= \int_A \sigma_{xy_i} \, dA \\ V_{z_i} &= \int_A \sigma_{xz_i} \, dA \\ M_{y_i} &= \int_A z \, \sigma_{xx_i} \, dA \\ M_{z_i} &= \int_A y \, \sigma_{xx_i} \, dA \end{aligned} \qquad (2.21)$$

where $i = 1,2$ which are the node points of the element.

The unbalanced stress resultants in the beam element, determined from the equilibrium condition, become

$$\begin{aligned}
\Delta P &= \int_A (\sigma_{xx_2} - \sigma_{xx_1})\, dA \\
\Delta V_y &= \Delta V_z = 0 \\
\Delta M_y &= \int_A z(\sigma_{xx_2} - \sigma_{xx_1})\, dA \\
\Delta M_z &= \int_A y(\sigma_{xx_2} - \sigma_{xx_1})\, dA
\end{aligned} \tag{2.22}$$

Or, when expressed in terms of the strain coefficients they are written in matrix notation as

$$\begin{aligned}
\Delta P &= EL\int_A [y \quad z] \begin{Bmatrix} \beta_3 \\ \beta_5 \end{Bmatrix} dA \\
\Delta M_y &= EL\int_A [yz \quad z^2] \begin{Bmatrix} \beta_3 \\ \beta_5 \end{Bmatrix} dA \\
\Delta M_z &= EL\int_A [y^2 \quad yz] \begin{Bmatrix} \beta_3 \\ \beta_5 \end{Bmatrix} dA
\end{aligned} \tag{2.23}$$

where L = length of the beam element.

These unbalanced forces are counteracted by introducing shearing forces at the nodes. The magnitude of the shearing stress resultants $\{\tilde{V}\}$, which satisfy the equilibrium condition of the element, are

$$\{\tilde{V}\} = \frac{1}{L}\{\Delta M\} \tag{2.24}$$

or, in terms of the axial forces $\{\Delta P\}$ as

$$\{\tilde{V}\} = \frac{1}{L}[\tilde{e}]\{\Delta P\} \tag{2.25}$$

where $[\tilde{e}]$ consists of the associated distances from the reference axis to the resultants of $\{\Delta P\}$. Substitution of Eq. 2.23 in Eq. 2.25 will furnish the shearing stress resultants, which are required for the overall equilibrium condition, in terms of $\{\beta\}$ and which are written in the form

$$\{\tilde{V}\} = E\ [J]\ \{\tilde{\beta}\} \tag{2.26}$$

where

$$[J] = \begin{bmatrix} y^2 & yz \\ yz & z^2 \end{bmatrix} dy\ dz$$

and

$$\{\tilde{\beta}\} = \begin{Bmatrix} \beta_3 \\ \beta_5 \end{Bmatrix}$$

It is noted that $[J]$ is equivalent to the inertia matrix of the cross section.

In the same manner, the shearing stress resultants of Eq. 2.20 may be expressed as

$$[V] = G\ [\tilde{P}]\ \{\tilde{\beta}\} \tag{2.27}$$

where

$$[\tilde{P}] = \int_A \begin{bmatrix} \varphi(y,z) & \chi(y,z) \\ \chi(y,z) & \psi(y,z) \end{bmatrix} dy\ dz$$

Obviously, the shearing stress resultants given by Eq. 2.27 are equivalent to those given by Eq. 2.26, thus

$$[V] = [\tilde{V}] \tag{2.28}$$

At this stage, a vector consisting of the average shearing strains $\{\bar{\gamma}\}$ is introduced to account for the variation in shearing strains over the cross section. The expression for $\{\bar{\gamma}\}$ can be written in the form

$$\{\bar{\gamma}\} = \frac{1}{AG} [\alpha] \{V\} = \frac{1}{A} [\alpha] [\tilde{P}] \{\tilde{\beta}\} \tag{2.29}$$

where

$$[\alpha] = \begin{bmatrix} \alpha_{yy} & \alpha_{yz} \\ \alpha_{zy} & \alpha_{zz} \end{bmatrix}$$

The matrix $[\alpha]$ is composed of numerical factors which are commonly known as shear deformation coefficients. A coefficient determines the shear deformation, by considering an average value of the shear induced transverse displacement, due to a transverse shearing force. For example, α_{yy} is the coefficient in the y direction due to a shear force in the same direction, α_{zz} is the counterpart of α_{yy} in the z direction, and α_{yz} is the coefficient that determines the shear deformation in the y direction due to a force in the z direction, and vice versa.

In order to evaluate the elements in $[\alpha]$, it is necessary to establish the general solution of the problem of bending by terminal transverse loads. The customary approach to the solution of this problem, based on the semi-inverse method of St. Venant, has been given by several authors(2,32,33). A recent contribution(34) reduces the elasticity solution, by introducing appropriate simplifying assumptions, in order to derive a formula for shear coefficients which is applicable to symmetric shapes only. Based on this formula, numerical values of $[\alpha]$ are calculated for simple geometric cross sections. The latest contributions[35,36], furnish a numerical solution based on displacement formulation by a finite element technique.

Comparison of Eq. 2.29 and Eq. 2.26 yields the following,

$$\{\bar{\gamma}\} = \frac{E}{GA}\,[\alpha]\,[J]\,\{\tilde{\beta}\} \tag{2.30}$$

Substitution of Eq. 2.30 in the strain field equations given by Eq. 2.19 results in defining the strain field explicitly as

$$\{\epsilon\} = [P]\,\{\beta\}$$

$$\begin{Bmatrix} \epsilon_{xx} \\ \epsilon_{xy} \\ \epsilon_{xz} \end{Bmatrix} = \begin{bmatrix} 1 & y & xy & z & xz \\ 0 & 0 & \dfrac{E\Gamma_{yy}}{GA} & 0 & \dfrac{E\Gamma_{yz}}{GA} \\ 0 & 0 & \dfrac{E\Gamma_{zy}}{GA} & 0 & \dfrac{E\Gamma_{zz}}{GA} \end{bmatrix} \begin{Bmatrix} \beta_1 \\ \beta_2 \\ \beta_3 \\ \beta_4 \\ \beta_5 \end{Bmatrix} \tag{2.31}$$

where

$$\Gamma_{yy} = \alpha_{yy}\,J_{yy} + \alpha_{yz}\,J_{zy}$$

$$\Gamma_{yz} = \alpha_{yy}\,J_{yz} + \alpha_{yz}\,J_{zz}$$

$$\Gamma_{zy} = \alpha_{zy}\,J_{yy} + \alpha_{zz}\,J_{zy}$$

$$\Gamma_{zz} = \alpha_{zy}\,J_{yz} + \alpha_{zz}\,J_{zz}$$

or, in tensor notation it may be expressed as

$$\Gamma_{ij} = \alpha_{ik}\,J_{kj}$$

where the summation convention for repeated indexes is employed.

Once the strain field is defined explicitly in terms of the undetermined coefficients, the stiffness matrix can be determined by following the outline described in Section 2.2. In Eq. 2.16 the stiffness matrix [k] is expressed in terms of the matrices [H] and [T]. These matrices are determined, by integrating over the volume of the beam element, the matrices [P], [D], [R] and [L] which are defined in Eq. 2.7 to 2.9.

The [H] matrix is written in the form

$$[H] = \int_V [P]^T [D] [P] \, dV \tag{2.12}$$

where the matrix [P] is given by Eq. 2.31 for the problem at hand. Substitution of [P] results in the following symmetric matrix

$$[H] = \int_V \begin{bmatrix} E & & & & & \\ Ey & Ey^2 & & & \text{SYMMETRIC} & \\ Exy & Exy^2 & Ex^2y^2+G[\Gamma_{yy}^{\ 2}+\Gamma_{yz}^{\ 2}] & & & \\ Ez & Eyz & Exyz & Ez^2 & & \\ Exz & Exyz & Ex^2y^2+G[\Gamma_{yy}\Gamma_{zy}+\Gamma_{yz}\Gamma_{zz}] & Exz^2 & Ex^2z^2+G[\Gamma_{zy}^{\ 2}+\Gamma_{zz}^{\ 2}] \end{bmatrix} dV \tag{2.32}$$

Obviously, the matrix reduces to a diagonal matrix when the centroidal-principal axes of the cross section are used.

In order to determine [T], the matrices [R] and [L] must be evaluated first. The matrix [R] is obtained by relating the boundary force vector $\{\sigma_b\}$ in terms of strain coefficients $\{\beta\}$. The boundary force vector $\{\sigma_b\}$ consists of six elements representing the y and z components of the boundary forces at the two nodes. Thus,

$$\{\sigma_b\} = [R]\,\{\beta\}$$

$$\begin{Bmatrix} \sigma_{xx_1} \\ \sigma_{xy_1} \\ \sigma_{xz_1} \\ \sigma_{xx_2} \\ \sigma_{xy_2} \\ \sigma_{xz_2} \end{Bmatrix} = \begin{bmatrix} -E & -Ey & E\ell y & -Ez & E\ell z \\ 0 & 0 & -E\Gamma_{yy}/A & 0 & -E\Gamma_{yz}/A \\ 0 & 0 & -E\Gamma_{zy}/A & 0 & -E\Gamma_{zz}/A \\ E & Ey & E\ell y & Ez & E\ell z \\ 0 & 0 & E\Gamma_{yy}/A & 0 & E\Gamma_{yz}/A \\ 0 & 0 & E\Gamma_{zy}/A & 0 & E\Gamma_{zz}/A \end{bmatrix} \begin{Bmatrix} \beta_1 \\ \beta_2 \\ \beta_3 \\ \beta_4 \\ \beta_5 \end{Bmatrix} \tag{2.33}$$

The matrix $[L]$ relates the displacements at the boundary $\{\tilde{u}\}$ and the generalized displacements $\{\delta\}$. For the problem at hand, there are six prescribed displacements at the boundary $\{\tilde{u}\}$ which are related to the ten generalized displacements $\{\delta\}$ at the nodes in the following form

$$\{\tilde{u}\} = [L]\,\{\delta\}$$

$$\begin{Bmatrix} u_1 \\ v_1 \\ w_1 \\ u_2 \\ v_2 \\ w_2 \end{Bmatrix} = \left[\begin{array}{ccccc|ccccc} 1 & 0 & -y & 0 & -z & & & & & \\ 0 & 1 & 0 & 0 & 0 & & & 0 & & \\ 0 & 0 & 0 & 1 & 0 & & & & & \\ \hline & & & & & 1 & 0 & -y & 0 & -z \\ & & 0 & & & 0 & 1 & 0 & 0 & 0 \\ & & & & & 0 & 0 & 0 & 1 & 0 \end{array}\right] \begin{Bmatrix} u_1 \\ v_1 \\ \theta_{z_1} \\ w_1 \\ \theta_{y_1} \\ u_2 \\ v_2 \\ \theta_{z_2} \\ w_2 \\ \theta_{y_2} \end{Bmatrix} \tag{2.34}$$

Once the matrices $[R]$ and $[L]$ are determined, the matrix $[T]$ is obtained by integrating the product over the boundary

$$[T] = \int_A [R]^T [L] \, dy \, dz$$

$$= \int_A \begin{bmatrix} -E & 0 & Ey & E & Ez & E & 0 & -Ey & 0 & -Ez \\ -Ey & 0 & Ey^2 & Ey & Ey^2 & Ey & 0 & -Ey^2 & 0 & -Ey^2 \\ E\ell y & -E\Gamma_{yy}/A & -E\ell y^2 & E\ell y & -E\ell y^2 & E\ell y & E\Gamma_{yy}/A & -E\ell y^2 & E_{zy}/A & -E\ell yz \\ -Ez & 0 & Eyz & Ez & Ez^2 & Ez & 0 & -Eyz & 0 & -Ez^2 \\ E\ell z & -E\Gamma_{yz}/A & -E\ell yz & E\ell z & E\ell z^2 & E\ell z & E\Gamma_{yz}/A & E\ell yz & E\Gamma_{zz}/A & -E\ell yz \end{bmatrix} dy \, dz \tag{2.35}$$

At this stage, the stiffness matrix [k] can be determined from Eq. 2.16 since the matrices [H] and [T] are known and are given by Eq. 2.33 and Eq. 2.35, respectively. This matrix is not evaluated here in the manner described above since it requires a rather tedious manipulation consisting of manual integrations and matrix operations. However, review of the derivation process discloses a complete sequence of numerical integration and matrix operations, which can be performed in a systematic manner, by developing a suitable computer program.

Alternatively, the manipulation required to evaluate the general stiffness matrix is significantly reduced from the viewpoint of manual computations, by performing transformations to the stiffness matrix computed for the centroidal-principal axes. For this particular set of axes the non-diagonal elements in [H] will vanish and most of the elements in [T] reduce to zero, thus the required matrix operation in Eq. 2.16 is simplified. Once the stiffness matrix for these sets of axes has been evaluated, the corresponding stiffness matrix for an arbitrarily assigned set of axes can be easily established following the standard transformation procedure of stiffness matrices used in structural mechanics.

The computation for the element stiffness matrix $[\bar{k}]$ corresponding to the centroidal-principal axes results as given below:

$$\{\bar{f}\} = [\bar{k}]\,\{\bar{\delta}\}$$

$$\begin{Bmatrix} \bar{P}_1 \\ \bar{V}_{z1} \\ \bar{M}_{y1} \\ \bar{V}_{y1} \\ \bar{M}_{z1} \\ \bar{P}_2 \\ \bar{V}_{z2} \\ \bar{M}_{y2} \\ \bar{V}_{y2} \\ \bar{M}_{z2} \end{Bmatrix} = \begin{bmatrix}
\frac{EA}{L} & & & & & & & & & \\
0 & \frac{12EJ_y}{L^3(1+\Phi_z)} & & & & & & & & \\
0 & \frac{6EJ_y}{L^2(1+\Phi_z)} & \frac{(4+\Phi_z)EJ_y}{L(1+\Phi_z)} & & & & & \text{SYMMETRIC} & & \\
0 & 0 & 0 & \frac{12EJ_z}{L^3(1+\Phi_y)} & & & & & & \\
0 & 0 & 0 & -\frac{6EI_z}{L^2(1+\Phi_y)} & \frac{(4+\Phi_y)EJ_z}{L(1+\Phi_y)} & & & & & \\
-\frac{EA}{L} & 0 & 0 & 0 & 0 & \frac{EA}{L} & & & & \\
0 & -\frac{12EJ_y}{L^3(1+\Phi_z)} & -\frac{6EJ_y}{L^2(1+\Phi_z)} & 0 & 0 & 0 & \frac{12EJ_y}{L^3(1+\Phi_z)} & & & \\
0 & \frac{6EJ_y}{L^2(1+\Phi_z)} & \frac{(2-\Phi_z)EJ_y}{L(1+\Phi_z)} & 0 & 0 & 0 & -\frac{6EJ_y}{L^2(1+\Phi_y)} & \frac{(4+\Phi_z)EJ_y}{L(1+\Phi_z)} & & \\
0 & 0 & 0 & -\frac{12EJ_z}{L^3(1+\Phi_y)} & \frac{6EJ_z}{L^2(1+\Phi_y)} & 0 & 0 & 0 & \frac{12EJ_z}{L^3(1+\Phi_y)} & \\
0 & 0 & 0 & -\frac{6EJ_z}{L^2(1+\Phi_y)} & \frac{(2-\Phi_y)EJ_z}{L(1+\Phi_y)} & 0 & 0 & 0 & \frac{6EJ_z}{L^2(1+\Phi_y)} & \frac{(4+\Phi_y)EJ_z}{L(1+\Phi_y)}
\end{bmatrix} \begin{Bmatrix} \bar{u}_1 \\ \bar{w}_1 \\ \bar{\theta}_{y1} \\ \bar{v}_1 \\ \bar{\theta}_{z1} \\ \bar{u}_2 \\ \bar{w}_2 \\ \bar{\theta}_{y2} \\ \bar{v}_2 \\ \bar{\theta}_{z2} \end{Bmatrix} \quad (2.36)$$

where

$$\Phi_y = \frac{12E\Gamma_{zz}}{GAL^2}$$

and

$$\Phi_z = \frac{12E\Gamma_{yy}}{GAL^2}$$

In the above expressions, the terms Γ_{yy} and Γ_{zz} are defined in Eq. 2.31. It is observed that use of the centroidal-principal axes sets the cross terms such as Γ_{yz}, J_{yz}, α_{yz}, etc. to zero thus resulting in a more simplified form of stiffness matrix.

In order to obtain the general stiffness matrix, for an arbitrary set of axes, the stiffness matrix $[\bar{k}]$ given by Eq. 2.36 is subjected to a transformation. The new set of axes which pass through point P, is shown in Fig. 2.3, where the axes are translated by v_p and w_p from the original point 0, (the centroid) and are rotated by an arbitrary angle α.

The transformation matrix, designated by $[T_r]$, is obtained by expressing the displacement field at the boundary as coordinates of each reference axes. This relationship is,

$$\{\delta\} = [T_r]\,\{\bar{\delta}\}$$

$$\begin{Bmatrix} u_1 \\ w_1 \\ \theta_{y1} \\ v_1 \\ \theta_{z1} \\ u_2 \\ w_2 \\ \theta_{y2} \\ v_2 \\ \theta_{z2} \end{Bmatrix} = \left[\begin{array}{ccccc|ccccc} 1 & 0 & -v_p & 0 & w_p & & & & & \\ 0 & -\sin\alpha & 0 & \cos\alpha & 0 & & & & & \\ 0 & 0 & -\sin\alpha & 0 & \cos\alpha & & & 0 & & \\ 0 & \cos\alpha & 0 & \sin\alpha & 0 & & & & & \\ 0 & 0 & \cos\alpha & 0 & \sin\alpha & & & & & \\ \hline & & & & & 1 & 0 & -v_p & 0 & w_p \\ & & & & & 0 & -\sin\alpha & 0 & \cos\alpha & 0 \\ & & 0 & & & 0 & 0 & -\sin\alpha & 0 & \cos\alpha \\ & & & & & 0 & \cos\alpha & 0 & \sin\alpha & 0 \\ & & & & & 0 & 0 & \cos\alpha & 0 & \sin\alpha \end{array}\right] \begin{Bmatrix} \bar{u}_1 \\ \bar{w}_1 \\ \bar{\theta}_{y1} \\ \bar{v}_1 \\ \bar{\theta}_{z1} \\ \bar{u}_2 \\ \bar{w}_2 \\ \bar{\theta}_{y2} \\ \bar{v}_2 \\ \bar{\theta}_{z2} \end{Bmatrix} \tag{2.37}$$

Since the transformation matrix $[T_r]$ is orthogonal the general flexural stiffness matrix is obtained from

$$[k] = [T_r]^T [\bar{k}] [T_r] \tag{2.38}$$

Stiffness Matrix in Torsion

In this section, the stiffness matrix is derived for a beam element having the characteristics of "thin-walled beams". A thin-walled beam is composed of plates which are assumed to undergo in-plane strains alone when subjected to loads. The theory of torsion of thin-walled beams, unlike solid beams, has as a distinctive feature the occurrence of considerable axial strains as a result of torsion. The general theory of thin-walled beams as developed by Vlasov[11] is essentially based on the assumptions that the cross section remains undeformed and the shearing deformation in the middle surface vanishes. In this study, the cross section will also be assumed to be rigid but the shearing strains at the middle surface are not neglected.

The stiffness matrix for the beam element subjected to torsion is derived by following the same procedure adopted in the flexural problem. Figure 2.4 shows a component plate of the beam model used for deriving this stiffness matrix. In order to simplify the computations, the z-axis is oriented parallel to the mid-surface of the element and the x-axis passes through the center of torsion.

The strain field for a torsional problem is approximated in a similar manner shown in Eq. 2.19 as

$$\{\epsilon\} = [P]\{\beta\}$$

$$\begin{Bmatrix} \epsilon_{xx} \\ \epsilon_{xy} \end{Bmatrix} = \begin{bmatrix} z & zx & 0 \\ 0 & \xi(z) & (y-a) \end{bmatrix} \begin{Bmatrix} \beta_6 \\ \beta_7 \\ \beta_8 \end{Bmatrix} \tag{2.39}$$

It is noted that the shear strain function $\xi(z)$ is assumed constant through the thickness. But the variation along the z-axis may be accounted for by introducing an average shearing strain $\bar{\epsilon}_{xz}$ and a shear deformation factor α_w in a similar manner described earlier in this section. Thus, the approximated strain field is defined explicitly as follows

$$\begin{Bmatrix} \epsilon_{xx} \\ \epsilon_{xy} \end{Bmatrix} = \begin{bmatrix} z & xz & 0 \\ 0 & \dfrac{\alpha_w E J_{yy}}{GA} & (y-a) \end{bmatrix} \begin{Bmatrix} \beta_6 \\ \beta_7 \\ \beta_8 \end{Bmatrix} \qquad (2.40)$$

The corresponding [H] matrix for the given strain field becomes

$$[H] = \int_V \begin{bmatrix} Ez^2 & & \text{SYMMETRIC} \\ Exz^2 & Ex^2z^2 + G\left[\dfrac{\alpha_w EJ_{yy}}{GA}\right]^2 & \\ 0 & G(y-a)(\alpha_w EJ_{yy}/GA) & G(y-a)^2 \end{bmatrix} dx\, dy\, dz \qquad (2.41)$$

Relating the boundary force vector $\{\sigma_b\}$ and the strain coefficients $\{\beta\}$ yields the matrix [R], thus

$$\{\sigma_b\} = [R]\{\beta\}$$

$$\begin{Bmatrix} \sigma_{xx1} \\ \sigma_{xz1} \\ \sigma_{xx2} \\ \sigma_{xz2} \end{Bmatrix} = \begin{bmatrix} -Ez & E\ell z & 0 \\ 0 & -\alpha_w EJ_{yy}/A & -G(y-a) \\ Ez & E\ell z & 0 \\ 0 & \alpha_w EJ_{yy}/A & G(y-a) \end{bmatrix} \begin{Bmatrix} \beta_6 \\ \beta_7 \\ \beta_8 \end{Bmatrix} \qquad (2.42)$$

There are four prescribed displacements $\{\tilde{u}\}$ at the boundary which are given in terms of four generalized displacements $\{\delta\}$ at the nodes. The relationship is written in the form,

$$\{\bar{u}\} = [L]\ \{\delta\}$$

$$\begin{Bmatrix} u_1 \\ w_1 \\ u_2 \\ \omega_2 \end{Bmatrix} = \left[\begin{array}{cc|cc} 0 & z & \multicolumn{2}{c}{0} \\ -a-2(y-a) & 0 & & \\ \hline \multicolumn{2}{c|}{} & 0 & 0 \\ \multicolumn{2}{c|}{0} & & \\ & & -a-2(y-a) & 0 \end{array}\right] \begin{Bmatrix} \varphi_1 \\ \omega_1 \\ \varphi_2 \\ \omega_2 \end{Bmatrix} \qquad (2.43)$$

It is noted that the term (y-a) in the displacement w given by Eq. 2.43 is multiplied by a factor of 2. The well known explanation given by Lord Kelvin and Tait(32,37) on the manner in which an applied torque is resisted by a bar having a thin rectangular cross section, refers to the stress distribution in the cross section. They have explained that one-half of the applied torque is carried by a system of shearing stresses parallel to the longer dimension of the cross section. The other half, is carried by the transverse shearing stresses which act normal to the plate. These transverse stresses are normally neglected even though they become of an appreciable magnitude near the short sides of the rectangle. However, since they act at a greater distance, their contribution to the torque is significant and thus they constitute the other half. In this study, the aforementioned difficulty is circumvented by establishing an appropriate kinematical model which will yield a solution consistent with the approximate elasticity solution.

The matrix [T] is computed as follows,

$$[T] = \int_A [R]^T\ [L]\ dy\ dz$$

$$[T] = \int_A \begin{bmatrix} 0 & Ez^2 & 0 & -Ez^2 \\ -G(a-2y)(\alpha_\omega EJ_{yy}/A) & -E\ell z^2 & G(a-2y)(\alpha_\omega EJ_{yy}/A) & -E\ell z^2 \\ -G(y-a)(a-2y) & 0 & G(y-a)(a-2y) & 0 \end{bmatrix} dy\, dz \tag{2.44}$$

The general stiffness matrix is obtained by substituting Eq. 2.41 and Eq. 2.44 in Eq. 2.16. If the y-axis passes through the centroid of the element, the stiffness matrix reduces to the following:

$$\{\bar{f}\} = [\bar{k}]\,\{\bar{\delta}\}$$

$$\begin{Bmatrix} M_{T1} \\ M_{\omega 1} \\ M_{T2} \\ M_{\omega 2} \end{Bmatrix} = \frac{12EI_\omega}{L^3(1+\Phi_\omega)} \begin{bmatrix} 1+\frac{\varkappa^2}{12}(1+\Phi_\omega) & & & \text{SYMMETRIC} \\ -\frac{L}{2} & \frac{L^2}{12}(4+\Phi_\omega) & & \\ -1-\frac{\varkappa^2}{12}(1+\Phi_\omega) & \frac{L}{2} & 1+\frac{\varkappa^2}{12}(1+\Phi_\omega) & \\ -\frac{L}{2} & \frac{L}{12}(2-\Phi_\omega) & \frac{L}{2} & \frac{L^2}{12}(4+\Phi_\omega) \end{bmatrix} \begin{Bmatrix} \varphi_1 \\ \omega_1 \\ \varphi_2 \\ \omega_2 \end{Bmatrix} \tag{2.45}$$

where

I_ω = warping moment of inertia about the shear center

K_T = St. Venant torsion constant

$$\Phi_\omega = \frac{12\alpha EJ_{yy}}{GAL^2}$$

$$\varkappa = \sqrt{GK_T L^2/EI_\omega}$$

Of course, for profiles with zero warping rigidity ($I_\omega = 0$), the factor $\varkappa$ must be expressed such that EI_ω does not become a denominator.

The torsional stiffness of a beam element may be derived consistently from the displacement approach also as a minimization of the total potential energy. In the following, two different forms of displacement functions are considered, namely, hyperbolic functions and polynomials. The stiffness matrices derived from these two forms of displacement functions are compared to that given by Eq. 2.45.

Hyperbolic Functions

According to Vlasov's beam theory[11] the governing differential equation for the beam element in torsion is given by

$$EI_{\omega}\varphi'''' - GK_{T}\varphi'' = 0 \tag{2.46}$$

The solution of Eq. 2.46 yields the following displacement functions written in matrix form as

$$\begin{Bmatrix} \varphi \\ \omega \end{Bmatrix} = \begin{bmatrix} 1 & x & \cosh kx & \sinh kx \\ 0 & 1 & k \sinh kx & k \cosh kx \end{bmatrix} \begin{Bmatrix} \alpha_1 \\ \alpha_2 \\ \alpha_3 \\ \alpha_4 \end{Bmatrix} \tag{2.47}$$

where

$$\omega = \varphi_{,x}$$

$$k = \sqrt{\frac{GK_T}{EI_{\omega}}}$$

Corresponding to the displacement function given by Eq. 2.47 the following stiffness matrix can be derived[38,39]

$$
\begin{Bmatrix} M_{T1} \\ M_{\omega 1} \\ M_{T2} \\ M_{\omega 1} \end{Bmatrix} = \frac{EI_{\omega}}{DL^3} \begin{bmatrix} \varkappa^3 \sinh\varkappa & & & \text{SYMMETRIC} \\ \varkappa^2 L(1-\cosh\varkappa) & \varkappa L^2(\varkappa\cosh\varkappa - \sinh\varkappa) & & \\ -\varkappa^3(1-\cosh\varkappa) & -\varkappa L^2(1-\cosh\varkappa) & \varkappa^2 \sinh\varkappa & \\ \varkappa^2 L(1-\cosh\varkappa) & \varkappa L^2(\sinh\varkappa - \varkappa) & -\varkappa L^2(1-\cosh\varkappa) & \varkappa L^2(\varkappa\cosh\varkappa - \sinh\varkappa) \end{bmatrix} \begin{Bmatrix} \varphi_1 \\ \omega_1 \\ \varphi_2 \\ \omega_2 \end{Bmatrix} \tag{2.48}
$$

where

$$D = 2(1 - \cosh\varkappa) + \varkappa \sin\varkappa$$

$$\text{and } \varkappa = kL$$

Polynomials

The displacement field for the beam element may be expressed by a polynomial of the third order as follows,

$$\{u\} = [P]\{\alpha\}$$

$$
\begin{Bmatrix} \varphi \\ \omega \end{Bmatrix} = \begin{bmatrix} 1 & x & x^2 & x^3 \\ 0 & 1 & 2x & (3x^2 + \frac{E\Gamma_{yy}}{GA}) \end{bmatrix} \begin{Bmatrix} \alpha_1 \\ \alpha_2 \\ \alpha_3 \\ \alpha_4 \end{Bmatrix}
$$

In order to take account of shearing deformations due to warping, an appropriate term is incorporated in [P] as described earlier in this section.

The vector $\{\alpha\}$ consists of the coefficients which are to be determined in terms of the nodal displacements $\{\delta\}$ from the relationship

$$\{\delta\} = [C]\,\{\alpha\} \tag{2.50}$$

The strain field $\{\epsilon\}$ corresponding to the displacement field of Eq. 2.49 may be written as follows,

$$\{\epsilon\} = [Q]\,\{\alpha\}$$

$$\begin{Bmatrix} \epsilon_{xx} \\ \epsilon_{xz} \end{Bmatrix} = \begin{bmatrix} -az\varphi_{,xx} & 0 & 0 & -6xz \\ z(y-a)\varphi_{,x} + \dfrac{E\Gamma_{yy}}{GA}\varphi_{,xxx} & 0 & 2(y-a) & 6[x^2(y-a)+\dfrac{E\Gamma_{yy}}{GA}] \end{bmatrix} \begin{Bmatrix} \alpha_1 \\ \alpha_2 \\ \alpha_3 \\ \alpha_4 \end{Bmatrix} \tag{2.51}$$

Following the standard finite element procedure, the stiffness matrix can be obtained from

$$[k] = [C^{-1}]^T \{\int_V [Q]^T [D] [Q]\, dV\} [C^{-1}] \tag{2.52}$$

Thus,

$$\{\bar{f}\} = [\bar{k}]\,\{\bar{\delta}\}$$

$$\begin{Bmatrix} \bar{M}_{T1} \\ \bar{M}_{\omega 1} \\ \bar{M}_{T2} \\ \bar{M}_{\omega 2} \end{Bmatrix} = \frac{12EI_\omega}{L^3(1+\Phi_\omega)^2} \begin{bmatrix} 1+\frac{\kappa^2}{12}[\frac{1}{5}+(1+\Phi_\omega)^2] & & \text{SYMMETRIC} & \\ -\frac{L}{2}[1+\frac{\kappa^2}{60}] & \frac{L^2}{12}[3+(1+\Phi_\omega)^2 + \frac{\kappa}{4}(\frac{1}{5}+\frac{(1+\Phi_\omega)^2}{3})] & & \\ -1-\frac{\kappa^2}{12}[\frac{1}{5}+(1+\Phi_\omega)^2] & \frac{L}{2}[1+\frac{\kappa}{60}] & 1+\frac{\kappa^2}{12}[\frac{1}{5}+(1+\Phi_\omega)^2] & \\ -\frac{L}{2}[1+\frac{\kappa}{60}] & \frac{L^2}{12}[3-(1+\Phi_\omega)^2 + \frac{\kappa}{4}(\frac{1}{5}-\frac{(1+\Phi_\omega)^2}{3})] & \frac{L}{2}[1+\frac{\kappa}{60}] & \frac{L^2}{12}[3+(1+\Phi_\omega)^2 + \frac{\kappa}{4}(\frac{1}{5}+\frac{(1+\Phi_\omega)^2}{3})] \end{bmatrix} \begin{Bmatrix} \bar{\varphi}_1 \\ \bar{\omega}_1 \\ \bar{\varphi}_2 \\ \bar{\omega}_2 \end{Bmatrix}$$

(2.53)

If warping shearing deformations are ignored, the parameters Φ_ω are set to zero, and the stiffness matrix will reduce to the following,

$$\begin{Bmatrix} M_{T1} \\ M_{\omega 1} \\ M_{T2} \\ M_{\omega 2} \end{Bmatrix} = \frac{12EI_\omega}{L^3} \begin{bmatrix} 1+\frac{\kappa^2}{10} & & & \text{SYMMETRIC} \\ -\frac{L}{2}[1+\frac{\kappa^2}{60}] & \frac{L^2}{3}[1+\frac{\kappa^2}{30}] & & \\ -1-\frac{\kappa^2}{10} & \frac{L}{2}[1+\frac{\kappa^2}{60}] & 1+\frac{\kappa^2}{10} & \\ -\frac{L}{2}[1+\frac{\kappa^2}{60}] & \frac{L^2}{6}[1-\frac{\kappa^2}{60}] & \frac{L}{2}[1+\frac{\kappa^2}{60}] & \frac{L^2}{3}[1+\frac{\kappa^2}{30}] \end{bmatrix} \begin{Bmatrix} \varphi_1 \\ \omega_1 \\ \varphi_2 \\ \omega_2 \end{Bmatrix} \quad (2.54)$$

The stiffness matrix given by Eq. 2.54, which is a special case of Eq. 2.53, is identical to previous derivations(40).

2.4 APPLICATIONS AND SAMPLE SOLUTIONS

Before any finite element solution can be used with confidence some idea of its accuracy and convergence characteristics are required. Suitable evidence is usually provided by comparing the finite element results with accurate results derived by alternate means. To illustrate the validity and application of the method the finite element formulation developed is applied to a number of the few numerical examples whose analytical solutions are straightforward. The procedure of analysis is based on the displacement method which is adequately covered in many publications(18,19,23).

The structural member under consideration is suitably idealized by a set of basic beam elements with a 7-degrees-of-freedom at each node. The stiffness matrix for such an element is given in Appendix I when the centroidal-principal axes system is used. Once the member is idealized as an assemblage of beam elements, the over-all unconstrained structural stiffness matrix is generated following the rules that govern the assembly process used in the matrix analysis of framed structures. This matrix is generated by a simple summation of the individual stiffnesses and loads at the nodes using nodal compatibility for this process. Alternatively, the variational concept may be used on the entire assemblage to derive a mathematical statement of the assembly rules. The assembly rules for the assemblage of the stiffness matrix and load vector is written as

$$[K] = \sum_{i=1}^{N} [k_i] \tag{2.55}$$

$$[F] = \sum_{i=1}^{N} [f_i] \tag{2.56}$$

where N is the total number of elements.

It is evident that structural members are subjected to boundary conditions in forms of tractions or displacements. The traction boundary conditions are incorporated automatically into the load vector $\{F\}$. When imposing the displacement boundary conditions, the standard procedure, which involves eliminating the equilibrium equation at which the particular displacements are specified, results in reducing the size of the master stiffness matrix and thus requires reorganization of the computer storage. However, the same conditions can be imposed without changing the size of the matrix, simply by modifying the stiffness matrix and the load vector. This is accomplished by multiplying with a very large number the element on the diagonal of the matrix $[K]$ at the location concerned and also by replacing the corresponding element in the load vector $\{F\}$ by the same large number multiplied by the specified displacement[15]. This procedure applies whether the prescribed displacements are homogeneous or nonhomogeneous. For the case of elastic restraints, the matrix $[K]$ is modified by adding the support stiffness on the appropriate matrix element on the diagonal of the stiffness matrix.

The resulting equilibrium equations of the complete system are expressed in the form

$$\{F\} = [K]\,\{\Delta\} \tag{2.57}$$

in which the number of simultaneous equations in the preceding relationship is equal to seven times the number of nodal points. The nodal displacements $\{\Delta\}$ are unknown and are determined by solving the set of simultaneous equations (Eq. 2.57) and then the stress resultants are evaluated by using the relationships of the individual elements.

Numerical Examples

The first numerical example to illustrate the application and validity of the procedure described is that of a cantilever beam subjected to a concentrated torque at the free end. The beam represented in Fig. 2.5 allows warping and twist at one end and these displacements are restrained at the other end. The twist and warping displacements are computed at the nodal points for different values of the parameter $\kappa = \sqrt{G\,K_t\,L^2/EI_\omega}$ in order to cover a wider range in cross-sectional properties. The computed values plotted in Fig. 2.5 agree very well with the charts given in Ref. 41.

The second example consists of the same beam used in the first example but loaded with a concentrated bimoment at the free end instead of a torque. The results are plotted in Fig. 2.6 where close agreement is observed with those given in Ref. 42.

In order to compare the differences in solutions that may arise when using the element stiffness matrices given by Eqs. 2.45, 2.48 and 2.54, the cantilever beam used in the earlier examples was used again. The stiffness matrices are determined based on three different formulations, namely, the strain field formulation, the polynomial formulation and the hyperbolic functions formulation as described in Section 2.3. The cantilever beam was loaded by a concentrated torque and bimoment at the free end as shown in Fig. 2.7. Different values of the cross sectional parameter $\varkappa$ were used in order to cover a wider spectrum in beam characteristics ranging from those having resistances in pure warping to those in pure torsion (St. Venant torsion). As indicated in Fig. 2.7, good correlation is observed for the values of $\varkappa$ normally regarded as thin-walled beams. However, for larger values of the parameter $\varkappa$, or when I_ω approaches zero, the differences in the solutions increase and the computational errors grow when using the stiffness matrix based on the strain formulation (Eq. 2.45). Moreover, for this particular formulation, the results oscillate for larger values of $\varkappa$ as shown in Fig. 2.8 whereas good agreement is observed for values of $\varkappa$ less than 10. This problem of numerical instability arises from the fact that the strain field formulation necessarily assumes that the cross section has warping resistance, I_ω. This is not regarded as a serious practical problem, since useful solutions can be obtained using ordinary analyses once it is known that the cross section has no warping resistance.

The final numerical example is intended to demonstrate the versatility of the method by considering a continuous beam with two equal spans subjected to a concentrated bimoment $M_\omega = 1.0$ acting at the right support as shown in Fig. 2.9. The shear centers of both spans are assumed to form one straight line which is considered as the axis of the beam. For both spans, the cross section parameter $\varkappa$ is assumed equal to 1.0. The variations of the torque M_T and the bimoment M_ω are shown in Fig. 2.9. It is important to distinguish the two components of the torque M_T which are present in thin-walled beams. The torque T_{sv} is the more familiar St. Venant's torsion, the other component T_ω is the warping torsion. The latter results not from warping but from the suppression of warping.

3. LINEAR STABILITY ANALYSIS OF BEAM-COLUMNS

3.1 INTRODUCTION

The theory of linear stability, which is based on the concept introduced by Euler, represents closely the circumstances of failure of beam-columns. Although the actual conditions of failure require the inclusion of nonlinear influences for the precise determination at the failure condition, as in determining the complete response of an imperfect column, the critical condition obtained from linear stability analysis is useful from the design standpoint. Linear stability analysis is defined here as the calculation of the bifurcation of equilibrium, the point of bifurcation occuring at the critical load which is characterized by the existence of a fundamental state of equilibrium.

In the conventional linear stability analysis of structural problems, two approaches are normally used. The first approach is to determine the lowest eigenvalue of the governing differential equations of the structural system for a given set of boundary conditions. Alternatively, if the governing differential equations are too difficult to prescribe, numerical methods are utilized by establishing a strain energy expression for large deflections which is subsequently minimized, leading to roots representing instability conditions.

The use of matrix methods in solving problems of stability based on the concept of discrete element idealization has recently received considerable attention. In particular, displacement formulations based on finite element idealization are found to be more suitable. The adoption of the matrix force method has been accomplished

(19) but is employed to a lesser extent. From the viewpoint of stability and finite displacement analyses, the possibility of incorporating geometric nonlinearities within a displacement method offers a suitable means of utilizing the finite element concept and its applications. Moreover, the finite element approach plays an important role through its ability to lead to solutions to problems with irregularities in loading and geometry which defy adequate treatment by the classical means. Another important characteristic for the use of finite elements has been their intrinsic simplicity. Useful reviews of the accomplishments in finite element stability analyses are found in Ref. 43 to 47.

As in other aspects of the finite element method, the treatment of problems dealing with linear stability consists of two component parts: the formulation of the element relationship and the solution of the complete system. Furthermore, the formulation of the element relationship involves the calculation of corrective terms to the linearized equations. Consequently, application of the conventional matrix displacement methods to problems in elastic stability has been concerned with the derivation of so-called geometric stiffness matrices to account for the instability effects. The inclusion of the geometric stiffness matrices into the formulation is performed by adding them directly to the elastic stiffnesses to form a resultant stiffness matrix. The derivation of the elastic stiffness matrix for the beam element is given in Section 2.3. In the following section, a formulation is presented for deriving the element geometric stiffness matrices.

3.2 A FINITE ELEMENT MODEL FOR DERIVING GEOMETRIC STIFFNESS MATRICES

In this section a general method for evaluating geometric stiffness matrices for the stability analysis of general discrete structural systems is presented. The formulation provides a means for a direct determination of geometric stiffness matrices that are consistent with any kinematically admissible displacement field assumed for the element. The derivation of stiffness matrices often is based on the approximate displacement field, as defined by suitable interpolation polynomials or shape functions $[N]$ of coordinates, and a set of nodal parameters $\{\delta\}$, element by element, as

$$\{u\} = [N]\,\{\delta\} \tag{3.1}$$

The displacement field may also be defined more conveniently by polynomial functions of the coordinates $[P]$ and a set of generalized coordinates or generalized displacement amplitudes $\{\alpha\}$ expressed by

$$\{u\} = [P]\,\{\alpha\} \tag{3.2}$$

A relationship between the vectors $\{\delta\}$ and $\{\alpha\}$ is established using a displacement transformation matrix $[C]$. This matrix is determined by substituting the coordinates of the nodes in Eq. 3.2 in the following form

$$\{\delta\} = [C]\,\{\alpha\} \tag{3.3}$$

When performing a stability analysis, use of the non-linear total strain-displacement equations is essential and leads to relevent solutions[48,49]. The strain-displacement equations as given by the general theory of deformations or known as the Lagrangian strain tensor[35] are written in tensor notation as

$$e_{jk} = \frac{1}{2} (u_{k,j} + u_{j,k} + u_{i,j} \, u_{i,k}) \tag{3.4}$$

In Eq. 3.4 the summation convention for repeated indexes is employed and a comma denotes partial derivation with respect to the variable that follows. A typical strain component, frequently used in structural analysis is the axial strain, e_{xx}, and can be expanded from Eq. 3.4 which is written in standard mathematical notation using the engineering definition as

$$e_{xx} = \frac{\partial u}{\partial x} + \frac{1}{2}\left[\left(\frac{\partial u}{\partial x}\right)^2 + \left(\frac{\partial v}{\partial x}\right)^2 + \left(\frac{\partial w}{\partial x}\right)^2\right] \tag{3.5}$$

In developing the strain-displacement relationships for beam-type bodies it is necessary to convert formally the relationships given by the three-dimensional theory of deformations into their one-dimensional analogue. An attempt is made here to formulate the stability problem of beam-columns by making use of the strain-displacement relationships provided by the classical theory of thin-walled beams(11,50,51).

The displacements of a thin-walled beam of rigid cross-section is adequately described by the lateral displacements v and w and by the rotation φ. The displacements at any point on the beam are functions of the coordinate x and are given by

$$\begin{aligned} u &= - z \frac{\partial \bar{w}}{\partial x} - y \frac{\partial \bar{v}}{\partial x} + \psi(y,z) \frac{\partial \bar{\varphi}}{\partial x} \\ v &= \bar{v}(x) + z \, \bar{\varphi}(x) \\ w &= \bar{w}(x) - y \, \bar{\varphi}(x) \end{aligned} \tag{3.6}$$

Where $\bar{u}$, $\bar{v}$ and $\bar{\varphi}$ are arbitrary functions of the coordinate x and $\psi(y,z)$ is the warping function. Based on the assumption that the elongations are negligible compared to unity, Novozhilov(48) has developed the strain-displacement relationships for thin rods by expanding the displacements u, v and w (Eq. 3.6) in series in the coordinates of y and z of the points of the cross section.

The expressions for the nonvanishing components of strains which become adequate for the problem at hand are:

$$\begin{aligned} \varepsilon_{xx} &= e_{xx} + z\,\varkappa_{zz}(x) + y\,\varkappa_{yy}(x) + \psi(y,z)\,\frac{d\varphi}{dx} \\ \varepsilon_{xz} &= e_{xz} + \left(\frac{\partial x}{\partial z} + y\right)\varphi \\ \varepsilon_{xy} &= e_{xy} + \left(\frac{\partial x}{\partial y} - z\right)\varphi \end{aligned} \tag{3.7}$$

where e_{ij} are the strain components given by Eq. 3.4, and $\varkappa_{zz}(x)$ and $\varkappa_{yy}(x)$ are the curvatures of the deformed axis of the beam which take into account large displacements in u, v and φ. The expressions for the curvatures for large displacements are found in Ref. 48.

The strain vector given above may be resolved into two components and is written in matrix notation

$$\{\varepsilon\} = \{\varepsilon_o\} + \{\varepsilon_L\} \tag{3.8}$$

where $\{\varepsilon_o\}$ is the usual linear, infinitesimal strain vector while $\{\varepsilon_L\}$ represents the non-linear strain contribution. It is well known that the mere presence of $\{\varepsilon_L\}$, without regard to magnitude, has a decisive influence on the behavior predicted in stability situations.

Having established the displacement field it would be logical to define the strain field in terms of the same parameters $\{\alpha\}$ used in Eq. 3.2 which may be written collectively as

$$\{\epsilon\} = \{\epsilon_o\} + \{\epsilon_L\} = [Q]\{\alpha\} + [Q_L]\{\tilde{\alpha}\} \tag{3.9}$$

The matrices $[Q]$ and $[Q_L]$ introduced in Eq. 3.9 represent derivatives of the displacements corresponding to the linear and non-linear strain contributions, respectively.

Following a similar development normally used in finite element formulation, the strain energy in the new configuration of equilibrium is evaluated as

$$U = \frac{1}{2}\int_V \{\epsilon\}^T [D] \{\epsilon\}\, dV \tag{3.10}$$

The matrix $[D]$ represents the generalized Hookean constant. On substituting Eq. 3.9 into Eq. 3.10 and neglecting the non-linear strain product $\{\epsilon_L\}^T [D] \{\epsilon_L\}$, since it is of much higher order, the strain energy functional reduces to

$$U = \frac{1}{2}\int_V \left[\{\sigma_o\}^T \{\epsilon_o\} + 2\{\sigma_o\}^T \{\epsilon_L\}\right] dV \tag{3.11}$$

where a new stress matrix

$$\{\sigma_o\} = [D]\{\epsilon_o\}$$

has been introduced to denote the stresses corresponding to the linear strains $\{\epsilon_o\}$.

From Castigliano's first theorem, which is applicable to non-linear strains provided that the total strain energy is evaluated, the following relationship is obtained

$$\{F_\alpha\} = \frac{\partial U}{\partial \alpha} = \int_V \left([Q]^T [D] [Q] + 2\, \sigma_o\, [Q_L] \right) dV \, \{\alpha\}$$
$$= \left[[K_E]_\alpha + [K_G]_\alpha \right] \{\alpha\} \tag{3.12}$$

In performing the differentiation with respect to the generalized coordinates $\{\alpha\}$ the linear stresses $\{\sigma_o\}$ have been assumed to remain constant. Introducing the displacement transformation matrix $[C]$ into Eq. 3.12 yields the force-displacement relationship

$$\{F\} = \left[[K_E] + [K_G] \right] \{\delta\} \tag{3.13}$$

where

$$[K_E] = [C^{-1}]^T \left[\int_V Q^T [D] [Q] \, dV \right] [C^{-1}] \tag{3.14}$$

is the usual stiffness matrix obtained by the linear theory, and

$$[K_G] = [C^{-1}]^T \left[2 \int_V \left(\sigma_o [Q_L] \right) dV \right] [C^{-1}] \tag{3.15}$$

is the geometric stiffness matrix. The geometric stiffness matrix derives its name from the fact that it depends on the geometry of the displaced element. It is noted that the geometric stiffness matrix can easily be determined from an integral of simple matrix products evaluated over the volume of the element. The approach avoids the usual procedure of determining strain energy in terms of displacements and its subsequent differentiation with respect to the displacement, which in this case would be more time consuming. Furthermore, the formulation allows for a systematic investigation of the effects of higher order terms in the strain-displacement relationship by introducing the appropriate matrices.

Application of the finite element model developed above is made to derive the geometric stiffness matrix of the beam element. This matrix may be derived in a single operation by formulating one general strain expression which includes all the strain components corresponding to the generalized displacements and substituting it into the strain energy functional given by Eq. 3.11. Although this approach may seem to offer simplicity it suffers from the drawback that the required computations become cumbersome. Alternatively, the derivation may be carried out more conveniently by treating separately each of the large displacements that introduce geometric nonlinearity. The stiffness matrices corresponding to each form of large displacement are finally aggregated together to constitute the general geometric stiffness matrix for the beam element.

The displacements that introduce geometric nonlinearity as they become 'large' may be put under three categories:

a) Axial displacements

b) Transverse displacements

c) Twist

In the following sections, the constitutive geometric stiffness matrices $[k_G]_i$ are derived corresponding to each large displacement given above. The derivation of the usual linear stiffness matrices $[k_E]_i$ is not given here; it is presented in Section 2.3.

3.3 LARGE AXIAL DISPLACEMENTS

When a beam-column is subjected to an axial force, it is well known that the stiffness of the beam in flexure and torsion become dependent on the magnitude of the applied axial force. In the following, the influence of the axial force on the flexural and torsional stiffnesses of the beam element are derived separately.

Flexural Geometric Stiffness Matrix

Consider a uniform beam element shown in Fig. 3.1a. The element sustains only flexural displacement in the x-y plane under the generalized forces P, V_y and M_z applied at the nodes. A simplified model is used here merely for convenience; however, a model capable of sustaining flexural displacements in both x-y and x-z planes simultaneously could also be used without introducing significant complications.

For the beam element shown in Fig. 3.1a, the axial displacement, u, is taken to be adequately represented by a linear polynomial and a cubic polynomial is assumed for the transverse displacement, v. The assumed displacement field is written in matrix notation as,(52)

$$\{u\} = [P]\,\{\alpha\}$$

$$\begin{Bmatrix} u \\ v \\ \theta \end{Bmatrix} = \begin{bmatrix} 1 & \xi & 0 & 0 & 0 & 0 \\ 0 & 0 & 1 & \xi & \xi^2 & \xi^3 \\ 0 & 0 & 0 & 1 & 2\xi & 3\xi^2 \end{bmatrix} \begin{Bmatrix} \alpha_1 \\ \alpha_2 \\ \alpha_3 \\ \alpha_4 \\ \alpha_5 \\ \alpha_6 \end{Bmatrix} \qquad (3.16)$$

where $\xi = x/L$

The approximate strain-displacement relationship based on the ordinary beam theory (Bernoulli's hypothesis) and which, in addition, included the predominant component of Eq. 3.5 to account for the large transverse displacement is given by

$$\epsilon_{xx} = \epsilon_o + \epsilon_L = [u_{,x} - yv_{,xx}] + \left[\frac{1}{2} v^2_{,x}\right] \tag{3.17}$$

Note that ϵ_{xx} is a nonlinear transformation under the assumption that the strain due to midline rotation is not small when compared to the midline axial strain.

The matrix $[Q_L]$ is determined by expressing the nonlinear strain component $\{\epsilon_L\}$ in terms of the parameter $\{\alpha\}$ as expressed in Eq. 3.9, thus,

$$[Q_L] = \frac{1}{2} \begin{bmatrix} 0 & 0 & 0 & 0 & 0 & 0 \\ 0 & 0 & 0 & 0 & 0 & 0 \\ 0 & 0 & 0 & 0 & 0 & 0 \\ 0 & 0 & 0 & 1 & 2\xi & 3\xi^2 \\ 0 & 0 & 0 & 2\xi & 4\xi^2 & 6\xi^3 \\ 0 & 0 & 0 & 3\xi^2 & 6\xi^3 & 9\xi^4 \end{bmatrix} \tag{3.18}$$

The transformation matrix $[C]$ is determined by substituting the coordinates of the nodes (Eq. 3.2) into the equations of the displacements given by Eq. 3.16. At this stage, the matrices $[Q_L]$ and $[C]$ are known. Finally, by substituting these matrices into Eq. 3.15, and integrating over the whole volume of the beam element the geometric stiffness matrix is evaluated as

$$[k_G] = \frac{P}{L}\begin{bmatrix} 0 & & & & & \\ 0 & 6/5 & & & \text{SYMMETRIC} & \\ 0 & L/10 & 2L^2/15 & & & \\ 0 & 0 & 0 & 0 & & \\ 0 & -6/5 & -L/10 & 0 & 6/5 & \\ 0 & L/10 & -L^2/30 & 0 & -L/10 & 2L^2/15 \end{bmatrix} \qquad (3.19)$$

The result agrees with that found in the literature(52).

Torsional Geometric Stiffness Matrix

A uniform beam element is considered here (Fig. 3.2b) which sustains only torsional and the associated warping displacements under the generalized forces P, M_T and M_ω at the nodes. For convenience, the x-axis is chosen such that it passes through the shear center of the beam section. As in the flexural analysis, the axial displacement, u, is taken to be adequately represented by a linear polynomial; the twist, φ, is represented by a cubic polynomial and a quadratic polynomial is assumed for the warping displacement, ω. The assumed displacement field when written in matrix notation is

$$\{u\} = [P]\,\{\alpha\}$$

$$\begin{Bmatrix} u \\ \varphi \\ \omega \end{Bmatrix} = \begin{bmatrix} 1 & 0 & 0 & 0 & 0 & 0 \\ 0 & 0 & 1 & \xi & \xi^2 & \xi^3 \\ 0 & 0 & 0 & -1 & -2\xi & -3\xi^2 \end{bmatrix} \begin{Bmatrix} \alpha_1 \\ \alpha_2 \\ \alpha_3 \\ \alpha_4 \\ \alpha_5 \\ \alpha_6 \end{Bmatrix} \qquad (3.20)$$

where $\xi = x/L$

It is noted that the displacement field given above is identical to Eq. 3.16, likewise, the transformation matrix [C] will be the same.

For open thin-walled beams, which are composed of plates assumed to undergo in-plane strains only, a strain-displacement relationship can be established based on the assumption that the cross section remains undeformed. The approximate axial strain, ϵ_{xx}, based on Vlasov's beam theory, and which includes, in addition, the second order effects of large twists is given by

$$\epsilon_{xx} = \epsilon_o + \epsilon_L = \left[u_{,x} - \sum_{i=1}^{n} \rho_i \, z \, \varphi_{,xx}\right] + \left[\frac{1}{2} \sum_{i=1}^{n} (\rho_i^2 \, \omega^2 + r_i^2 \, \omega^2)\right] \quad (3.21)$$

where n = number of component plates of the shape

ρ = the perpendicular distance between the shear center of the section and the middle line of a plate

r = the distance from the center of twist of a component plate (due to St. Venant torsion) to a general point on the middle of the plate

The kinematics of the beam section under torsion, from which the strain-displacement relationship was established (Eq. 3.21), and the dimensions defined above are shown in Fig. 3.2.

By expressing the nonlinear component of the axial strain (Eq. 3.9), ϵ_{xx}, in terms of the parameters $\{\alpha\}$ the matrix $[Q_L]$ is determined, thus

$$[Q_L] = \frac{(\rho_i + r_i)}{2} \begin{bmatrix} 0 & 0 & 0 & 0 & 0 & 0 \\ 0 & 0 & 0 & 0 & 0 & 0 \\ 0 & 0 & 0 & 0 & 0 & 0 \\ 0 & 0 & 0 & 1 & 2\xi & 3\xi^2 \\ 0 & 0 & 0 & 2\xi & 4\xi^2 & 6\xi^3 \\ 0 & 0 & 0 & 3\xi^2 & 6\xi^3 & 9\xi^4 \end{bmatrix} \quad (3.22)$$

At this level, the matrices $[Q_L]$ and $[C]$, required for the computation of $[k_G]$, are known; on substituting these into Eq. 3.15 and performing the required integration over the volume of the beam element, the torsional geometric stiffness matrix of a beam element under axial load is obtained as

$$[k_G] = \frac{PI_o}{LA} \begin{bmatrix} 0 & & & & & \\ 0 & 6/5 & & & \text{SYMMETRIC} & \\ 0 & -L/10 & 2L^2/15 & & & \\ 0 & 0 & 0 & 0 & & \\ 0 & -6/5 & L/10 & 0 & 6/5 & \\ 0 & -L/10 & L^2/30 & 0 & L/10 & 2L^2/15 \end{bmatrix} \qquad (3.23)$$

where I_o = polar moment of inertia of the section about the shear center.

3.4 LARGE LATERAL DISPLACEMENTS

When a beam is subjected to a major axis bending, the minor axis flexural stiffness and the torsional stiffness become dependent on the applied moment. For a perfect member, there is a critical load at which the beam buckles in a combined mode involving twist and lateral deflection. In the following, the influence of the major axis bending on the stiffnesses in torsion and in flexure about the weak axis are investigated.

Flexural-Torsional Geometric Stiffness Matrix

Consider a uniform beam element that undergoes only translational displacements v, in the y direction, when subjected to unequal moments M_{z1} and M_{z2} at the two nodes (Fig. 2.2). Just prior to buckling, the initial axial stress at any point in the beam, according to the elementary beam theory, is given by

$$\sigma_o = \frac{M_{oz} y}{I_z} + \frac{V_y xy}{I_z} \tag{3.24}$$

where

$$M_{oz} = \frac{1}{2}(M_{z1} + M_{z2})$$

$$V_y = \frac{1}{2L}(M_{z1} - M_{z2})$$

Obviously, the initial stress σ_o must be modified for the case when, in addition, the beam element carries distributed loads between the nodes. For instance, the additional term becomes quadratic in x for a uniformly distributed load. However, such additional terms may not be required whenever a finer discretization is used and a proper lumping of the nodal forces is performed.

At the critical state, the adjacent equilibrium configuration assumes lateral displacements associated with twisting. For a finite element formulation, these displacements may be represented adequately by polynomial functions which are written in matrix form as

$$\{u\} = [P]\,\{\alpha\}$$

$$\begin{Bmatrix} v \\ \theta_z \\ w \\ \theta_y \\ \varphi \\ \omega \end{Bmatrix} = \begin{bmatrix} 1 & \xi & \xi^2 & \xi^3 & 0 & 0 & 0 & 0 & 0 & 0 & 0 & 0 \\ 0 & 1 & 2\xi & 3\xi^2 & 0 & 0 & 0 & 0 & 0 & 0 & 0 & 0 \\ 0 & 0 & 0 & 0 & 1 & \xi & \xi^2 & \xi^3 & 0 & 0 & 0 & 0 \\ 0 & 0 & 0 & 0 & 0 & 1 & 2\xi & 3\xi^2 & 0 & 0 & 0 & 0 \\ 0 & 0 & 0 & 0 & 0 & 0 & 0 & 0 & 1 & \xi & \xi^2 & \xi^3 \\ 0 & 0 & 0 & 0 & 0 & 0 & 0 & 0 & 0 & -1 & -2\xi & -3\xi^2 \end{bmatrix} \begin{Bmatrix} \alpha_1 \\ \alpha_2 \\ \alpha_3 \\ \alpha_4 \\ \alpha_5 \\ \alpha_6 \\ \alpha_7 \\ \alpha_8 \\ \alpha_9 \\ \alpha_{10} \\ \alpha_{11} \\ \alpha_{12} \end{Bmatrix} \tag{3.25}$$

where $\xi = x/\ell$

In deriving the geometric stiffness matrix, it is important to identify the nonlinear strain components when establishing the strain-displacement relationship. The total axial strain ε_{xx} may be obtained from the general strain-displacement relationship for beams (Eq. 3.7) by substituting the appropriate curvatures due to large displacements. The relevent terms, in the case of lateral torsional displacements, are those which are products of φ and ω and their derivatives. It is believed that inclusion of all the terms in the analysis will result in furnishing a more complete geometric stiffness matrix. In the study presented herein, only a limited number of these terms are adopted merely to constitute a formulation which is compatible with the classical analysis of lateral-torsional buckling. In the classical approach, for example, it is assumed that the flexural rigidity about the major axis is very much greater than about the minor axis. This is equivalent to the assumption that the deflections prior to buckling are small and can be neglected. However, if the flexural rigidities about both principal axes are of the same order of magnitude, the deflections may be of importance and should be considered.[37]

In the energy formulation for lateral buckling of a beam as given by Timoshenko[53], or in the kinematical model demonstrated by Bleich[54], the equivalent strain-displacement relationship is written as

$$\varepsilon = \varepsilon_o + \varepsilon_L = [- yv_{,xx} - \rho z\varphi_{,xx}] + [y\varphi w_{,xx}] \tag{3.26}$$

Once the nonlinear strain component is defined, the matrix $[Q_L]$ is determined by establishing the strain-displacement relationship in terms of the parameters $\{\alpha\}$, as expressed in Eq. 3.9, thus

$$[Q_L] = \begin{bmatrix} 0 & 0 & 0 & 0 & 0 & 0 & 0 & 0 \\ 0 & 0 & 0 & 0 & 0 & 0 & 0 & 0 \\ 0 & 0 & 0 & 0 & 2 & 2\xi & 2\xi^2 & 2\xi^3 \\ 0 & 0 & 0 & 0 & 3\xi & 3\xi^2 & 3\xi^3 & 3\xi^4 \\ 0 & 0 & 2 & 3\xi & 0 & 0 & 0 & 0 \\ 0 & 0 & 2\xi & 3\xi^2 & 0 & 0 & 0 & 0 \\ 0 & 0 & 2\xi^2 & 3\xi^3 & 0 & 0 & 0 & 0 \\ 0 & 0 & 2\xi^3 & 3\xi^4 & 0 & 0 & 0 & 0 \end{bmatrix} \tag{3.27}$$

The transformation matrix $[C]$ is evaluated by substituting the coordinates of the nodes into the equations of the displacements (Eq. 3.3).

On substituting the matrices $[Q_L]$, $[C]$ and $\{\sigma_o\}$ into Eq. 3.15 and performing the required integration over the volume of the beam element, the geometric stiffness is obtained. The resulting matrix, where the columns and rows corresponding to the torsional displacements are eliminated since they are all zero, is written as

$$[k_G] = \frac{M_{oz}}{30L} \begin{bmatrix} 0 & & & & & & & \\ 0 & 0 & & & & \text{SYMMETRIC} & & \\ -36 & -33L & 0 & & & & & \\ 3L & 4L^2 & 0 & 0 & & & & \\ 0 & 0 & 36 & -3L & 0 & & & \\ 0 & 0 & -3L & -L^2 & 0 & 0 & & \\ 36 & 3L & 0 & 0 & -36 & 33L & 0 & \\ 3L & -L^2 & 0 & 0 & -3L & 4L^2 & 0 & 0 \end{bmatrix}$$

$$+\frac{V}{60}\begin{bmatrix} 0 & & & & & & & \\ 0 & 0 & & & & \text{SYMMETRIC} & & \\ 30 & 21L & 0 & & & & & \\ -3L & -2L^2 & 0 & 0 & & & & \\ 0 & 0 & -30 & 3L & 0 & & & \\ 0 & 0 & 9L & -L^2 & 0 & 0 & & \\ 30 & 9L & 0 & 0 & -30 & 21L & 0 & \\ 3L & L^2 & 0 & 0 & -3L & 2L^2 & 0 & 0 \end{bmatrix} \tag{3.28}$$

3.5 LARGE TORSIONAL DISPLACEMENTS

A straight shaft may become unstable under the action of a torque. Similar to the case of Euler buckling in flexure when subjected to an action of axial compressive force, the bending moment in the shaft remains zero so long as the axis remains straight. However, as soon as a deflection occurs, bending moments are introduced about both principal axes at various sections of the shaft. The deformed configuration in this case is not a plane curve, and the bending moments vary accordingly as components of the applied axial torque. A comprehensive treatment of buckling of shafts, based on the conventional approach of establishing the governing differential equations, is given by Ziegler[55] for different loading and support conditions.

Torsional-Lateral Geometric Stiffness Matrix

In the finite element formulation, the displacement of the beam is represented adequately by a system of third order polynomial as given by Eq. 3.25. Just prior to buckling, the initial torsional stress at any point in the beam is given by

$$\sigma_o = \frac{M_x \rho}{I_o} \tag{3.29}$$

where ρ = radial distance from the center of twist

I_o = polar moment of inertia of the section about the shear center

In deriving the geometric stiffness matrix, it is important to identify the linear and nonlinear displacement components. For a beam subjected to a large torsional displacement, Fig. 3.3 shows schematically the displacement components. The total unit torsional displacement is written as

$$\theta = \theta_o + \theta_L = [(\theta_x)_{,x}] + [\theta_y(\theta_z)_{,x} - \theta_z(\theta_y)_{,x}] \tag{3.30}$$

where a comma denotes a differentiation.
When these generalized displacements are expressed in terms of the displacement functions of the beam, the relationship becomes

$$\epsilon = \epsilon_o + \epsilon_L = [\varphi_{,x}] + [w_{,x}\, v_{,xx} - v_{,x}\, w_{,xx}]\, \rho \tag{3.31}$$

Note that the nonlinear strain components are associated with the curvature of the beam.

The matrix $[Q_L]$ is determined by expressing the nonlinear strain component $\{\epsilon_L\}$ in terms of the parameter $\{\alpha\}$ as expressed in Eq. 3.9, thus

$$[Q_L] = \begin{bmatrix} 0 & 0 & 0 & 0 & 0 & 0 & 0 & 0 \\ 0 & 0 & 0 & 0 & 0 & 0 & 0 & 0 \\ 0 & 0 & 0 & 0 & 0 & 2/\ell^3 & 4x/\ell^4 & 6x^2/\ell^5 \\ 0 & 0 & 0 & 0 & 0 & 6x/\ell^4 & 12x^2/\ell^5 & 18x^3/\ell^6 \\ 0 & 0 & 0 & 0 & 0 & 0 & 0 & 0 \\ 0 & 0 & 2/\ell^3 & 6x/\ell^4 & 0 & 0 & 0 & 0 \\ 0 & 0 & 4x/\ell^4 & 12x^2/\ell^5 & 0 & 0 & 0 & 0 \\ 0 & 0 & 6x^2/\ell^5 & 18x^3/\ell^6 & 0 & 0 & 0 & 0 \end{bmatrix} \tag{3.32}$$

The displacement transformation matrix [C] is determined by substituting the coordinates of the nodes into the displacement function given by Eq. 3.25. At this level, the matrices $[Q_L]$ and [C], required for the evaluation of the geometric stiffness matrix $[k_G]$, are known; on substituting these into Eq. 3.15 and performing the required integration over the volume of the beam element, the geometric stiffness matrix of a beam element under pure tension is obtained as

$$K_G = \frac{M_x}{L} \begin{bmatrix} 0 & & & & & & & \\ 0 & 0 & & & \text{SYMMETRIC} & & & \\ 0 & 1.0 & 0 & & & & & \\ -1.0 & 0 & 0 & 0 & & & & \\ 0 & 0 & 0 & 1.0 & 0 & & & \\ 0 & 0 & -1.0 & -L/2 & 0 & 0 & & \\ 0 & -1.0 & 0 & 0 & 0 & 1.0 & 0 & \\ 1.0 & L/2 & 0 & 0 & -1.0 & 0 & 0 & 0 \end{bmatrix} \tag{3.33}$$

3.6 LINEAR EIGENVALUE PROBLEMS

Solution Technique

Once the elastic and geometric stiffness matrices are determined for each structural element, the element stiffnesses can be transformed into a common displacement system and the assembled stiffness matrix is obtained using conventional procedures from the summation of the element stiffnesses. The resulting equations for the complete system, which take into account the nonlinear effects of large displacements, are expressed in general form

$$\{F\} = [K_E]\{\Delta\} + F_1 [K_G]_1 \{\Delta\} + F_2 [K_G]_2 \{\Delta\} + \ldots + F_n [K_G]_n \{\Delta\} \tag{3.34}$$

where the matrices $[K_G]_i$ $(i = 1,2,\ldots n)$ represent various components of geometric stiffness matrices which are conveniently resolved such that the generalized forces become the scalar multipliers. Since the geometric stiffness matrix depends on the nodal displacement vector $\{\Delta\}$, the system of equation given by Eq. 3.34 becomes nonlinear.

In dealing with linear stability problems, it is tacitly assumed that the buckling deformations are independent of the deformations prior to instability. This leads to the possibility of expressing the load vectors of each element as ratios of those particular loads that introduce instability to the whole structure. Since the critical load is unknown, a factor λ and an arbitrary measure (scale factor) of the normalized load vector $\{\overline{F}\}$ is introduced to represent the relative magnitude of the applied loads only

$$\{F\} = \lambda \{\bar{F}\} \tag{3.35}$$

The factor λ is the instability factor or eigenvalue. Since the geometric stiffness matrix is proportional to the internal forces, it follows that

$$[K_G] = \lambda [\bar{K}_G] \tag{3.36}$$

where $[K_G]$ is the geometric stiffness matrix for the reference value of the applied loading.

In performing the numerical analysis, the stiffness matrices are resolved into two components: the effective elastic stiffness matrix, which includes the effect of prestress in the element, and the geometric stiffness matrices whose instability factors are unknown. The effective elastic stiffness matrix $[\tilde{K}_E]$ is composed of the initial elastic stiffness matrix and those geometric stiffness matrice whose load parameters λ_o are known,

$$[\tilde{K}_E] = [\bar{K}_E] + \lambda_{o_i} [\bar{K}_G]_i \quad (i = 1, 2, \ldots m) \tag{3.37}$$

For small displacements $\{\bar{\Delta}\}$ the effective elastic stiffness matrix may be taken as a constant. Hence, Eq. 3.37 reduces to

$$[\tilde{K}_E] \{\bar{\Delta}\} + \lambda_{cr} [\bar{K}_G] \{\Delta\} = \{0\} \tag{3.38}$$

The requirement for a non-trivial solution is

$$\text{Det} \left| [\tilde{K}_E] + \lambda_{cr} [\bar{K}_G] \right| = 0 \tag{3.39}$$

or

$$\frac{1}{\lambda_{cr}} \{\Delta\} = [\tilde{K}_E]^{-1} [\bar{K}_G] \{\Delta\} \tag{3.40}$$

From Eq. 3.40 the eigenvalues λ_{cr}, which represent the critical loads, and the associated eigenvectors $\{\Delta\}_{cr}$, representing the buckling modes, are determined using standard matrix methods. The eigenvalue routine used in this study is based on the Jacobi reduction scheme. The routine yields the complete eigenvalues and eigenvectors corresponding to the order of the matrix $[K_G]$. Consequently, the higher buckling modes and the associated critical loads are obtained without introducing extra provision.

Numerical Examples and Results

At this stage it is appropriate to examine the numerical accuracy that may be attained in the solution of actual problems. In general, the adequacy and validity of a numerical formulation is measured by its performance on problem cases for which accurate solutions have been derived by alternate means. A simple and fundamental measure of accuracy may be furnished by referring to the case of the flexural buckling of the Euler column. In Fig. 3.4 the results of the finite element solutions are shown for centrally loaded columns with different forms of end conditions, where the percent error of the solutions are plotted versus the number of elements in the idealization. The convergence of the numerically computed critical loads toward the exact solution is remarkably good as indicated in Fig. 3.4. A similar plot is made in Fig. 3.5 of the results obtained from the application of the finite differences[56] to the governing differential equations for the case of a centrally loaded pinned-end column, where also a comparison is made with a finite element solution. It is noted that the error in a two element idealization, which is regarded as the coarsest possible grid, is less than 0.8% for the finite element solution.

Of course, the finite element method is not intended as a procedure for calculation of problems given above which can be treated rather efficiently by the classical method. However, there are numerous problems whose solutions are not straightforward when conventional approaches are used especially when there are irregularities in loading and geometry. Such problems lead to mathematical problems which are usually intractable. The formulation given here will enable the solution of a wide variety of problems. In order to demonstrate the efficacy of the finite element method in the solution of linear stability problems, several basic problem cases are selected whose solutions by classical means are not straightforward. Another aspect taken into consideration in the selection of the demonstrative problem cases is that each case possesses a distinctive feature from a finite element standpoint. In the following, several basic examples, which are encountered in many engineering situations are studied and the numerical results are presented.

a) Columns with Distributed Axial Loads

Variations in axial loads in columns is a condition encountered in many engineering situations. A vertical column having significant self-weight, the decrease in axial load with depth in a pile embedded in a frictional medium, guyed towers, industrial racks and library stacks are but a few examples. Solutions to such problems by conventional means are not straightforward especially when there are irregularities in loading and geometry. For instance, the solution of the governing differential equation for a pinned-end prismatic column under a uniformly distributed axial load requires the application of Bessel functions[53]. For such problems, the finite element method furnishes solutions in a simple manner.

In formulating a finite element relationship consider a column having general boundary conditions and carrying some arbitrarily distributed axial load of intensity q(x) per unit length together with an end load P. Both the distributed load and the end load may be compressive as shown in Fig. 3.6, or either one may be tensile while the other is compressive. In all cases, however, the conditions for buckling are represented by the critical combination of the two sets of loads. The influence of the initial load can readily be introduced by modifying the elastic stiffness matrix $[k_E]$ of each element by adding a scalar multiple of the associated geometric stiffness matrix.

For the case when the end load P is the initial load (prestress load), the modified elastic stiffness matrix is

$$[\tilde{k}_E]_i = [k_E]_i + P\,[k_G]_i \tag{3.41}$$

Or, when the initial load is a distributed axial load, the corresponding modified stiffness matrix becomes

$$[\tilde{k}_E]_i = [k_E]_i + \alpha_i\, q_i\, [k_G]_i \tag{3.42}$$

where q_i = resultant axial load at element i

α_i = consistent load factor of element i

Once the modified matrix for each element is evaluated, the critical loads are determined by finding the non-trivial solution for the homogeneous equations of the complete system given by Eq. 3.40.

To illustrate the advantages of the finite element method, examples are selected whose closed-form solution are available. Very few analytical solutions are found in the literature since the solutions involve integrals which are difficult, and usually impossible, to evaluate[37]. The examples selected are prismatic columns, having the four conventional boundary conditions, and loaded by end loads together with uniformly distributed axial loads $q(x) = q_o$. The analytical solutions for the critical combinations of buckling loads, as evaluated by Dalal[57] are compared to the results obtained through the application of the finite element method. The results are compared in graphical form in Fig. 3.7. A very good agreement is observed for all ranges of combinations of loads. The results from the finite element solutions are also given in tabular form in Table 1. For two of the numerical examples solved, the first buckling modes, under different combinations of loads, are shown in Fig. 3.8.

Unlike the conventional approaches, which require additional and usually tedious computational scheme to determine the higher buckling loads and the associated modes, the finite element approach readily furnishes these values as part of the original operational scheme.

b) Tapered Columns

Tapered columns of different cross-sectional shapes are used for structural purposes in a variety of applications. Their use is attractive in many situations where the applied load can closely be specified and a saving in weight is encountered. Analysis of tapered columns of different shapes and end conditions by classical means is difficult and has been the subject of a number of investigations [53,58,59,60]. Such problems, however, can be treated in a simple manner by the use of the finite element method.

In formulating the finite element relationship, the column is idealized as an assemblage of discrete elements, where either piecewise prismatic elements or uniformly tapered elements may be used. For the stepped representation, the section properties at the mid-length of the element sufficiently describe the element. However, such idealization may furnish less accurate results when coarse discretication is employed and when the member has a high gradient of taper. For such members, use of tapered elements will yield results with a better accuracy. The derivation of the stiffness matrix for beams with a uniform taper in either one or both principal axes is given in Appendix I.

The assembled stiffness matrix of the complete system is obtained from the summation of the geometric stiffness matrices, which are independent of the cross-sectional properties, and the elastic stiffness matrices of each element. The critical loads are then determined by finding the non-trivial solution of the homogeneous equation (Eq. 3.40).

To illustrate the advantages of the method, the critical loads of tapered columns with one end fixed and free at the other end are computed for uniformly tapered columns. For these columns, a taper parameter is defined as the ratio of moment of inertia at the two ends $\eta = I_T/I_B$, where I_T is the moment of inertia at the free end (top) and I_B represents for the fixed end (bottom). For columns with $\eta \leq 1.0$, the results obtained by the finite element method are compared to the theoretical solutions given by Timoshenko[37]. The comparison is shown both in graphical and tabular form in Fig. 3.9 and Table 2, respectively. A very close correlation is observed for all values of η. The critical loads for $\eta \geq 1.0$ is shown in Fig. 3.10 and a study on convergence is demonstrated in Fig. 3.11.

c) Columns on Elastic Foundations

The behavior of axially loaded columns with continuous elastic support can be considered as the idealized form of a number of related problems in engineering. Embedded piles receive lateral support from the surrounding soil, compression flanges of beams and girders are laterally supported through the web system, and railway tracks or continuous crane rails subjected to axial loads, such as during temperature changes, also receive lateral elastic support.

A considerable amount of literature exists regarding the analysis of beams supported on elastic foundations by seeking solutions to the governing differential equations[53,61,62]. This approach becomes more difficult to solve those problems with variations in loading, the supporting medium and on the geometry of the member.

In formulating the finite element relationship, a column supported on a Winkler-type foundation[61] is assumed, that is, the elastic foundation can be replaced by a continuous set of springs each of which can deflect independently.(*) The supporting medium may have a variation in the foundation modulus $k(x)$ along the column length and may be capable of developing lateral, rotational and torsional restraints.

The discrete element stiffness formulation results in a simple matrix relationship of the form

$$\left[[k_E]_i + [k_F]_i + [k_G]_i\right] \{\delta_i\} = \{F_i\} \tag{3.43}$$

where a new stiffness matrix $[k_F]$ is introduced to represent the consistent stiffness matrix of the foundation. The derivation of $[k_F]$ for a Winkler-type foundation is given in Appendix II. Once the evaluation of the element stiffness matrices is completed, they are assembled to obtain the equations of the complete system. The critical loads are determined by finding the non-trivial solution of the homogeneous equation (Eq. 3.40).

To demonstrate the usefulness of the method, the critical loads of axially loaded pinned-end columns on elastic foundations (lateral springs) are evaluated for various values of foundation modulii $k(x) = \bar{k}$. In Fig. 3.12, the results are compared, in graphical form, to the analytical solutions obtained by Hetenyi[61]. A very good agreement of results is observed even when a coarse discretization is used ($N = 4$).

(*)There are also other types of foundation models which have been suggested by Wieghart(63), Filenko-Bordich (64), Vlasov (65) and Biot (66). The use of such models may also be incorporated by developing the appropriate consistent stiffness matrices of the foundation as demonstrated in Appendix II for the case of a Winkler-type foundation.

d) Piecewise Prismatic Columns

Piecewise prismatic columns are occasionally encountered in special situations in engineering. The main differing feature which is characteristic of such columns, when compared to the example cases studied above, is the variation of the direction of the principal axes of the cross section along the length. During buckling of a piecewise prismatic column, the deflected configuration does not necessarily become perpendicular to the axis of the least moment of inertia and thus will exhibit a non-planar configuration. This feature causes the governing differential equations to be nonlinear, consequently the solution by the classical approach becomes difficult. For the particular case of elastic buckling of a two-component column composed of identical components, the solution was given by Hsu[67] using classical methods.

In order to demonstrate the application of the finite element method to stability problems of piecewise prismatic columns, consider a two-component column composed of two prismatic columns of the same cross section. The components are assumed to be rigidly connected, with one component on top of the other (Fig. 3.13), in such a manner that their centoidal axes are coincident but the principal axes are offset by an arbitrary angle α. The shear center of each column cross section is assumed to coincide with its centroid.

In formulating the finite element relationship, two local coordinate systems, namely the x-y-z system and the x-y'-z' system (Fig. 3.13) are used such that y-z and y'-z' coincide with the principal axes of the cross-section of the lower and upper components of the column, respectively. The x-axis is identical to both segments and coincides with the centroidal axis of the column. The stiffness expressions, when written with reference to the local coordinate system, are

$$\{F\} = [k_E]\{\delta\} + P[k_G]\{\delta\} \tag{3.44}$$

for the lower component, and

$$\{F'\} = [k_E]\{\delta'\} + P[k_G]\{\delta'\} \tag{3.45}$$

for the upper component. In Eq. 3.45, $\{F'\}$ and $\{\delta'\}$ are the force and displacement vectors corresponding to the y'-z' axes system.

To obtain the equations of the complete system, a common displacement system is used by choosing a global system of axes which coincides with the y-z system of the lower component. Following conventional procedures, the generalized displacements of the upper component $\{\delta'\}$ are transformed to the global system, through the relations

$$\begin{Bmatrix} u' \\ w' \\ \theta_y' \\ y' \\ \theta_z' \\ \varphi' \\ \omega' \end{Bmatrix} = \begin{bmatrix} 1 & 0 & 0 & 0 & 0 & 0 & 0 \\ 0 & \cos\alpha & 0 & -\sin\alpha & 0 & 0 & 0 \\ 0 & 0 & \cos\alpha & 0 & \sin\alpha & 0 & 0 \\ 0 & \sin\alpha & 0 & \cos\alpha & 0 & 0 & 0 \\ 0 & 0 & -\sin\alpha & 0 & \cos\alpha & 0 & 0 \\ 0 & 0 & 0 & 0 & 0 & 1 & 0 \\ 0 & 0 & 0 & 0 & 0 & 0 & 1 \end{bmatrix} \begin{Bmatrix} u \\ w \\ \theta_y \\ y \\ \theta_z \\ \varphi \\ \omega \end{Bmatrix} \tag{3.46}$$

where α is the angle of offset shown in Fig. 3.13. In a similar manner, the force vector $\{F'\}$ is determined using the same transformation matrix, thus

$$\{F'\} = [T]\,\{F\} \tag{3.47}$$

Since the matrix [T] is orthogonal, Eq. 3.47 may be written as

$$\{F\} = [T]^T\,[k_E]\,[T]\,\{\delta\} + P\,[T]^T\,[k_G]\,[T]\,\{\delta\}$$

Finally, the evaluation of the element stiffness matrices is performed with reference to the global system and the element stiffness matrices are assembled to form the equation of the complete system. The critical loads, P_{cr}, are obtained from the non-trivial solution of Eq. 3.15.

In order to demonstrate the application of the finite element solution procedure described above, the critical loads of two-component columns with arbitrary offset angle α are determined for various values of the stiffness factor $\eta = I_1/I_2$. The analytical solutions for such columns are given by Hsu(67) for limited values of the factor η. For the available analytical results, the finite element counterparts are compared. Figure 3.14 compares the critical loads of columns supported on spherical pins, and in Fig. 3.15 for columns with fixed end conditions. Additional results, which cover a wider range in values of the factor η, are given in graphical form (Fig. 3.14 and Fig. 3.15) and also in tabular form (Table 3).

As a second example, the critical loads of multi-segment columns, where the segments are offset orthogonally ($\alpha = 90^o$) in consecutive order, are determined for different values of the factor $\eta = I_1/I_2$. The approximate analytical solutions are given by Fischer (68). The results are compared in Fig. 3.16 for columns with pin ends and in Fig. 3.17 for fixed columns, where in both cases good correlation is observed. The results are also given in Table 4.

e) Pretwisted Columns

A pretwisted column is a structural member that has a natural twist about the longitudinal axis which may vary in some arbitrary manner along the length. While pretwisted beams are used in a variety of applications, as in turbine blade and aircraft propellers, pretwisted columns are also encountered occasionally. More than its practical justification, the study of pretwisted columns here offers a good example to demonstrate the efficacy of the finite element method to beam-column problems. In the buckling of pretwisted columns, as in the case of piecewise prismatic columns, the column assumes a non-planar deformed configuration and the resulting deflection is no longer perpendicular to the axis of least stiffness. This characteristic makes the equilibrium equations to be nonlinear differential equations whose solution may be difficult to obtain in a simple manner.

Little information is available on the study of pretwisted columns. Ziegler[(69)] investigated the buckling of pretwisted beams and columns. Later, Zickel[(70)] developed a theory concerned with the behavior of pretwisted beams and columns of thin-walled section. More recently, Fischer[(71)] investigated the influence of pretwisting on the buckling load of a column for different boundary conditions and moments of inertia. These investigations deal essentially with approximating the nonlinear differential equations by a set of uncoupled homogeneous linear differential equations, introducing certain simplifying assumptions.

In formulating the finite element relationship, the pretwisted column is idealized as an assemblage of either uniformly pretwisted beam elements or prismatic beam elements which are piecewise twisted with respect to one another along the centroidal axis. For the piecewise prismatic representation, the section properties and the incremental twist at the mid-length of the element may sufficiently describe the interval modeled. However, for situations when coarse discritization are used and when the member has a high gradient in twist, the use of pretwisted elements will furnish results with better accuracy. The derivation of the stiffness matrix for a uniformly pretwisted element is given in Appendix III.

Once the stiffness matrices for the elements are determined with reference to the local coordinates they are subsequently transformed to the global coordinates using Eq. 3.48. The transformed matrices are finally assembled following the conventional procedure of summation of the element stiffnesses. The critical loads are determined by finding the non-trivial solution for the homogeneous equation of the complete system (Eq. 3.15).

In order to obtain a verification of the finite element solution, a short test program was carried out to compare the experimental and theoretical strengths of pretwisted columns. It appears that very little theoretical study and no experimental work is found in the literature on the elastic buckling of pretwisted columns. The test program conducted in this study consists of four high-strength steel wide flange shapes (2-5/8 x 1-1/2 WF). The specimens were prepared from beams which were originally prismatic by twisting the beams, to simulate a natural twist along the length, until a permanent twist of the desired magnitude was attained. In order to induce a uniform twist along the length, pure torque was applied to the specimens in an engine lathe as shown in Fig. 3.18, by controlling the rotational displacements. Four specimens were prepared having natural twists of 0^o (prismatic), 90^o, 180^o and 360^o.

The pretwisted columns were tested under a hydraulic testing machine (Fig. 3.19) following a standard testing procedure for centrally loaded prismatic columns(72). For each column test, a boundary condition consisting of a knife edge condition along the web of the cross section (the minor principal axis) was used at each end of the column. The test data and the experimental results of the stability tests are summarized in Table 5. The Table also gives the theoretical critical loads predicted by the finite element method and estimates of the experimental critical loads which were derived by extrapolating from the load and deflection using a Southwell Plot method(37). The results are also shown graphically in Fig. 3.20. It can be seen, in general, that the critical loads are consistently more than the experimental loads and there is good correlation between the theoretical and experimental critical loads. Comparisons between the theoretical and experimental buckling modes of the tested columns are shown in Fig. 3.21.

Theoretical predictions of critical loads of pretwisted columns for various angles of pretwist α and different values of the factor $\eta = I_1/I_2$ are shown graphically in Fig. 3.22 and also in tabular form in Table 6. A knife edge condition about the minor principal axis is imposed at each end of the pretwisted column. It is seen that, for cross sections with $\eta > 1.0$, the critical load is always greater than that of the prismatic column counterpart. The increase in strength becomes significant for larger values of the factor η and for certain ranges in values of α as shown in Fig. 3.22.

It is instructive to note the variation in strength for the particular case $\eta = 1.0$ shown in Fig. 3.22. Hypothetically, within the context of the beam theory, pretwisting has no effect on the buckling strength of columns whose cross sections have equal moment of inertia about all centroidal axes ($\eta = 1.0$). However, the variation in strength shown in Fig. 3.22 is attributed to the directions of the knife edge condition imposed at the ends. For the particular case when $\alpha = 90^o$, the strength of the pretwisted column is equivalent to that of a prismatic column with pinned-fixed end conditions or to that of crossed pin end conditions oriented orthogonally. The latter view leads to the classic problem of the buckling of prismatic columns with crossed pins or ginglymus joints, that is, the pins that permit rotations in a single plane at the column ends are oriented at an arbitrary angle to each other. Ashwell(73) solved the problem of buckling of prismatic columns with crossed pins for cross sections with $\eta = 1.0$. Analytical solutions for cross sections with unequal moment of inertias about the principal axes become difficult since, in pretwisted columns, the column deflections during buckling are non-planar.

These complications do not arise when using the finite element method, since it is needed only to have an additional transformation at the node where the arbitrarily oriented pinned end condition is imposed. At this node, transformation is performed from the local to the global system using the matrix given by Eq. 3.48. Applying the finite element method described, the critical loads were determined for prismatic columns of arbitrary cross sections with crossed pins. The results are shown graphically in Fig. 3.23. For the particlar case when $\eta = 1.0$ the theoretical solution given by Ashwell(73) is compared to that of the finite element solution. Prismatic columns fixed at one end and pinned at an arbitrary angle at the other end are also solved and the numerical results are shown graphically in Fig. 3.24.

f) Lateral-Torsional Buckling Problems

The importance of lateral-torsional buckling in governing the strength of thin-walled beams has long been recognized. For perfectly straight beams subjected to major axis bending, failure in the lateral-torsional buckling mode may occur at loads considerably below those necessary to cause failure in the plane of the applied loads.

The classical procedure for determining the buckling loads of beams involves the formation and solution of the governing differential equations. Alternatively, the solution is obtained by employing energy methods such as the Ritz procedure(53,54). These methods are not, however, sufficiently general to deal with many situations which occur in practice, such as in handling complex loading and support conditions and irregularities in the beam geometry. The advantages of the finite element approach are therefore considerable since a general formulation once established may then be applied to a wide variety of lateral-torsional problems.

In order to demonstrate the accuracy and convergence characteristics of the finite element formulation (Sec. 3.4), a few examples are examined whose solutions are available by alternate means. The convergence characteristics are demonstrated by examining a simply-supported beam subjected by equal end moments M_{cr}. The results are shown in Fig. 3.25 where the percent error is plotted versus the number of elements used in the idealization, using the elastic stiffness matrices based on cubic polynomial and strain field formulation (Sec. 2.3). For a four element idealization, the percent error is less than 0.1% which may be regarded as a remarkable convergence characteristic. Note that the convergence characteristics of torsional buckling under axial loading are identical to the case of lateral-torsional buckling as shown in Fig. 3.25. To demonstrate the accuracy of the formulation, a simply-supported beam subjected to a concentrated load at the midspan of the beam is examined. In Fig. 3.26, the finite element solution is compared graphically to the analytical solution given by Timoshenko[53] for a wide range of cross section properties (see also Table 7).

The application of the finite element formulation to complex problems may be demonstrated sufficiently by examining the experimental investigations performed by Trahair on the elastic stability of continuous beams[74] and simply supported tapered beams[75]. In both cases the loads were applied at the top of the flange. In the finite element approach, effects of applying a load P at distance $\bar{a}$ from the shear center are taken into the formulation simply by adding a moment term ($P\bar{a}$) in the $[k_G]$ matrix corresponding to the degree of freedom φ at the node where the load is applied.

The experimental results of two-span aluminum beams tested by Trahair[74], which are presented in the form of an interaction diagram, are compared to the finite element solution in Fig. 3.27. The agreement with the experimental results is satisfactory. The theoretical values are obtained by taking the appropriate displacement and loading conditions during the assembly of the element stiffnesses. The moment diagram prior to buckling is taken as the loading condition which consists of terms as multiples of the unknown load parameter P_{cr} applied at one span and the known load P at the other span. The effect of the known load P is added to the elastic stiffness matrix $[k_E]$. For different values of P the corresponding P_{CR} is determined by solving the eigenvalue problem.

In the case of the buckling of tapered beams, the only differing feature is the elastic stiffness matrix $[k_E]$ which varies for each element. As in the case of tapered columns a stepped representation may sufficiently describe each element by taking the section properties at mid-length of each element. However, when beams with high taper gradients are encountered, the elastic stiffness matrix of uniformly tapered elements may be used (Appendix II). The experimental results of simply supported aluminum beams (Fig. 3.28) tested by Trahair [75] are compared to finite element solution in Fig. 3.29. Also, the theoretical values given by Trahair[75], where the differential equations are solved by numerical methods, are compared in Fig. 3.30. In both cases, the agreement is satisfactory. Using the finite element method, additional numerical results are given in Fig. 3.31 for different combinations of taper parameters.

g) Space Frames

The study of the overall stability of a space frame to obtain the actual buckling condition of the entire system has been a subject of numerous investigations. A number of methods are now available for obtaining exact or approximate solutions. A detailed account of the work in this field is found in Ref. 54 and 76. The application of the finite element method in solving problems of space frame buckling is now presented.

In formulating the finite element relationship, the internal forces in each member prior to buckling are first evaluated. The frame is then idealized as an assembly of discrete beam elements. The members which are not subjected to axial forces during the prebuckling state are sufficiently represented by single elements since the geometric stiffness matrices for such elements are null matrices. In such situations, a one-element representation does not introduce additional numerical errors since the displacement expression of the element, which is a third order polynomial, describes consistently the assumed deflection of a beam with constant shear.

Once the element stiffness matrices are determined in terms of the local coordinate systems, a displacement transformation is performed for each element involving the direction cosines when relating the local and global systems. The equilibrium equations for an element when expressed in terms of the global coordinate system is

$$\left[[k_E]_g + [k_G]_g \right] \{\delta\}_g = \{F\}_g \tag{3.49}$$

where

$$[k_E]_g = [T]^T [k_E]_\ell [T]$$

$$[k_G]_g = [T]^T [k_G]_\ell [T]$$

$$\{F\}_g = [T]^T \{F\}_\ell$$

The subscript g and ℓ represent the global and local reference axes systems, respectively.

Applying the procedure described above, numerical results of a few sample problems are now presented. In order to demonstrate the convergence characteristics of the method, knee-bent frames subjected by axial forces and having two different boundary conditions are considered. The results are compared to analytical solutions in Fig. 3.32 where the percent errors are plotted versus the number of elements used in discretizing the columns. The accuracy of the method is demonstrated by comparing the results to the analytical solutions of the four standard cases of single-story portal frames. The results are shown graphically in Fig. 3.33.

The application of the method to more complex problems is illustrated by solving the space frame used in the investigation by Morino[77] based on the determinantal approach which makes use of the concept that the determinant of the overall stiffness matrix becomes zero at the critical load. The space frame is shown in Fig. 3.34 and is subjected to vertical loads P at each joint. All members are made of the W10x49 shape and the columns are oriented as indicated in the Figure. Also shown is the idealization of the frame for the finite element analysis. The critical loads and the associated buckling modes are obtained in one operation as in the previous examples and do not require iteration. In Table 8 the results from this analysis are compared to the results in Ref. 77.

h) Buckling of Shaft under Torsion

In order to demonstrate the use of the geometric stiffness matrix derived in Section 3.5, which corresponds to large torsional displacements, the buckling strength of shafts under pure torsion is now presented. For the purpose of simplicity, two shafts are considered having simple boundary conditions: pinned and fixed in flexural rotations at both ends. In both cases concentrated torques are applied at the ends and the shafts are assumed to have equal moment of inertias about all axes. The buckling analysis of shafts having unequal moments of inertia about the principal axes is not straightforward. For such members, just prior to buckling, it is possible that the member is excessively deformed in torsion, thus, the stiffness of the beam at buckling is better represented by a pretwisted beam. However, the pretwist of the beam at the instant of buckling is unknown since the buckling load is yet to be determined. In such situations, therefore, it is suggested to employ iterative schemes in solving the problem.

In order to study the convergence characteristics of shafts having equal moments of inertia about all axes, the shaft is discretized into different numbers of elements. For a specified number of elements, the assembled stiffness matrix of the complete system is obtained in the usual manner from the summation of the individual matrices. The critical loads are determined by finding the non-trivial solution of the homogeneous equations (Eq. 3.40). The results are given in Table 9 and are compared to the analytical solution. For both shafts the eigenvalues corresponding to the first buckling modes are shown in Fig. 3.35.

4. NONLINEAR ANALYSIS OF BEAM-COLUMNS

4.1 INTRODUCTION

Nonlinear behavior in structural systems arises from two distinct sources, namely, material nonlinearities and geometric nonlinearities, the former being reflected in nonlinearities in the constitutive equations and the latter in the nonlinear terms in the kinematical equations of large displacements.

The application of nonlinear theory to conduct the conventional closed form analysis of structural responses leads to mathematical problems which are usually intractable. In order to obtain quantitative solutions, it is natural, therefore, to resort to numerical methods. In general, numerical methods of structural analysis may be described under two categories. In the first category are the methods that lead to numerical solution of the governing algebraic or differential equations, by approximating the mathematical functions, which are then solved by either finite differences or by numerical integration. In the second category is the finite element method which is based on the concept of piecewise approximating continuous fields. The adaption of the finite element method has been accelerated in recent years and is employed extensively in a wide range of nonlinear problems mainly due to its simplicity and generality. A comprehensive treatment on the theoretical foundations of the method to nonlinear problems is given in Ref. 16.

The problem of material nonlinearity arises from the nonlinearity of the constitutive equations as a consequence of describing the laws of material behavior under multiaxial stress states. The relationships do not involve only the current state of stresses as in the case of elastic behavior; rather, they depend as well upon the past histories of these components. Despite these complexities, substantial progress has been made in developing the finite element method based on the principles of the general theory of plasticity. Useful reviews of accomplishments in finite element inelastic analysis are found in Refs. 16 and 17 and also in Refs. 78 to 80.

The problem of geometric nonlinearity may be considered as having several levels of nonlinearity. For a more realistic evaluation of actual behavior, additional measures of nonlinearities must be considered. Such measures, however, will result in increasing the complexity of the formulation and of the solution.

The problems that may be considered at the lowest level in this hierarchy of nonlinearity comprise those that can be transformed into linear eigenvalue problems. This is the classical stability problem, such as in the buckling of perfectly straight columns, where satisfactory predictions can be made for critical loads (eigenvalues) and the corresponding buckling modes (eigenvectors) by solving a typical eigenvalue problem. These problems involve a bifurcation of equilibrium, the point of bifurcation occurring at the critical load, which is characterized by the existence of a fundamental state of equilibrium. A detailed treatment of such problems is given in Chapter 3.

The problems dealing with predicting post-buckling behavior or those characterized by initial imperfections extend to the next level in the hierarchy of geometric nonlinearity. The investigation of post-buckling behavior requires higher order approximations, which, unlike the linear eigenvalue problem, depend on the type of singularity occurring at the critical load. In a similar manner, the presence of geometric imperfections will introduce nonlinearity, but of a different nature when compared to the linear analysis, since the load-deflection relationships are no longer based on the initial geometry. The critical load for an imperfect system is characterized by the load for which the deflections increase indefinitely. Further higher levels in the hierarchy of nonlinearity include problems with large rotations and axial strains as in snap-through type instability problems arising in arches.

4.2 SOLUTION TECHNIQUES

The solution techniques for nonlinear problems are fundamentally the same despite the sources of nonlinearities. A variety of solution procedures utilizing the finite element concept and its applications have been employed extensively in recent years. Basically, most of the numerical procedures fall into two broad classes: namely, incremental and iterative methods. The incremental methods do not necessarily satisfy equilibrium conditions, whereas the iterative methods tend to stay on the true equilibrium path at all steps of the computation.

The procedures are described by considering the nonlinear equilibrium equations of the complete system

$$[K]\{\delta\} = \{F\} \tag{4.1}$$

The nonlinearity occurs in the stiffness matrix [K] which itself is a function of the load {F} and displacement {δ}. In the following, the fundamental principles in the two solution techniques are presented.

Incremental Methods

The application of the piecewise linear incremental procedure to the finite element analysis of nonlinear structural behavior was first proposed by Turner et al[81]. In this method nonlinear behavior is determined by solving a sequence of linear problems. The load is applied as a sequence of sufficiently small increments so that during the application of each increment the structure is assumed to respond linearly; consequently, the equations become linear. For each load increment, the corresponding increment of displacement is computed; it is accumulated to give the total displacement at any stage of loading. A subsequent increment of load is applied and the incremental process is continued until the desired number of load increments has been completed. The solution procedure takes the following form,

$$\left[[K] + [K_I]\right]_{i-1} \{\dot{\delta}\}_i = \{\dot{F}\}_i \tag{4.2}$$

where $[K]$ = linear stiffness matrix

$[K_I]$ = incremental stiffness matrix at load step (i-1)

$\{\dot{\delta}\}$ = incremental displacement

$\{\dot{F}\}$ = incremental load

Essentially, the incremental procedure solves a sequence of linear problems where the stiffness properties are recomputed based on the current geometry prior to each load increment. This process is basically the Euler-Cauchy integration scheme applied to Eq. 4.1 with the load $\{F\}$ playing the role of the dependent parameter. The method is schematically indicated in Fig. 4.1.

One of the principal advantages of the incremental method is its complete generality and simplicity in application to many types of problems with nonlinear behavior. In addition, it provides a relatively complete description of the load-displacement behavior. Nevertheless, the method has the disadvantage that a real estimate of the solution accuracy is not possible since, in general, equilibrium is not satisfied at any given load level. In some situations, the incremental method may lead to a deviation from the true load-displacement relationship especially in the neighborhood of instability conditions.

In order to reduce the deviation from the true behavior, an effect which is prominent with Euler type integration schemes, more accurate schemes such as the Runga-Kutta method may be used. The addition of a corrective term to the incremental method, for instance, which requires only insignificant computational effort, has been demonstrated by Haisler et al.[82] to increase the accuracy considerably. This procedure includes a load vector representing the out-of-balance force $\{F_R\}$ determined from equilibrium considerations. Consequently, the self-correcting incremental procedure becomes

$$\Big[[K] + [K_I]\Big]_{i-1} \{\dot{\delta}\}_i = \{\dot{F}\}_i + \{F_R\} \tag{4.3}$$

Iterative Methods

The iterative approach is one of the oldest procedures used by many investigators for solving systems of nonlinear algebraic equations. In this procedure a sequence of linearized equations is solved to obtain an improved solution by starting with an initial estimate to the displacement solution. This improved solution is back-substituted into the equations and the process is repeated until an acceptable convergence measured by a prescribed tolerance is obtained. For the nonlinear equilibrium equations given by Eq. 4.1 the iterative procedure consists of successive corrections to the solution until equilibrium condition under the total load $\{F\}$ is satisfied. The success of iterative methods, in general, depend estimates of the displacements.

To obtain rapid convergence for problems exhibiting high nonlinearities, many investigators have utilized the Newton-Raphson iterative approach. This method is accurate and converges rapidly, whenever a realistic initial estimate of the solution is made, and is considered as one of the most reliable[82]. Based upon an initial estimate of the displacement $\{\delta\}_i$ at a given load $\{F\}$ in Eq. 4.1, and using a first-order Taylor series expansion corresponding to $\{\delta + \dot{\delta}\}_i$ a linear incremental relationship is established

$$\Big[[K] + [K_I]\Big]_i \{\dot{\delta}\}_i = \{\dot{F}\}_i \qquad (4.4)$$

An increment to the displacements $\{\dot{\delta}\}_i$ is computed during the i th cycle of iteration; it is added to the approximate displacement $\{\delta\}_i$ to obtain a more nearly correct $(i + 1)$th approximate solution, thus

$$\{\delta\}_{i+1} = \{\delta\}_i + \{\dot{\delta}\}_i \tag{4.5}$$

This new solution $\{\delta\}_{i+1}$ is then substituted into Eq. 4.4 to obtain a further correction by utilizing the tangent stiffness at the end of the previous iterative step. This process is repeated until the increments of displacements $\{\dot{\delta}\}_i$ become sufficiently null. The method is described schematically in Fig. 4.2(a).

The Newton-Raphson method requires updating and subsequently inverting the stiffness matrix at each cycle. This process may become lengthy in particular for larger systems of equations. In such situations, it may be advantageous to employ the modified Newton-Raphson procedure[45,82]. In this method the stiffness matrix is held constant for several iterations or load increments after which the stiffness matrix is updated based on the current displacements. Obviously, the procedure necessitates a greater number of iterations; however, it guarantees a substantial saving of computations as it does not require an inversion of the matrix at each cycle. A schematic representation of the method is shown in Fig. 4.2(b).

4.3 GEOMETRIC NONLINEARITY

This section deals with the general instability problems of beam-columns in which the displacements are large but the engineering strains remain 'small'. Geometric nonlinearities enter the finite element formulation as a result of nonlinear strain-displacement relationships, which consist of strain products of the same order of magnitude as the engineering strains, and also from the effect of large displacements on the equilibruim equations.

A formulation that takes into account geometric nonlinearities can be used to study the response of imperfect structures as well as the post-critical behavior of perfect structures. In general, actual structural systems are never built precisely as planned and thus inevitably contain small imperfections associated with geometric errors. These imperfections can change the response of the system.

The nonlinear response of a structure is obtained by utilizing linearized incremental methods[44]. The resulting incremental equilibrium equation may be written in the form

$$\Big[[K_E] + [K_G]\Big]_{i-1} \{\dot{\delta}\}_i = \{\dot{F}\}_i \tag{4.6}$$

where $[K_E]$ is the conventional linear stiffness matrix and $[K_G]$ is the geometric stiffness matrix. The subscript (i-1) indicates the stiffness matrices are evaluated for the state of displacement at the beginning of the increment. At each load increment the local displacement vector, the overall stiffness matrix and load vector are related to those in the global system by the transformations

$$\{\delta_g\} = [T]^T \{\delta_\ell\} \tag{4.7}$$

$$[K_g] = [T]^T [K_\ell] [T] \tag{4.8}$$

$$\{F_g\} = [T]^T \{F_\ell\} \tag{4.9}$$

The subscripts ℓ and g represent the local and global systems, repsectively. In incremental formulations, the direction cosines in the transformation matrix [T] become also functions of the current displacement state in addition to the initial geometry. Thus, the transformation matrix [T] is modified at each load increment. The load {F}, which is the scalar multiplier of the geometric stiffness matrix $[K_G]$, is also evaluated at the beginning of each load increment.

In the iterative method, a load increment $\{\dot{F}\}$ is applied to the structure and the resulting displacements are used to revise the new configuration of the structure. At each cycle of iteration, the new geometry is used to recompute the stiffness matrix and the load vector by using a linear analyses. The solution procedure takes the following form

$$[K]_{i-1} \{\dot{\delta}\}_i = [\dot{F}]_{i-1} \tag{4.10}$$

where $\{\dot{F}\}_{i-1} = [T]^T_{i-1} \{F_\ell\}$

$$[K]_{i-1} = [T]^T_{i-1} \left[[K_E] + [K_G] \right]_\ell [T]_{i-1}$$

4.4 <u>MATERIAL NONLINEARITY</u>

The stiffness matrix for problems of material nonlinearity is computed from the relationship given by Eq. 2.16

$$[k] = [T]^T [H]^{-1} [T] \tag{2.16}$$

$$\text{where } [H] = \int_V [P] [D_{ep}] [P] \, dV$$

The matrix $[D_{ep}]$, which describes the material behavior under multiaxial stress, is now a variable and depends not only on the state of stresses but also upon the history of loading. The constitutive relationship for an inelastic material can be expressed in terms of finite increments

$$\{\dot{\sigma}\} = [D_{ep}] \{\dot{\epsilon}\} \tag{4.11}$$

The matrix $[D_{ep}]$ is modified by updating the components of the matrix according to the deformation laws of plasticity. For metallic structures, in general, idealization of the material by a Prandtl-Ruess material obeying the von Mises yield criterion is universally used.

Two general methods, which are based on essentially different concepts, have been developed for inelastic analysis of solid bodies. These are the method of "initial strain" and the method of "tangent modulus".(78)

The initial strain method is based on the idea of modifying the equations of equilibrium so that completely elastic behavior may be assumed. This approach introduces modifications to compensate for the fact that the inelastic strains do not cause any change in the stresses. Details on the development of the method are found in Ref. 80.

The tangent modulus method is based on the linearity of the incremental laws of plasticity and approaches the problem in a piece-wise linear fashion. As the load is applied in increments, a new set of coefficients is obtained for the equilibrium equations. This approach is used now more extensively among many investigators due to its consistency with the classical methods of plasticity analysis and also due to its computational efficiency. In Ref. 79 the use of this method is described in detail.

In this study further investigation on the material nonlinearity aspect is not made. The problem of material nonlinearity in beam-columns is identical to those problems of solid mechanics or plates and shells. Substantial information is available in the literature on the application of finite elements to problems of material non-linearity.(16,17,78,79,80)

4.5 SAMPLE PROBLEMS AND RESULTS

The first numerical example to illustrate the validity of the procedure described is that of a cantilever column with an initial out-of-straightness δ_o at the free end. The out-of-straightness along the length of the column is assumed to be expressed by

$$\delta_x = \delta_o \ (1 - \cos\pi \ x/L) \tag{4.12}$$

For this column the analytical solution for the complete load-displacement relationship is given in Ref. 53. In the application of the finite method, the direct incremental procedure is used in evaluating the load-displacement relationship. The effect of the number of load increments in the final solution is shown in Fig. 4.3 when using the direct incremental procedure. It is observed that the results agree closely to the analytical solution as the load increments become small.

In Fig. 4.4 a set of load-displacement relationships is shown for the same column for different values of δ_o ranging from L/500 to L/5000. The results indicate fairly close correlation to the analytical solutions. In Fig. 4.5 the finite element and analytical solutions are compared when the column is bent excessively to large displacements having the order of magnitude of the length of the column.

5. CONCLUSIONS AND RECOMMENDATIONS FOR FUTURE DEVELOPMENTS

The principal objective of this study is to develop a finite element formulation for the analysis of beam-columns and to demonstrate the applicability of the method to general beam-column problems as a practical tool. In the formulation of the finite element model, the beam column is regarded as a one-dimensional body.

The contributions achieved in this dissertation are:

- A one-dimensional finite element model is developed to analyze general linear static beam-column problems.
- A systematic procedure is presented to evaluate geometric stiffness matrices for beam-columns which are required to perform a finite element analysis of stability problems.
- The geometric stiffness matrices are derived which correspond to large lateral and torsional displacements.
- The advantages of the finite element method are demonstrated in the solution of a few stability problems, such as the buckling of pretwisted columns and the lateral buckling of tapered beams, the analytical solutions of which are not yet available.

The study has served in demonstrating the use of the finite element method in conducting linear static, linear stability and non-linear analyses of beam-columns. Furthermore, the advantages of the method are demonstrated in solving a wide variety of problems having irregularities in geometry, loading and support conditions which defy adequate treatment by the classical means.

In the linear static analysis, a one-dimensional finite element model is developed by making use of variational principles. The evaluation of the element properties is performed by developing a formulation based on a functional constituting of two independent fields: a polynomial approximation of the strain field in the domain, and displacements at the boundary. The beam element has two nodes with seven degrees-of-freedom at each node: three linear displacements, three rotations about the cartesian system, and a warping displacement. The formulation has an advantage when compared to previous work in that the required manipulation to evaluate the element properties is simple especially when additional kinematical assumptions are introduced such as shearing deformations due to bending and warping. Reviews of the derivation process disclose a complete sequence of numerical integration and matrix operations which can be operated in a systematic manner.

In the linear stability analysis, a systematic procedure is developed to evaluate the so-called geometric stiffness matrices for beam-columns by making use of the nonlinear strain-displacement relationships. The model developed is used in deriving the geometric stiffness matrices for beam-columns when the displacements are large in axial and transverse directions and also in twist. The use of these matrices is demonstrated in solving a variety of stability problems through a direct eigenvalue determination. The examples are selected such that each has a differing feature from the finite element standpoint. The types of examples include: columns with distributed axial loads, tapered columns, columns on elastic foundations, pretwisted columns, space frames and lateral-stability problems. In all cases, a remarkable convergence is observed and satisfactory accuracy is obtained by using relatively few elements. Moreover, the required computational effort is found to be minimal.

In nonlinear analysis of beam columns, the use of geometric stiffness matrices is found to play an important role in determining nonlinear responses of structures. The use of the direct incremental method is demonstrated on a few numerical examples whose analytical solutions are available. For beam-columns with geometric nonlinearity, it is found that the direct incremental method furnishes satisfactory results, especially when the load increments are small. In addition, the method is straightforward and requires very little computational effort.

While the applications presented in this study are very simple the finite element method enables the study of complex and practical problems. The method derived here should find applications in linear static and linear stability analyses of novel structures. The stability analysis, in particular, should find immediate application to ordinary structural problems such as space frames. Other applications of the method include performing optimization studies on the strength of structural members such as tapered columns and piecewise prismatic members.

For a more general application of the method, the formulation should be extended to enable analysis of thin-walled closed beams, multi-cellular beams, curved beams and the like.

Finally, extension of the method to include material non-linearity will encourage studies on a wider variety of practical problems. Among the many possible applications, the validity of some of the universally accepted assumptions used in inelastic analysis of beam-columns can be investigated. For instance, the universally accepted assumption that the shear response is always elastic for an inelastic beam-column is but one of the many possible items for investigation. Other problems of interest are related to the investigation of structures under repeated loading, cyclic loading and shake-down.

6. APPENDICES

APPENDIX I

ELASTIC STIFFNESS MATRIX FOR THE BEAM ELEMENT

The linear elastic stiffness matrix for a straight beam element of uniform cross section is now presented. A cartesian reference axes system is used which coincides with the centroidal-principal axes of the cross section. The element is represented by two nodes with seven degrees of freedom at each node; three linear displacements, three rotations about the reference axes and a set of warping displacements. The stiffness matrix is derived based on the formulation given in Section 2.3 which take into account the shearing deformations due to flexural and torsional-warping loadings. In the stiffness matrix given below the following expressions are used:

$$\Psi = 1 + \frac{\alpha^2 L^2}{12}\left[\frac{1}{5} + (1 + 1.5\ \Phi_z)^2\right] \tag{A1.1}$$

$$\Lambda = \left[1 + \frac{\alpha^2 L^2}{60}\right] \tag{A1.2}$$

$$\Omega = 3 + (1 + 1.5\ \Phi_z)^2 + \frac{\alpha^2 L^2}{4}\left[\frac{1}{5} + (1 + 1.5\ \Phi_z)^2\right] \tag{A1.3}$$

$$\theta = 3 - (1 + 1.5\ \Phi_z)^2 + \frac{\alpha^2 L^2}{4}\left[\frac{1}{5} - \frac{(1+1.5\Phi_z)^2}{3}\right] \tag{A1.4}$$

where $\Phi_y = \dfrac{12EJ_z}{GA_{sy}L^2}$

$\Phi_z = \dfrac{12EJ_y}{GA_{sz}L^2}$

$\alpha = \sqrt{GK_T/EI_\omega}$

A_{sy}, A_{sz} = Effective shear area for V_y and V_z, respectively.

$$
[k] = \left[\begin{array}{cccccccccccccc}
\frac{EA}{L} & & & & & & & & & & & & & \\
 & \frac{12EJ_y}{L^3(1+\Phi_z)} & & & & & & & & & & & & \\
 & \frac{6EJ_y}{L^2(1+\Phi_z)} & \frac{(4+\Phi_z)EJ_y}{L(1+\Phi_z)} & & & & & & & & & & & \\
 & & & \frac{12EJ_z}{L^3(1+\Phi_y)} & & & & & & & & & & \\
 & & & -\frac{6EJ_z}{L^2(1+\Phi_y)} & \frac{(4+\Phi_y)EJ_z}{L(1+\Phi_y)} & & & & & & & & & \\
 & & & & & \frac{12EI_\omega\Psi}{L^3(1+1.5\Phi_z)^2} & & & & & & & & \\
 & & & & & \frac{6EI_\omega\Lambda}{L^2(1+1.5\Phi_z)^2} & \frac{EI_\omega\Omega}{L(1+1.5\Phi_z)^2} & & \text{SYMMETRIC} & & & & & \\
-\frac{EA}{L} & & & & & & & \frac{EA}{L} & & & & & & \\
 & -\frac{12EJ_y}{L^3(1+\Phi_z)} & -\frac{6EJ_y}{L^2(1+\Phi_z)} & & & & & & \frac{12EJ_y}{L^3(1+\Phi_z)} & & & & & \\
 & \frac{6EJ_y}{L^2(1+\Phi_z)} & \frac{(2-\Phi_z)EJ_y}{L(1+\Phi_z)} & & & & & & -\frac{6EJ_y}{L^2(1+\Phi_z)} & \frac{(4+\Phi_z)EJ_y}{L(1+\Phi_z)} & & & & \\
 & & & -\frac{12EJ_z}{L^3(1+\Phi_y)} & \frac{6EJ_z}{L^2(1+\Phi_y)} & & & & & & \frac{12EJ_z}{L^3(1+\Phi_y)} & & & \\
 & & & -\frac{6EJ_z}{L^2(1+\Phi_y)} & \frac{(2-\Phi_y)EJ_z}{L(1+\Phi_y)} & & & & & & \frac{6EJ_z}{L^2(1+\Phi_y)} & \frac{(4+\Phi_y)EJ_z}{L(1+\Phi_y)} & & \\
 & & & & & \frac{12EI_\omega\Psi}{L^3(1+1.5\Phi_z)^2} & \frac{6EI_\omega\Lambda}{L^2(1+1.5\Phi_z)^2} & & & & & & \frac{12EI_\omega\Psi}{L^3(1+1.5\Phi_z)^2} & \\
 & & & & & \frac{6EI_\omega\Lambda}{L^2(1+1.5\Phi_z)^2} & \frac{EI_\omega\theta}{L(1+1.5\Phi_z)^2} & & & & & & \frac{6EI_\omega\Lambda}{L^2(1+1.5\Phi_z)^2} & \frac{EI_\omega\Omega}{L(1+1.5\Phi_z)^2}
\end{array}\right]
$$

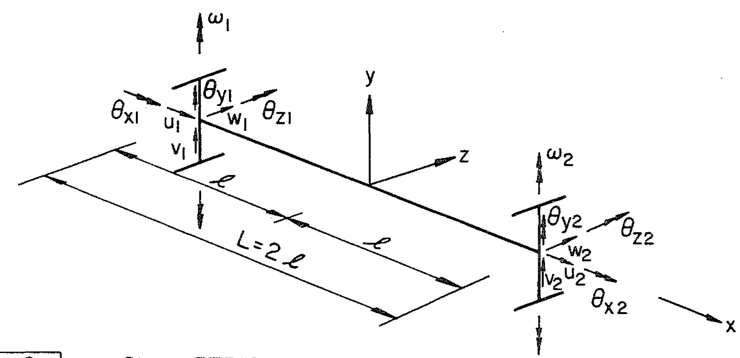

APPENDIX II

FLEXURAL STIFFNESS MATRIX OF TAPERED BEAMS

Consider a beam element with the smaller end denoted as end i and the larger as end j. The element may have uniform taper in either one or both principal axes. Gere and Carter(58) defined the depth, d_x, and the moment of inertia, I_x, at a distance x from end i of the member as

$$d_x = d_i \left[1 + \left(\frac{d_j}{d_i} - 1\right) \frac{x}{L}\right] \tag{A2.1}$$

$$I_x = I_i \left[1 + \left(\frac{d_j}{d_i} - 1\right) \frac{x}{L}\right]^{\alpha} \tag{A2.2}$$

in which α refers to the shape factor that depends upon the shape of the cross section and may be obtained from

$$\alpha = \frac{\log_e (I_j/I_i)}{\log_e (d_j/d_i)} \tag{A2.3}$$

The values of α for various types of cross sections are found in Ref. 59.

Once all values of α are known for various sectional properties, such as cross-sectional area and moments of interia, the flexibility matrix may be determined by the matrix integration

$$[f_{jj}] = \int_L [T_{xj}]^T [U_x] [T_{xj}] \, dx \tag{A2.4}$$

where $[T_{xj}]$ = translational matrix from j to x

$[U_x]$ = the basic sectional property matrix which are defined as

$$[T_{xj}] = \begin{bmatrix} 1 & 0 & 0 & 0 & 0 \\ 0 & 1 & 0 & 0 & 0 \\ 0 & 0 & 1 & 0 & 0 \\ 0 & 0 & -(L-x) & 1 & 0 \\ 0 & (L-x) & 0 & 0 & 1 \end{bmatrix}$$

and

$$[U_x] = \begin{bmatrix} \frac{1}{EA_{xx}} & 0 & 0 & 0 & 0 \\ 0 & \frac{1}{GA_{yx}} & 0 & 0 & 0 \\ 0 & 0 & \frac{1}{GA_{zx}} & 0 & 0 \\ 0 & 0 & 0 & \frac{1}{EI_{yx}} & 0 \\ 0 & 0 & 0 & 0 & \frac{1}{EI_{zx}} \end{bmatrix}$$

The flexibility matrix is determined by performing the integration of Eq. A2.4 over the length of the beam[59],

$$[f_{jj}] = \begin{bmatrix} \frac{\beta_1 L}{EA_{xi}} & 0 & 0 & 0 & 0 \\ 0 & \left(\frac{\beta_3 L^3}{3EI_{zi}} + \frac{\beta_1 L}{GA_{yi}}\right) & 0 & 0 & \frac{\beta_2 L^2}{2EI_{zi}} \\ 0 & 0 & \left(\frac{\beta_3 L^3}{3EI_{yi}} + \frac{\beta_1 L}{GA_{zi}}\right) & -\frac{\beta_2 L^2}{2EI_{yi}} & 0 \\ 0 & 0 & -\frac{\beta_2 L^2}{2EI_{yi}} & \frac{\beta_1 L}{EI_{yi}} & 0 \\ 0 & \frac{\beta_2 L^2}{2EI_{zi}} & 0 & 0 & \frac{\beta_1 L}{EI_{zi}} \end{bmatrix} \qquad (A2.5)$$

The values of β_1, β_2 and β_3 are given in Ref. 59 for various types of cross sections.

Finally, the stiffness submatrix is determined from

$$[k_{jj}] = [f_{jj}]^{-1} \tag{A2.6}$$

the other stiffness matrices are found through the use of equilibrium equations[19] and symmetry considerations as follows.

$$[k_{ij}] = - [T_{ij}] [k_{ji}]$$

$$[k_{ji}] = [k_{ij}]^T \tag{A2.7}$$

and

$$[k_{ii}] = - [T_{ij}] [k_{jj}] [T_{ij}]^T$$

Or, the element stiffness matrix may be determined in a simple operation from

$$[k] = [N]^T [f_{jj}]^{-1} [N] \tag{A2.8}$$

where $[N] = [T, I]$, $[I]$ = identity matrix.

APPENDIX III

CONSISTENT STIFFNESS MATRIX FOR BEAMS ON ELASTIC FOUNDATION

Consider a beam element on a Winkler-type elastic foundation with spring constant (foundation modulus) k over the length of the element. For a consistent formulation, the deformation of the foundation must be identical to that of the beam it supports. Accordingly, the displacement field for the foundation is expressed as a polynomial of the third order which is written in matrix notation, as

$$\{u\} = [P]\ \{\alpha\}$$

$$y = [1 \quad x \quad x^2 \quad x^3] \begin{Bmatrix} \alpha_1 \\ \alpha_2 \\ \alpha_3 \\ \alpha_4 \end{Bmatrix} \tag{A3.1}$$

The displacement, y, can be either lateral or torsional, depending on whether the foundation is represented by lateral or torsional springs. The vector $\{\alpha\}$ consists of the coefficients which are to be determined in terms of the nodal displacements $\{\delta\}$ from

$$\{\delta\} = [C]\ \{\alpha\} \tag{A3.2}$$

Using the principle of vietual work, the total external work is written as

$$W_{ext} = \{\delta\}^T\ \{F\} \tag{A3.3}$$

where $\{F\}$ is the vector of nodal forces. The total internal work is

$$W_{int} = \int_L \{u\}^T\ [k]\ \{u\}\ dx \tag{A3.4}$$

Assuming a homogeneous foundation modulus over the element length, the total internal work is expressed in terms of the nodal displacements

$$W_{int} = k \{\delta\}^T [C^{-1}]^T \left(\int_L [P]^T [P]\, dx\right) [C^{-1}] \{\delta\} \tag{A3.5}$$

Comparison of Eq. A3.4 and Eq. A3.5 yields

$$[k_F] = k [C^{-1}]^T \left(\int_L [P]^T [P]\, dx\right) [C^{-1}] \tag{A3.6}$$

Substituting the values of $[C^{-1}]$ and $[P]$ and integrating over the length L furnishes the consistent stiffness matrix as follows

$$[k_F] = \frac{kL}{420} \begin{bmatrix} 156 & & & \\ 22L & 4L^2 & \text{SYMMETRIC} & \\ 54 & 13L & 156 & \\ -13L & -3L^2 & -22L & 4L^2 \end{bmatrix} \tag{A3.7}$$

APPENDIX IV

FLEXURAL STIFFNESS MATRIX OF PRETWISTED BEAMS

Consider a uniform beam element of length L with natural twist about the centroidal axis which varies linearly with the axial coordinate x. The element has a total angle of pretwist α. Let the end at x = 0 be denoted as end i and the other as end j. At distance x from end i, the angle of pretwist about the centroid line α_x is defined as

$$\alpha_x = \alpha_i + \frac{x}{L}\,\alpha_j \tag{A4.1}$$

By assigning $\alpha_i = 0$ and $\alpha_j = \alpha_o$, the y and z axes become aligned with the principal axes of the cross section at x = 0. The flexural stiffnesses about the minor and major principal axes of the beam cross section are EI_1, and EI_2, respectively, and are independent of x.

A direct evaluation of the stiffness matrix for a pretwisted beam, in the manner performed for the case of a prismatic beam (Section 2.3) is difficult and is not attempted here. Nevertheless, the determination is simplified by evaluating the flexibility matrix first, such as by utilizing previous investigations which have dealt with establishing the governing differential equations for pretwisted beams.

The equations governing displacements of pretwisted beams due to terminal loads are found in Refs. 83 and 84. For matrix applications, these governing equations are separated and integrated[85] to establish explicit displacement functions describing the transverse displacements and rotations of the beam about the y and z axes. The flexibility matrix is found by imposing the displacement boundary conditions at end j where unit terminal loads are assigned, thus,

$$[f_{ij}] = \frac{L^3}{EI_1 EI_2} \begin{bmatrix} f_{11} & & \text{SYMMETRIC} & \\ f_{21} & f_{22} & & \\ f_{31} & f_{32} & f_{33} & \\ f_{41} & f_{42} & f_{43} & f_{44} \end{bmatrix} \tag{A4.2}$$

where

$$f_{11} = \frac{1}{6}(EI_1 + EI_2) - (EI_2 - EI_1)(\alpha - \sin\alpha)/\alpha^3$$

$$f_{21} = \frac{1}{2}(EI_2 - EI_1)[2(1 - \cos\alpha)/\alpha^3 - 1/\alpha]$$

$$f_{22} = \frac{1}{6}(EI_1 + EI_2) + (EI_2 - EI_1)(\alpha - \sin\alpha)/\alpha^3$$

$$f_{32} = -\frac{1}{4L}[EI_1 + EI_2 + 2(EI_2 - EI_1)(1 - \cos\alpha)/\alpha^2]$$

$$f_{33} = \frac{1}{2L^2}[EI_1 + EI_2 + (EI_2 - EI_1)(\sin\alpha)/\alpha]$$

$$f_{41} = \frac{1}{4L}[EI_1 + EI_2 - 2(EI_2 - EI_1)(1 - \cos\alpha)/\alpha^2]$$

$$f_{42} = -\frac{1}{2L}(EI_2 - EI_1)(\alpha - \sin\alpha)/\alpha^2$$

$$f_{43} = \frac{1}{2L^2}(EI_2 - EI_1)(1 - \cos\alpha)/\alpha$$

$$f_{44} = \frac{1}{2L^2}[EI_1 + EI_2 - (EI_2 - EI_1)(\sin\alpha)/\alpha]$$

Once the flexibility matrix is determined, the evaluation of the stiffness matrix is accomplished following the same procedure of matrix operations described in Appendix II, thus

$$[k] = [N]^T [f_{jj}]^{-1} [N] \tag{A4.3}$$

where

$$[N] = [T, I], \ [I] = \text{identity matrix.}$$

7. NOTATIONS

A	= cross sectional area
$[C]$	= displacement transformation matrix
$D,[D]$	= generalized Hookean constant
E	= Young's modulus of elasticity
$\overline{F}$	= body force
$\{F\},\{F'\},\{\overline{F}\}$	= load vector of assembled system
$\{\dot{F}\}$	= incremental load vector
G	= shearing modulus
$[H]$	= stiffness matrix in terms of generalized displacement amplitude
I,I_B,I_T	= moment of inertia
I_o	= moment of inertia about the shear center
I_ω	= warping moment of inertia
J_y,J_z	= moment of inertia about the y and z axes, respectively
$[J]$	= inertia matrix
K_T	= St. Venant torsional constant
$[K]$	= assembled (master) stiffness matrix
$[K_E]$	= linear stiffness matrix
$[K_G]$	= geometric stiffness matrix
$[K_I]$	= incremental stiffness matrix
L	= length of beam element, column length
$[L]$	= displacement interpolating function matrix
M	= bending moment
M_{cr}	= critical moment
M_T	= total torque

$(M_x)_{CR}$	= critical torque
M_ω	= bimoment
N	= number of elements
[N]	= shape function
P	= axial thrust
P_{CR}	= axial critical load
P_E	= Euler load
[P]	= polynomial functions of coordinates
$[Q],[Q_L]$	= polynomial functions of generalized displacement amplitudes
[R]	= suface coordinates of tractions
S,S_σ,S_u	= surface area and portions of boundaries
$\bar{T}$	= traction on boundary S_σ
$[T],[T_r]$	= transformation matrices
U	= strain energy
$[U_x]$	= basic sectional property matrix
V	= volume
V_y,V_z	= shear force in y and z directions, respectively
W	= work or energy
a	= distance from rotation axis to shear center
$\bar{a}$	= point of load application from shear center
d	= depth of beam
e	= Lagrangian strain tensor
{f}	= element load vector
h	= frame height

k	=	foundation modulus, cross sectional parameter
$[k]$	=	element stiffness matrix
n	=	directional vector
p	=	traction on boundary S
q_o, q	=	intensity of distributed load
r	=	distance from axis of twist
u	=	displacement in x-direction
$\bar{u}$	=	displacement on boundary S_u
$\tilde{u}$	=	interelement boundary displacement
v	=	displacement in y-direction
w	=	displacement in z-direction
x,y,z	=	reference axes
Γ	=	cross sectional parameter
$\{\Delta\}$	=	displacement vector of complete system
Λ	=	cross sectional property
$\Phi_y, \Phi_z, \Phi_\omega$	=	cross sectional property
Ψ	=	cross sectional property
Ω	=	cross section property
α	=	angle between pins, angle of pretwist
$\{\alpha\}, \{\tilde{\alpha}\}$	=	generalized displacement amplitudes
$[\alpha]$	=	shear coefficient matrix
β	=	critical load parameter
$\{\beta\}$	=	strain coefficients
γ	=	average shearing strain

δ	= variational convention
$\{\delta\},\{\bar{\delta}\}$	= element displacement
$\{\dot{\delta}\}$	= incremental displacement
$\{\epsilon\}$	= strain field
$\{\epsilon_o\}$	= linear strain
$\{\epsilon_L\}$	= nonlinear strain
η	= ratio of moment of inertia
θ,θ_y,θ_z	= rotational displacements
κ	= cross sectional parameter
λ	= instability factor or eigenvalue, frame parameter
ξ	= nondimensionalized length
π,π_ω	= functional or objective function
ρ	= radial distance of component plate from shear center
σ	= stress
$\{\sigma\},\{\sigma_o\}$	= stress field
φ	= shear strain function, angle of twist
χ	= shear strain function
ψ	= cross sectional property
ω	= warping displacement

8. TABLES AND FIGURES

TABLE 1 CRITICAL LOADS OF COLUMNS WITH DISTRIBUTED AXIAL LOADS(*)

A. When the end loads (P) are prescribed:

$\frac{P}{P_E}$	Q_{CR}/P_E			
	Case 1	Case 2	Case 3	Case 4
-2.0	5.1875	6.6611	8.5779	5.2296
-1.0	3.5931	4.7505	6.0030	3.6146
-0.5	2.7565	3.7088	4.6199	2.7694
0.0	1.8846	2.5849	3.1633	1.8909
0.2	1.5242	2.1072	2.5584	1.5285
0.5	0.9692	1.3553	1.6257	0.9712
0.8	0.3949	0.5561	0.6613	0.3956
1.0	0.0000	0.0000	0.0000	0.0000

B. When the distributed loads ($Q = q_w$) are prescribed:

$\frac{Q}{P_E}$	P_{CR}/P_E			
	Case 1	Case 2	Case 3	Case 4
-2.0	1.9351	1.6471	1.5786	1.9391
-3.0	2.3564	1.9405	1.8542	2.3653
-4.0	2.7502	2.2171	2.1214	2.7664

(*) Refer to Fig. 3.7 for identification of cases

TABLE 2 CRITICAL LOADS OF UNIFORMLY TAPERED COLUMNS(*)

Boundary condition: Free at top

Fixed at bottom

$$P_{CR} = \beta \, (EI_T/L^2)$$

Values of β:

$\eta = \dfrac{I_T}{I_B}$	Timoshenko Solution(53)	Finite Element Solution (N = No. of Elements)		
		N = 2	N = 4	N = 10
0.1	1.202	1.0906	1.1740	1.1985
0.2	1.505	1.1409	1.4818	1.5014
0.3	1.710	1.6309	1.6906	1.7071
0.4	1.870	0.8036	1.8535	1.8672
0.5	2.002	1.9482	1.9890	2.0002
0.6	2.116	2.0740	2.1060	2.1149
0.7	2.217	2.1861	2.2097	2.2163
0.8	2.308	2.2879	2.3032	2.3075
0.9	2.391	2.3816	2.3886	2.3907
1.0	2.467	2.4687	2.4675	2.4674
2.0		3.1328	3.0502	3.0286
4.0		4.0098	3.7658	3.7025
10.0		5.6887	4.9892	4.8071
20.0		7.5899	6.2088	5.8447
40.0		10.3745	7.7947	7.1029
100.0		16.3334	10.7359	9.2046

(*) Compare with Figs. 3.9 and 3.10.

TABLE 3 CRITICAL LOADS OF TWO-COMPONENT COLUMNS(*)

$P_{CR} = \beta P_E$ where P_E = Euler load for a prismatic column

α = angle of offset

Values of the factor β:

A. Columns with spherical pins

$\eta = I_1/I_2$	$\alpha = 0^o$	30^o	60^o	75^o	90^o
2	1.0000	1.0315	1.1280	1.2037	1.2994
4	1.0000	1.0452	1.1917	1.3146	1.4810
10	1.0000	1.0530	1.2292	1.3818	1.5947
20	1.0000	1.0555	1.2415	1.4042	1.6327
30	1.0000	1.0563	1.2456	1.4116	1.6453
50	1.0000	1.0570	1.2489	1.4175	1.6554
1000	1.0000	1.0580	1.2536	1.4298	1.6697

B. Columns with fixed ends

$\eta = I_1/I_2$	$\alpha = 15^o$	30^o	45^o	60^o	75^o	90^o
2	1.0116	1.0446	1.0901	1.1524	1.2298	1.3209
4	1.0152	1.0854	1.1790	1.3029	1.4468	1.6091
10	1.0456	1.1822	1.3984	1.6620	1.9429	2.1876
20	1.0965	1.3536	1.7461	2.2240	2.6740	2.9509
50	1.2238	1.8438	3.2228	3.5044	3.6792	3.7818
100	1.4352	2.6498	3.5864	3.7836	3.8884	3.9483
1000	3.6315	3.9380	4.0037	4.0273	4.0388	4.0442

(*) Compare with Figs. 3.14 and 3.15.

TABLE 4 CRITICAL LOADS OF PIECEWISE PRISMATIC COLUMNS(*)

$$P_{CR} = \gamma P_E \text{ where } P_E = \text{Euler Load}$$

M = Number of segments

$\alpha = 90^\circ$

Values of the factor γ:

A. Pinned columns

$\eta = I_1/I_2$	M = 2	M = 4
2	1.3121	1.3243
5	1.5428	1.6210
10	1.6246	1.7447
15	1.6520	1.7892
20	1.6658	1.8121
30	1.6796	1.8355

B. Fixed columns

$\eta = I_1/I_2$	M = 2	M = 4
2	1.3209	1.4346
5	1.7184	2.2937
10	2.1876	3.0442
15	2.5948	3.3870
20	2.9434	3.5605
30	3.4262	3.7399

(*) Compare with Figs. 3.16 and 3.17

TABLE 5 EXPERIMENT ON PRETWISTED COLUMNS

Cross Section Properties:

Shape: $2\frac{5}{8} \times 1\frac{1}{2}$ WF

B = 1.838 in.	A = 1.110 in^2
D = 2.628 in.	I_{xx} = 1.246 in^4
T = 0.202 in.	I_{yy} = 0.210 in^4
W = 0.165 in.	I_{ω} = 0.308 in^6
L = 75 in.	K_T = 0.0131 in^4

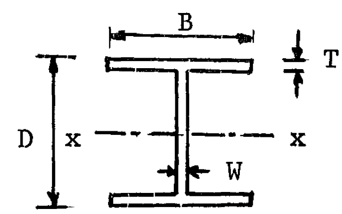

Modulus of Elasticity, E = 31,374,000 psi

Summary of Test Results:

Specimen No.	Angle of Pretwist	Failure Load (lb)	Critical Load (lb) (Southwell Plot)	P_{CR}/P_E	
				Experiment	Theory
01	0^o	7800	8403	1.00	1.00
02	90^o	20000	25500	3.04	3.14
03	180^o	14050	21212	2.52	2.54
04	360^o	10600	12800	1.52	1.71

TABLE 6 CRITICAL LOADS OF PRETWISTED COLUMNS(*)

End Conditions: Knife edge along minor axis

$P_{cr} = \beta P_E$ where P_E = Euler load for a prismatic column

α = angle of prestwist

Values of the factor β:

α	$\eta = I_1/I_2 = 1.0$	$\eta = 2.0$	$\eta = 5.0$	$\eta = 10.0$
0^o	1.0	1.0	1.0	1.0
60^o	1.5086	1.8629	2.9037	3.6967
90^o	2.0499	2.7409	3.0990	3.2178
120^o	1.5086	2.0543	2.4849	2.6436
180^o	1.0000	1.5126	2.3539	3.1961
210^o	1.1388	1.9968	3.6843	5.4572
270^o	2.0499	2.8252	3.5910	3.9160
360^o	1.0000	1.3391	1.6684	1.8129

(*) Compare with Fig. 3.22

TABLE 7 LATERAL TORSIONAL BUCKLING LOADS(*)

Beam: Simply supported, free warping at ends

Loading: Concentrated load at mid span of beam (at shear center)

$$P_{CR} = \lambda \left\{ \frac{\sqrt{EI_y \; GK_T}}{L^2} \right\}$$

Values of the factor λ

$\frac{L^2 GK_T}{EI_w}$	Timoshenko Solution[53]	Finite Element Solution	
		N = 4	N = 6
0	86.4	85.6827	86.2257
4	31.9	31.4772	31.6772
16	21.8	21.4772	21.6110
32	19.6	19.3055	19.4225
64	18.3	18.1135	18.2184
160	17.5	17.3448	17.4393
400	17.2	17.0136	17.1057

(*) Compare with Fig. 3.26

TABLE 8 SPACE FRAME BUCKLING

STRUCTURE: One-story space frame (Fig. 3.34)

SHAPE: W10x48 (all members)

DIMENSIONS: Height, $h = 20\ r_y$

Span, $L = 60\ r_y$

BOUNDARY CONDITION: Fixed at bases

Comparison of results:

Mode of Buckling	CRITICAL LOAD, P (kips)	
	Determinantal[77]	Finite Element
SWAY	11.93	11.73
TWIST	11.96	12.21

TABLE 9 BUCKLING OF SHAFTS UNDER PURE TORSION

Cross Section: $I_x = I_y$

Critical Torque, $(M_x)_{CR} = \alpha \frac{EI}{L}$

Values of α

Number of Elements	End Condition in Flexure	
	Pinned	Fixed
2	6.405	---
3	6.322	9.862
4	6.298	9.305
5	6.289	9.182
6	6.284	9.094
Analytical[55]	6.283 ($=2\pi$)	8.988

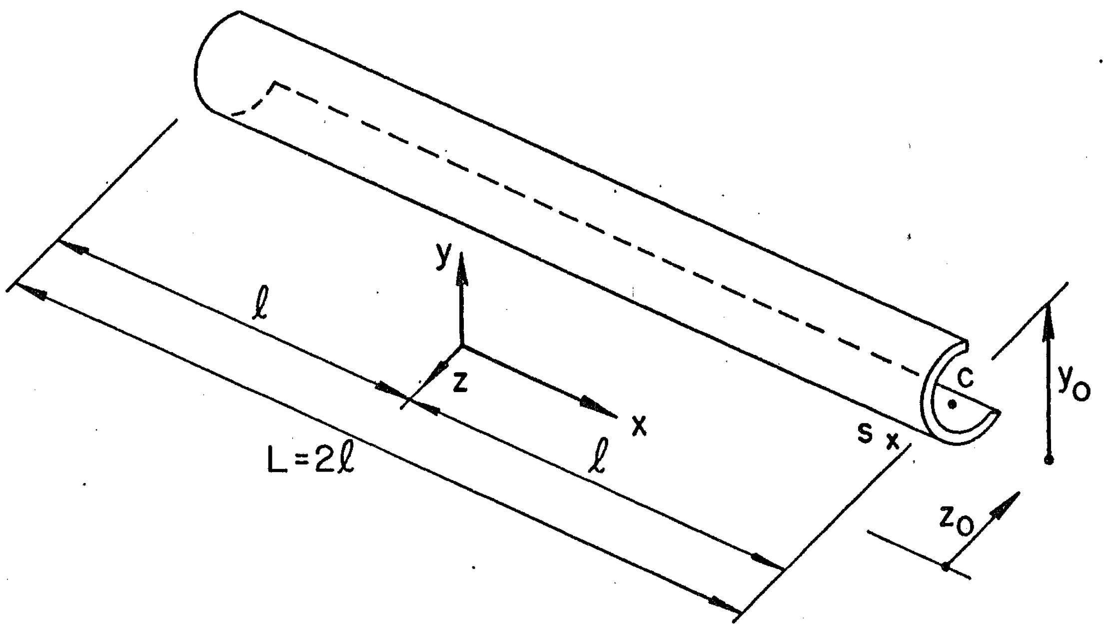

Fig. 2.1 Reference Axes System for the Beam Element

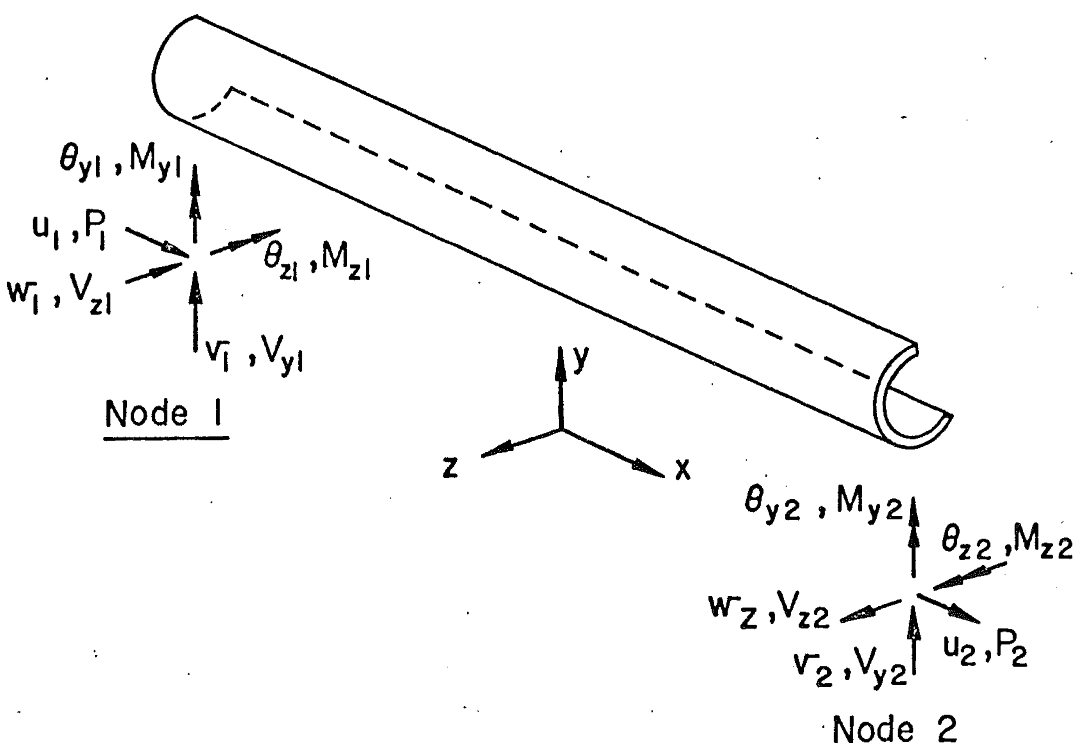

Fig. 2.2 Notations for Generalized Stresses and Displacements of the Beam Element in Flexure and Extension

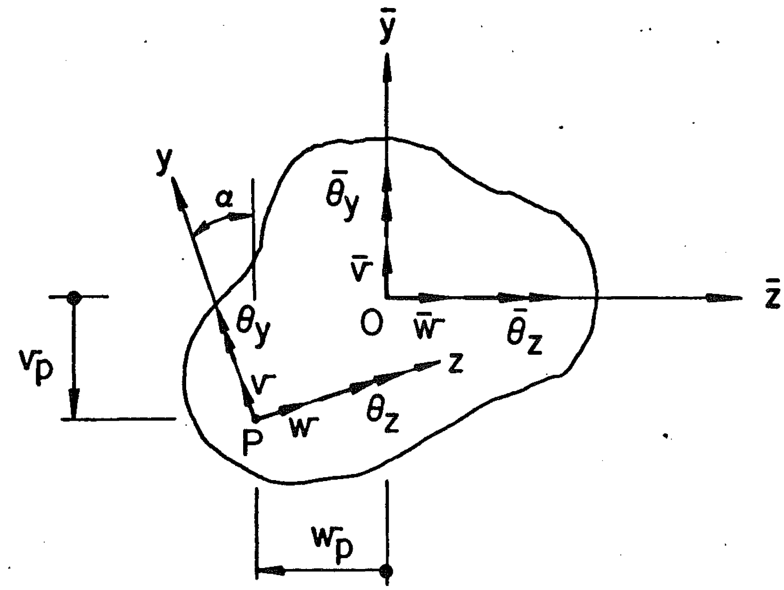

Fig. 2.3 The Centroidal-Principal Axes and the Generalized Coordinate System

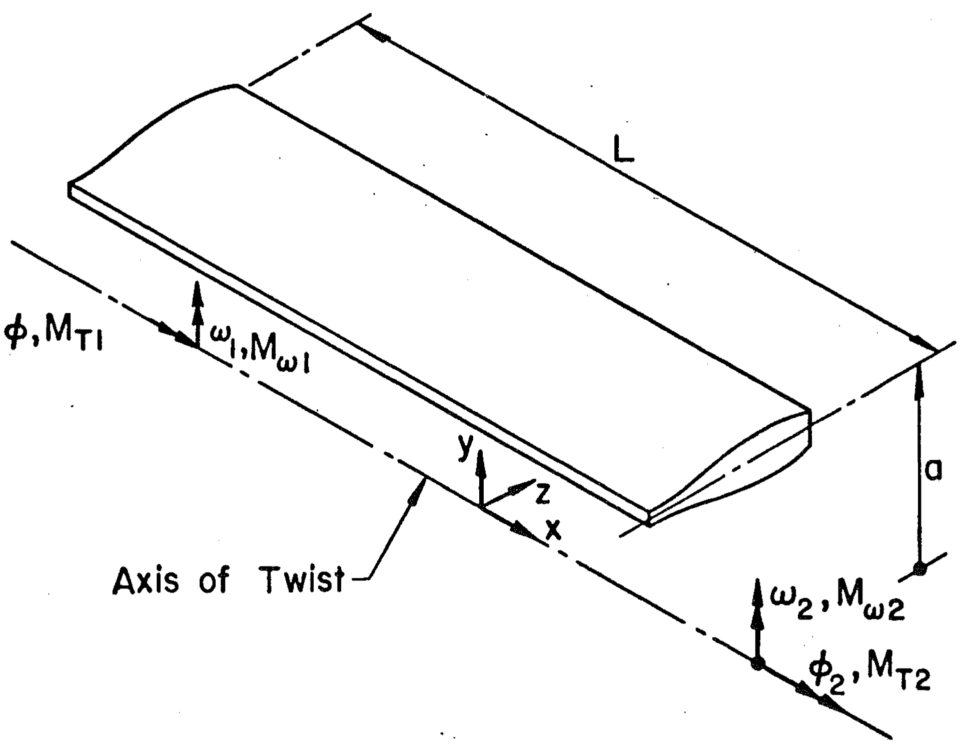

Fig. 2.4 Notations for a Beam Component Subjected to Torsion and Warping

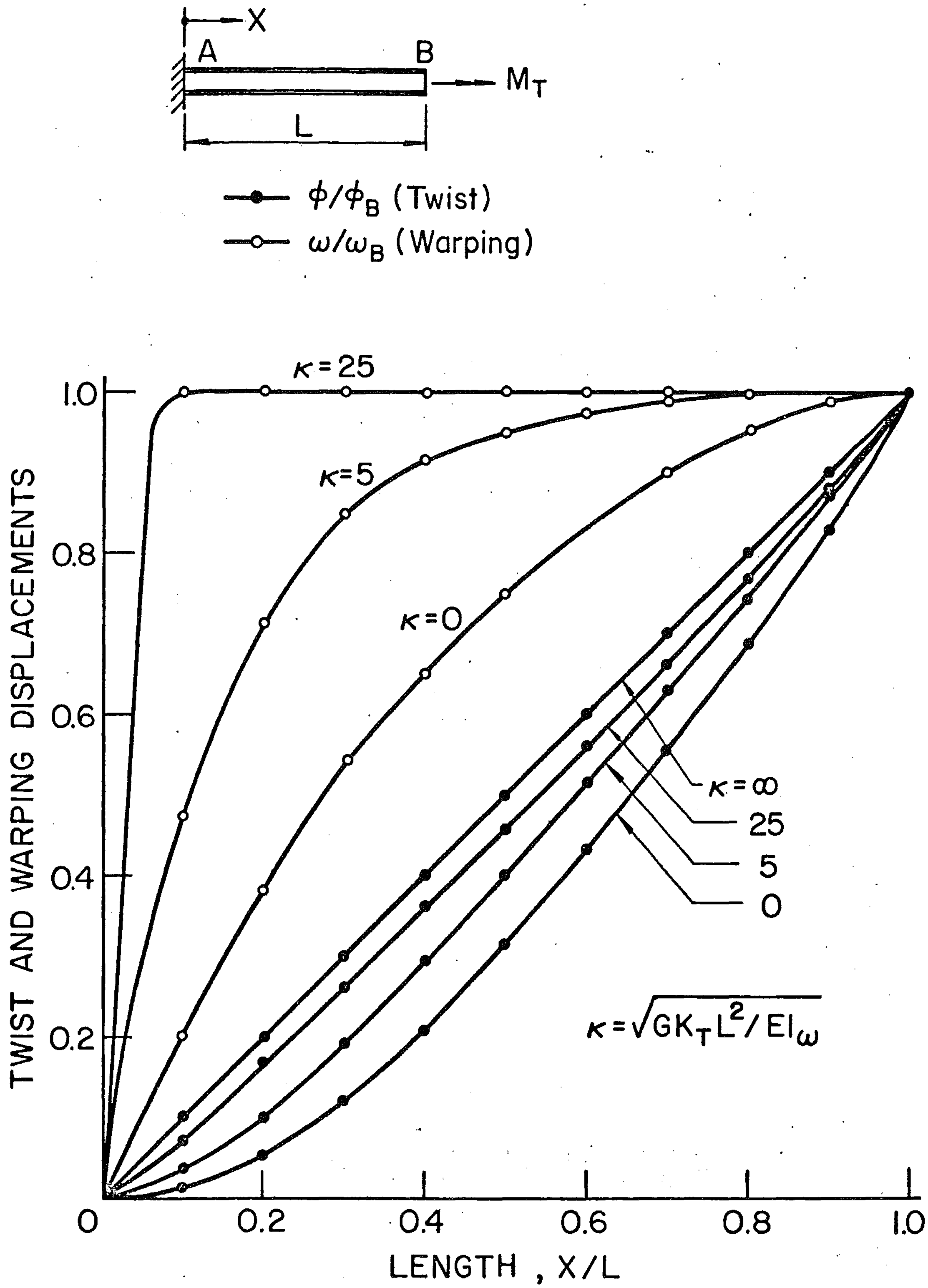

Fig. 2.5 A Cantilever Beam Loaded by Torque

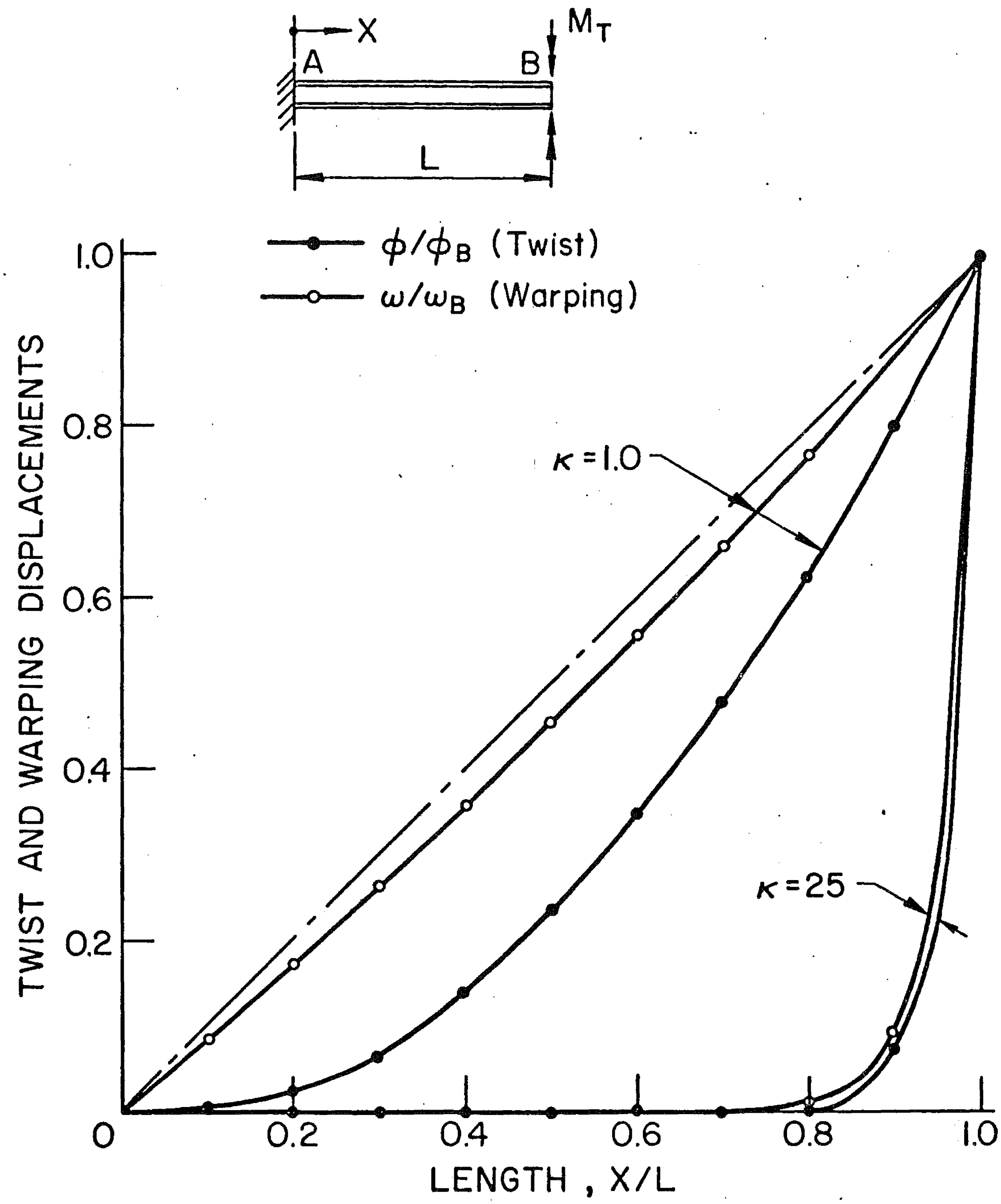

Fig. 2.6 A Cantilever Beam Loaded by a Concentrated Bimoment

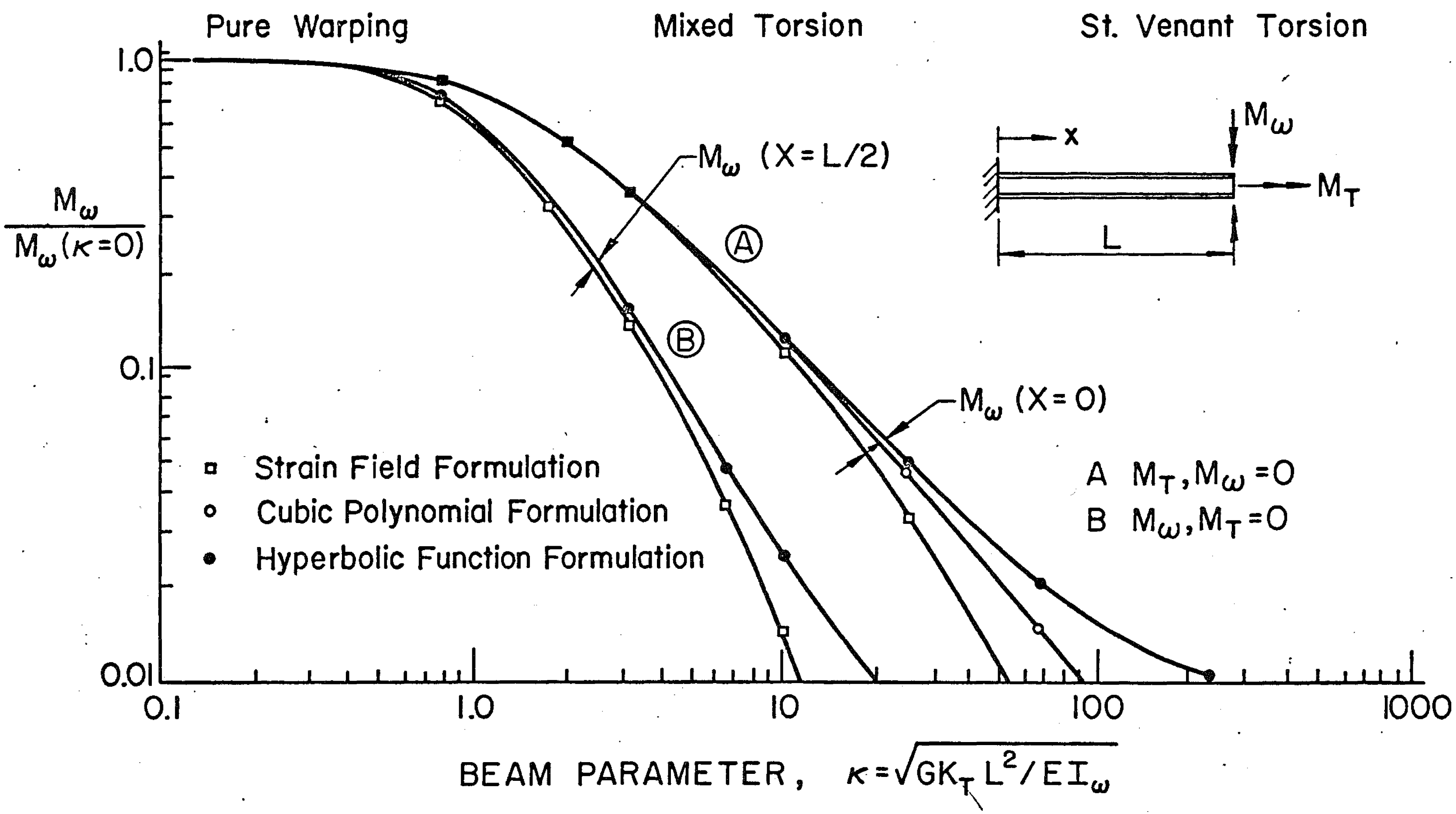

Fig. 2.7 Comparison of Beam Element Stiffness Matrices using a Cantilever Beam under Torsion and Bimoment

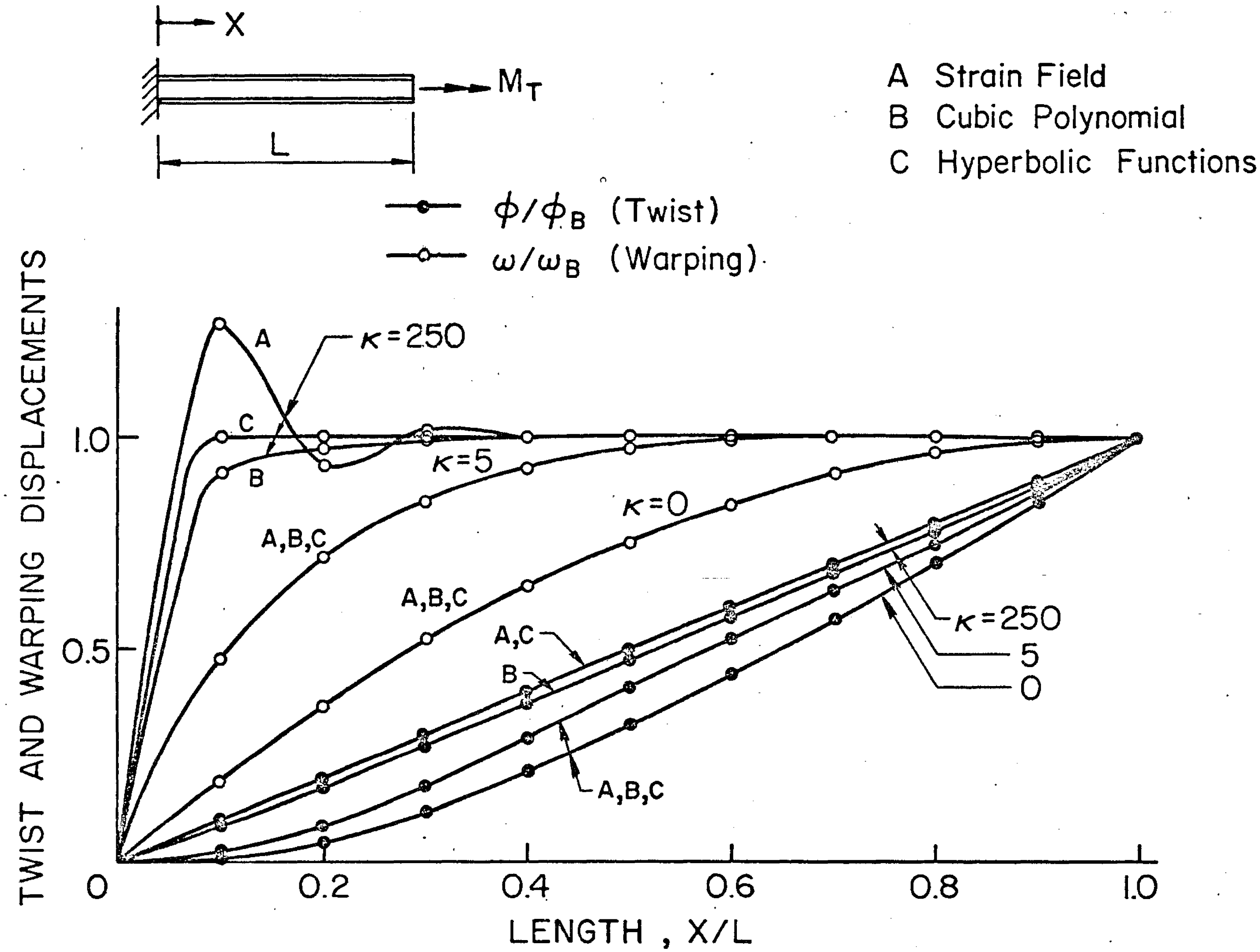

Fig. 2.8 Comparison of Beam Stiffness Matrices

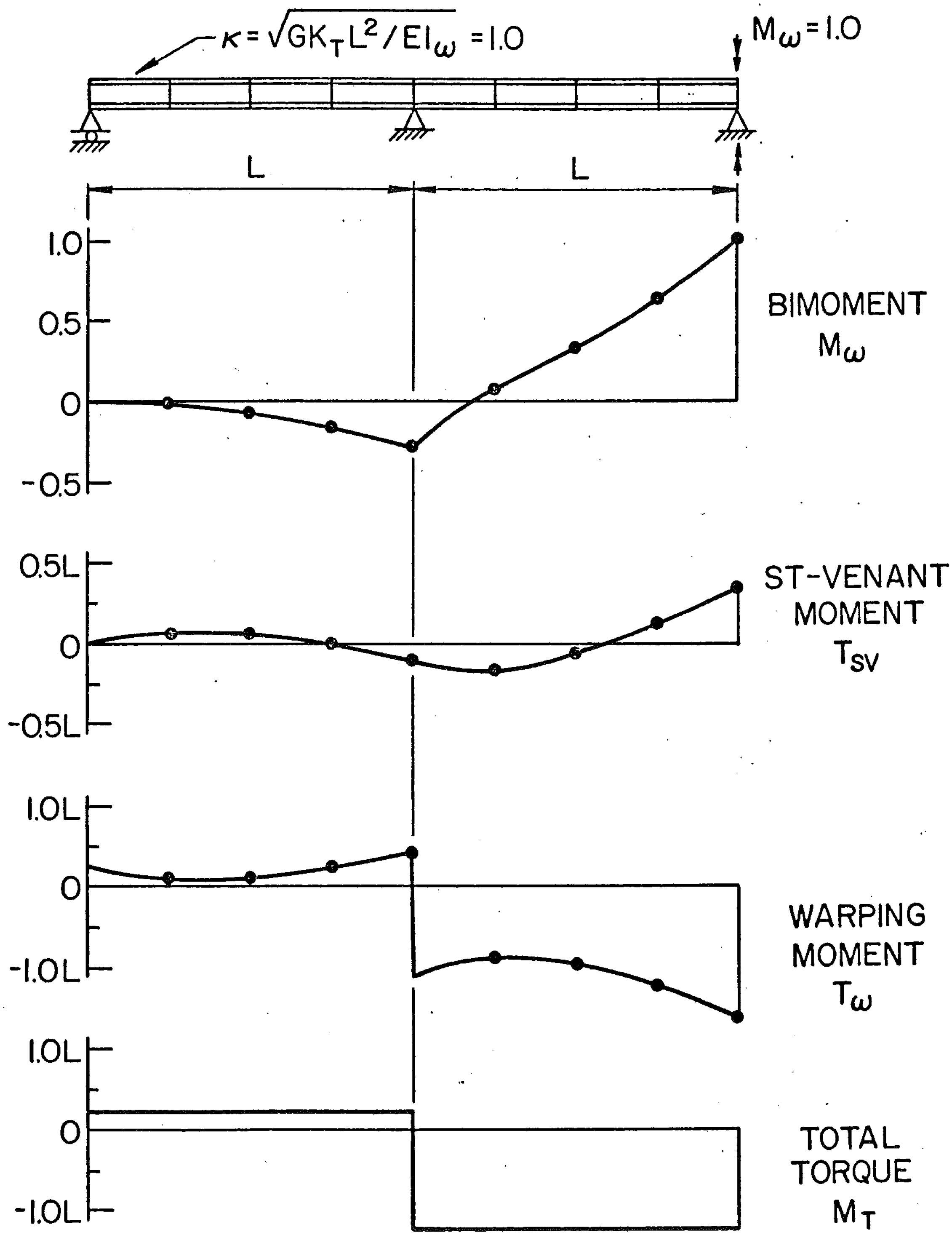

Fig. 2.9 Continuous Beam Loaded by Concentrated Bimoment

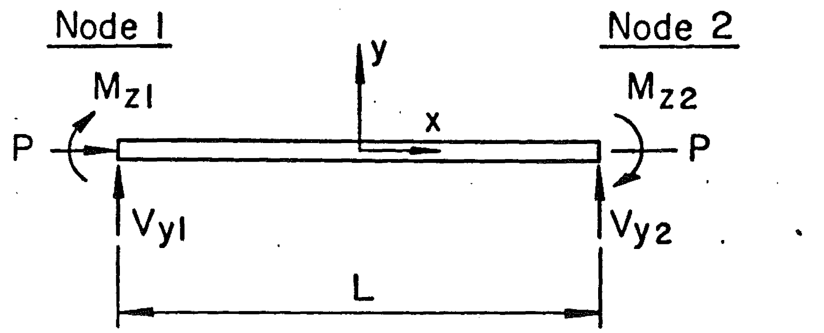

(a)

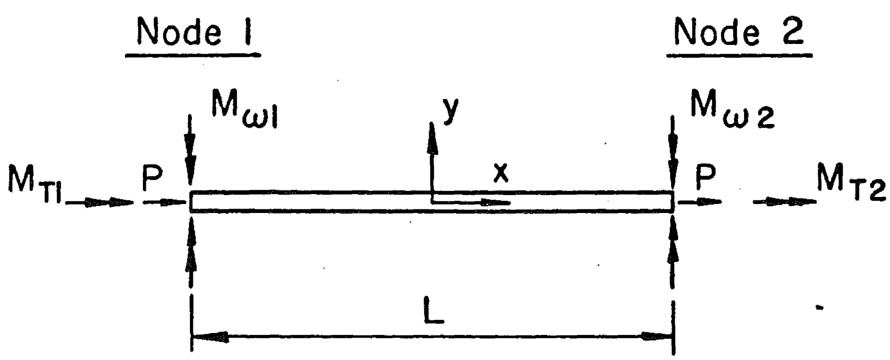

(b)

Fig. 3.1 Beam Element Under Axial and Torsional Loading

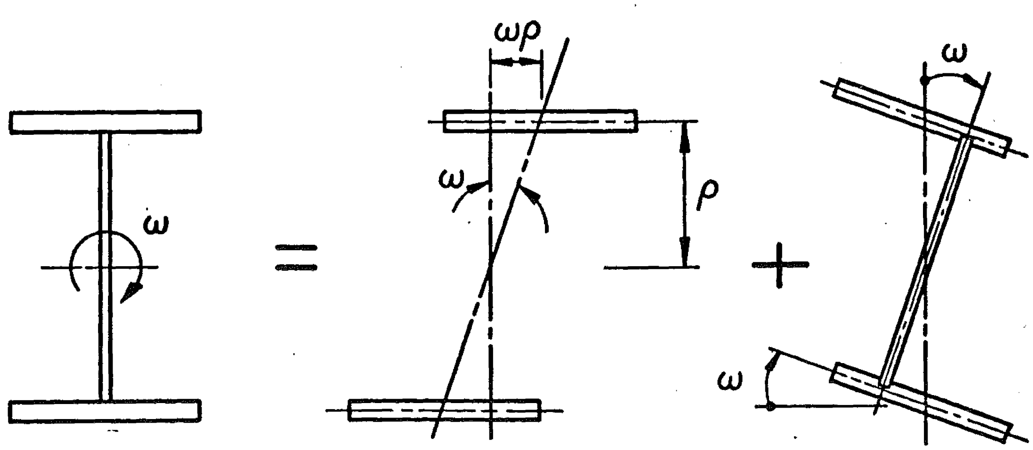

Fig. 3.2 Kinematics of Wide Flange Shape Under Torsion

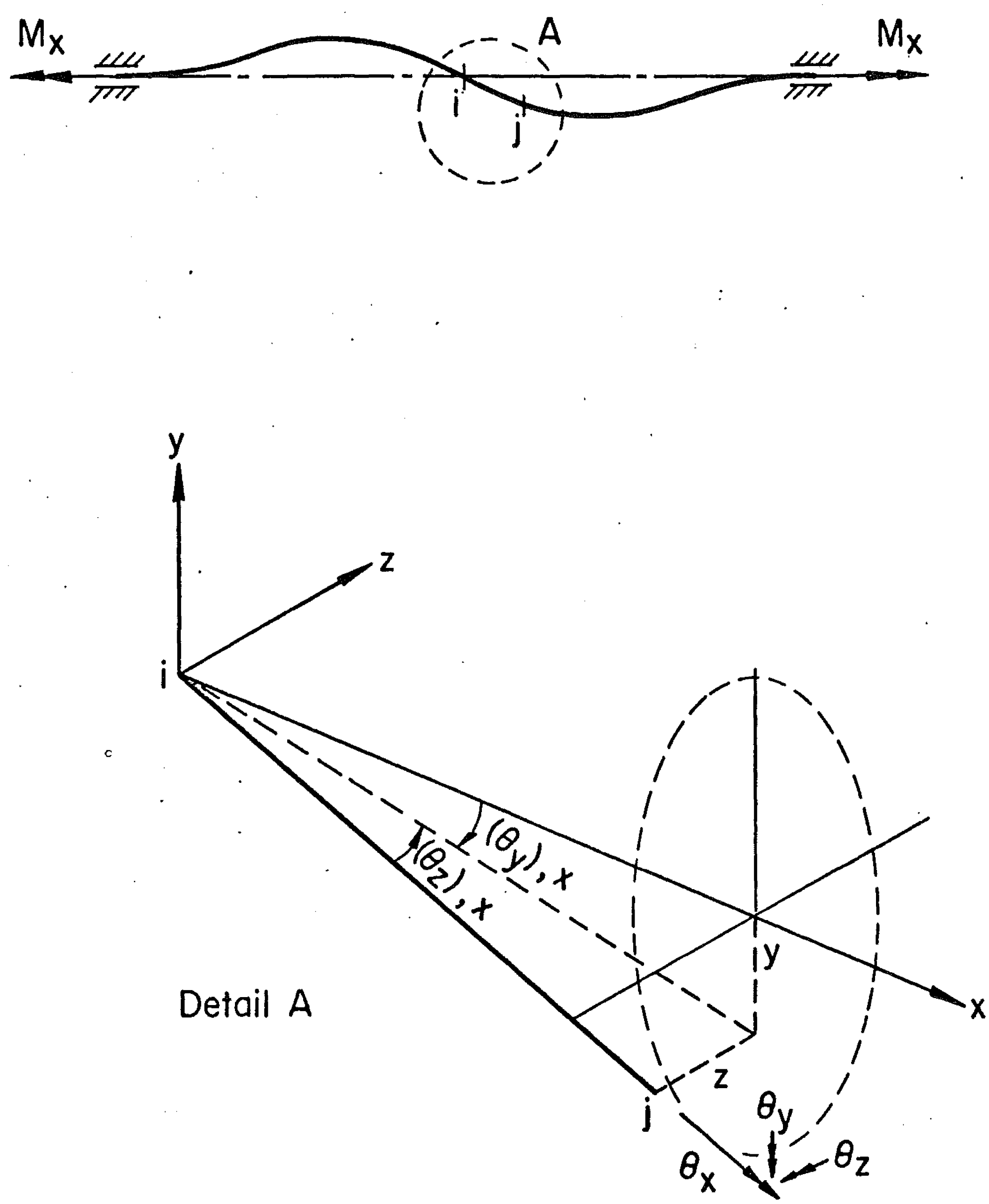

Fig. 3.3 Schematic Description of the Kinematics of a Shaft Under Large Torsional Displacement

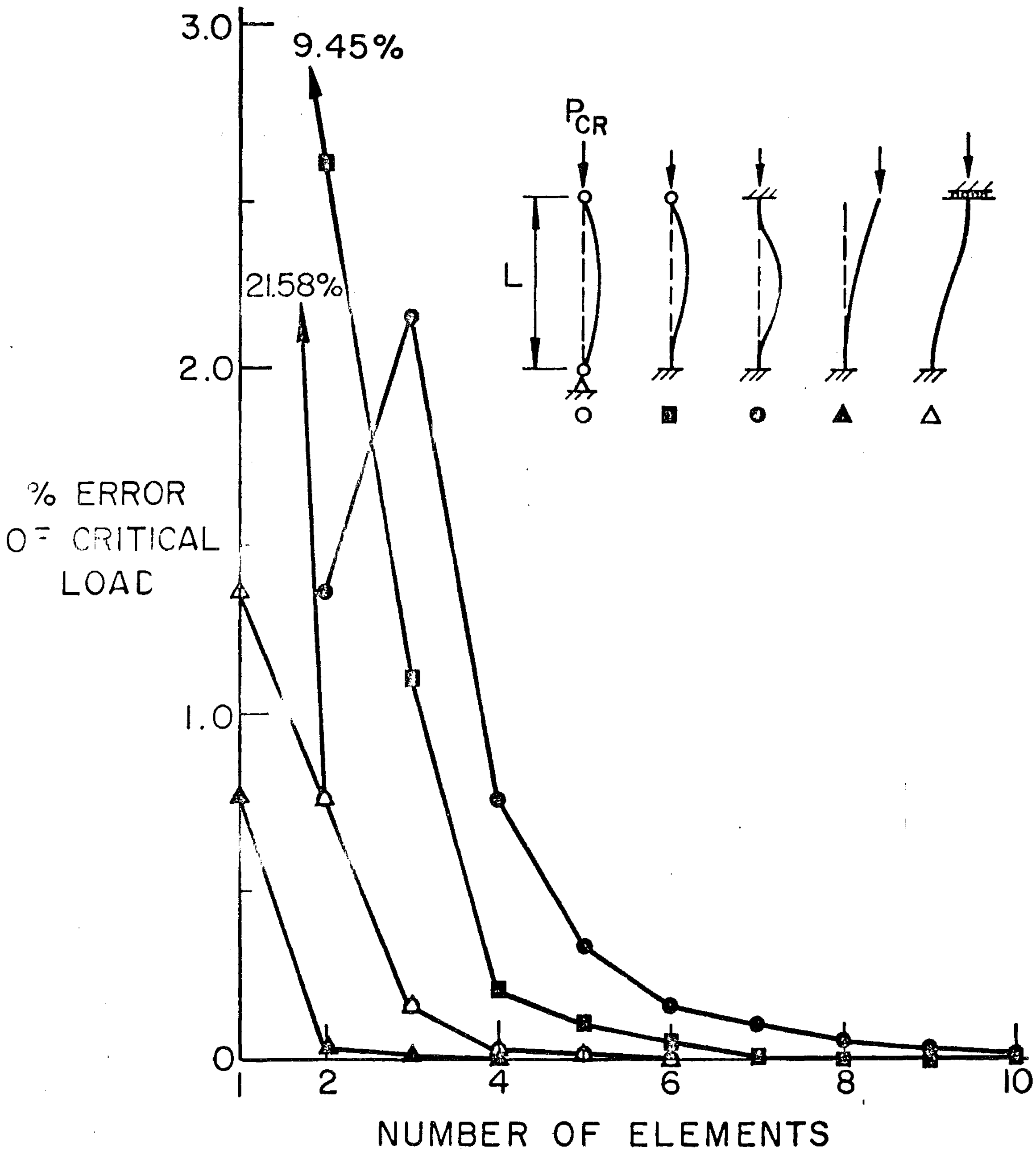

Fig. 3.4 Convergence of Finite Element Solution for Axially Loaded Columns

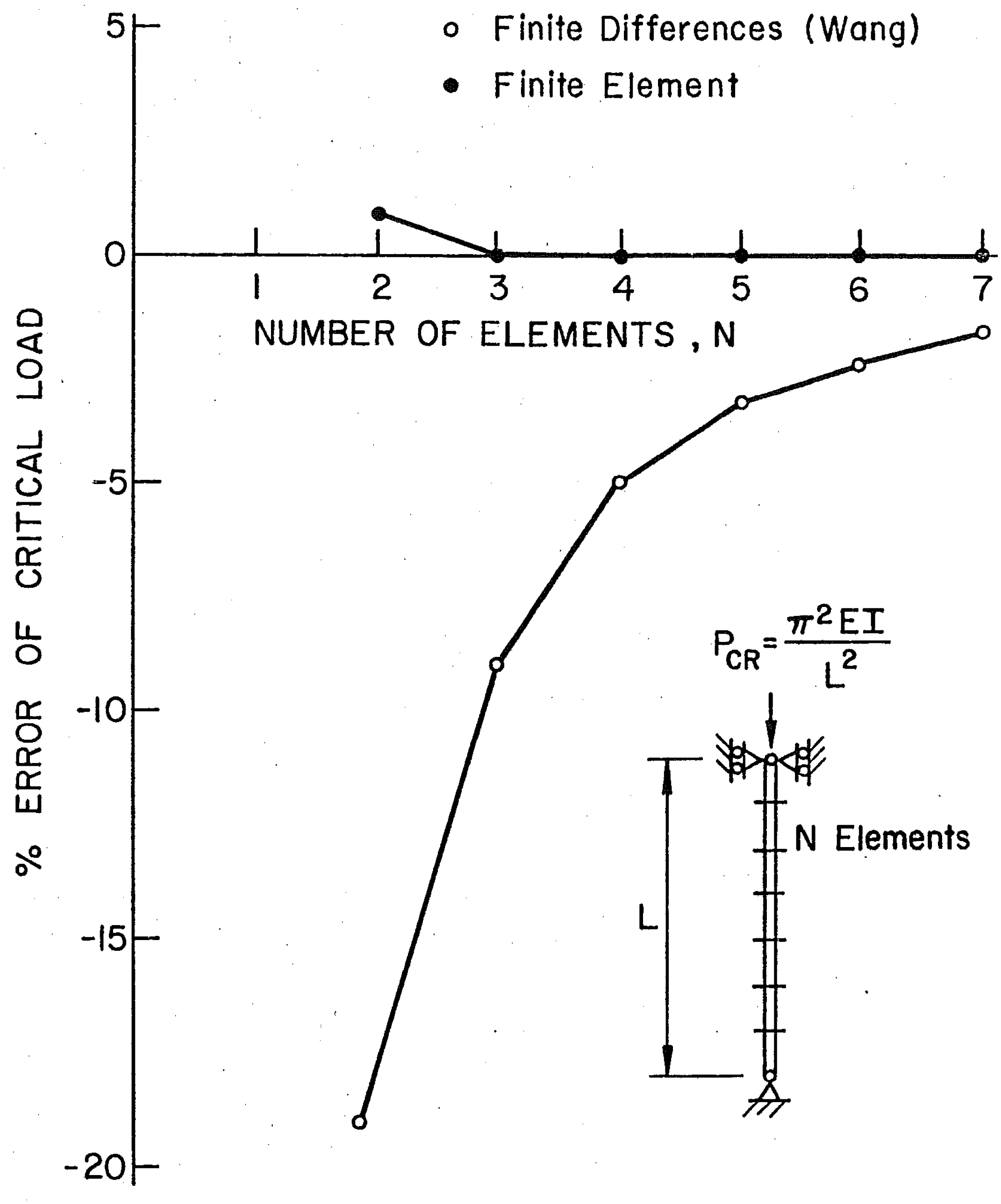

Fig. 3.5 Comparison of Convergence Between Finite Element and Finite Differences Solutions for the Euler Column

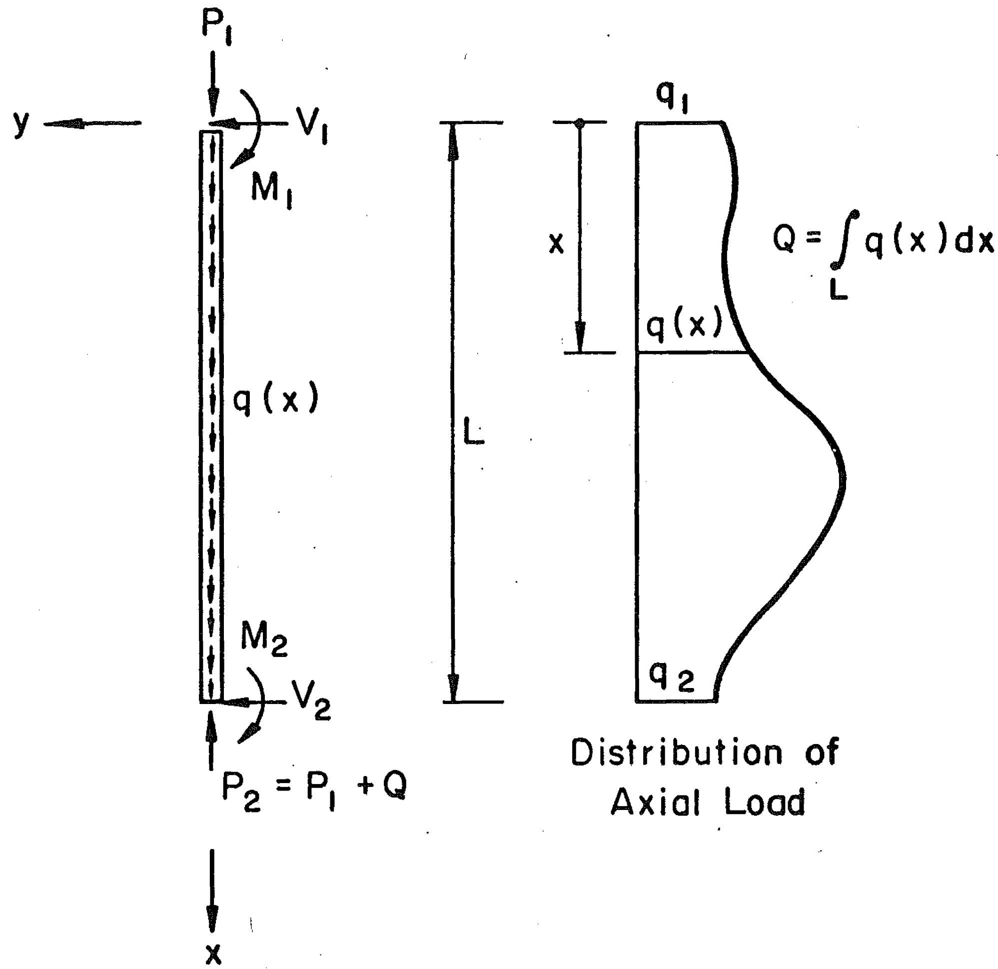

Fig. 3.6 A Column Under Distributed Axial Loads

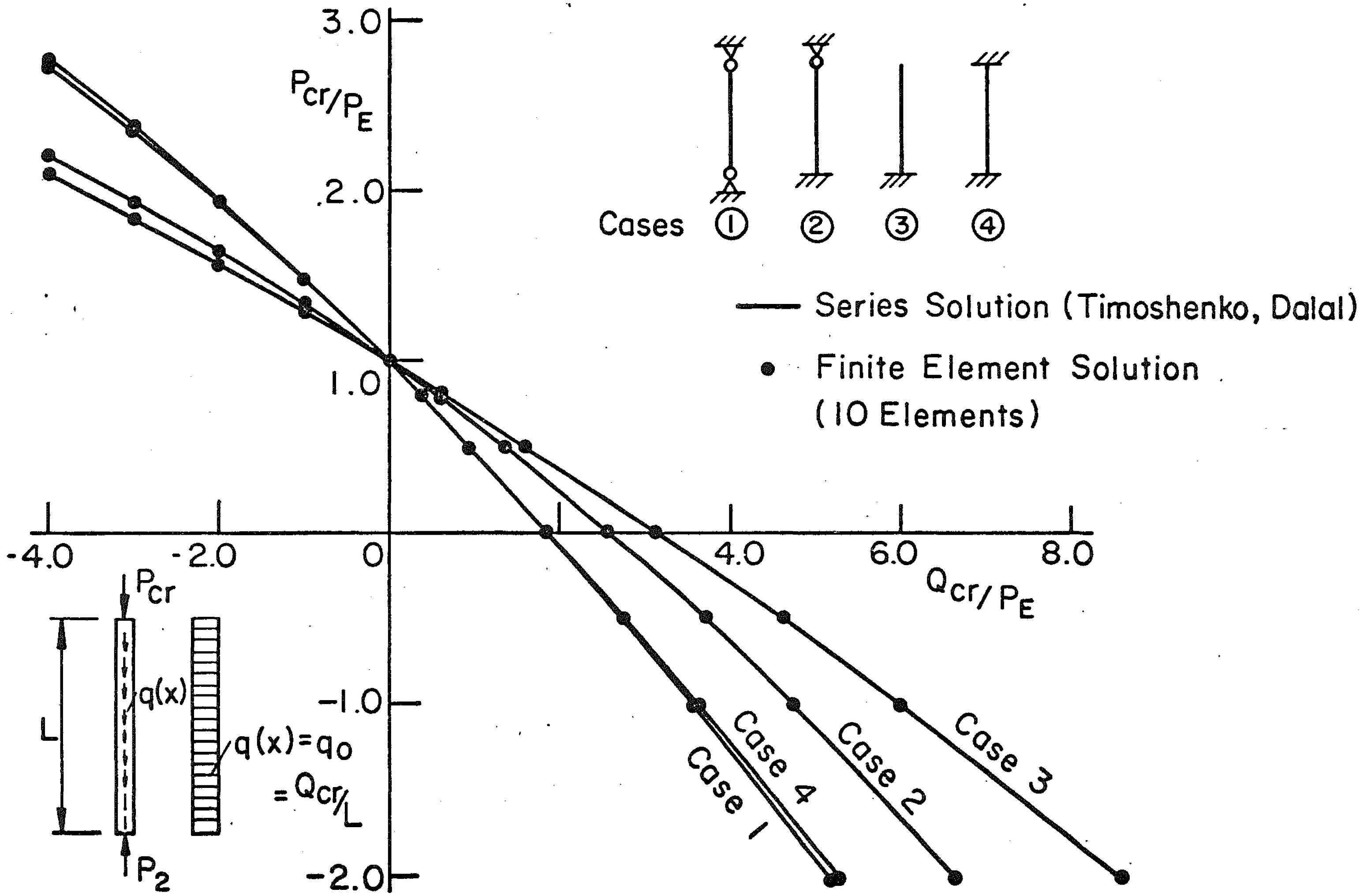

Fig. 3.7 Comparison of Finite Element and Analytical Solutions of Columns with Distributed Axial Loads

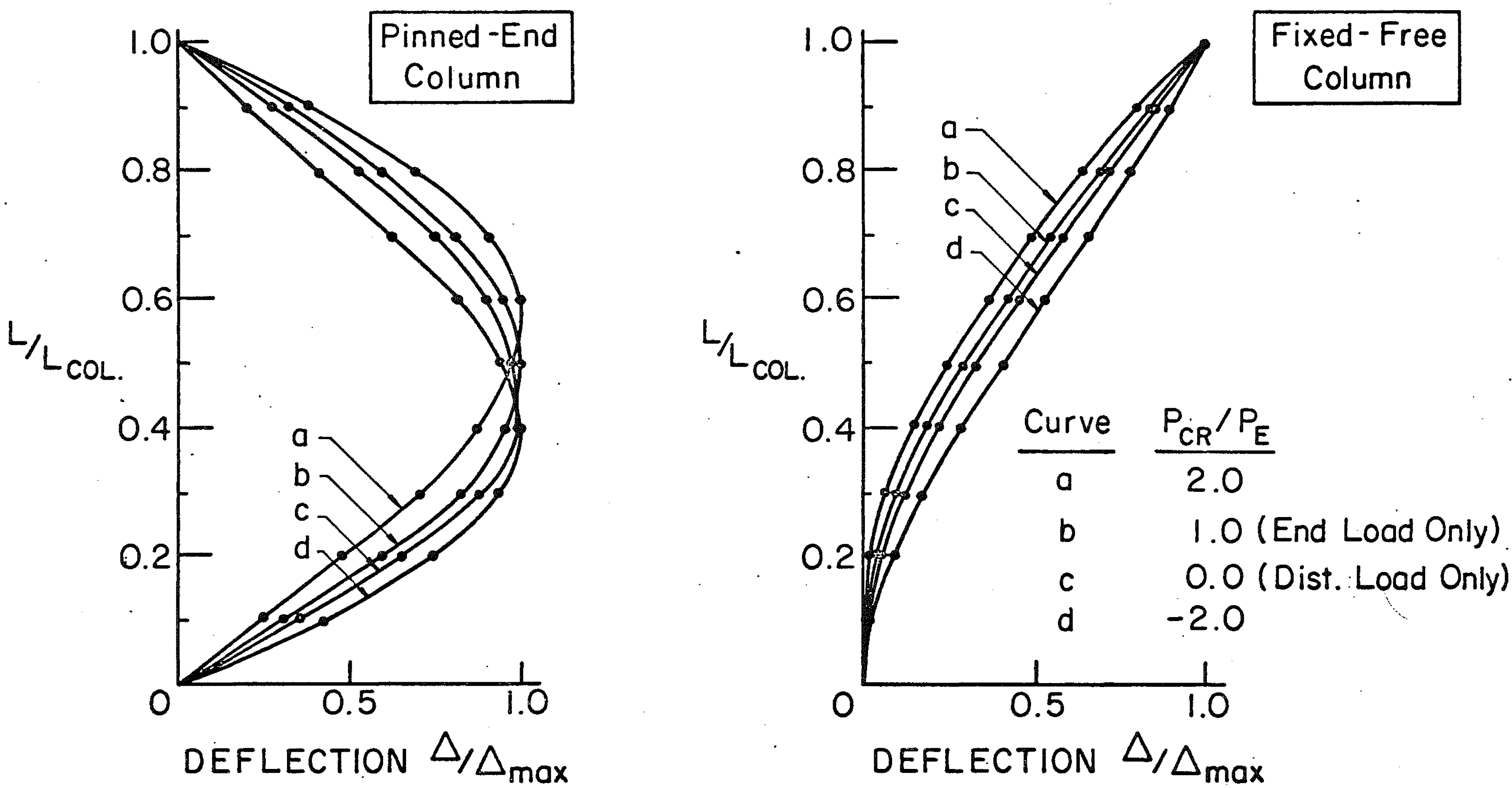

Fig. 3.8 The First Buckling Modes of Columns with Distributed Axial Loads

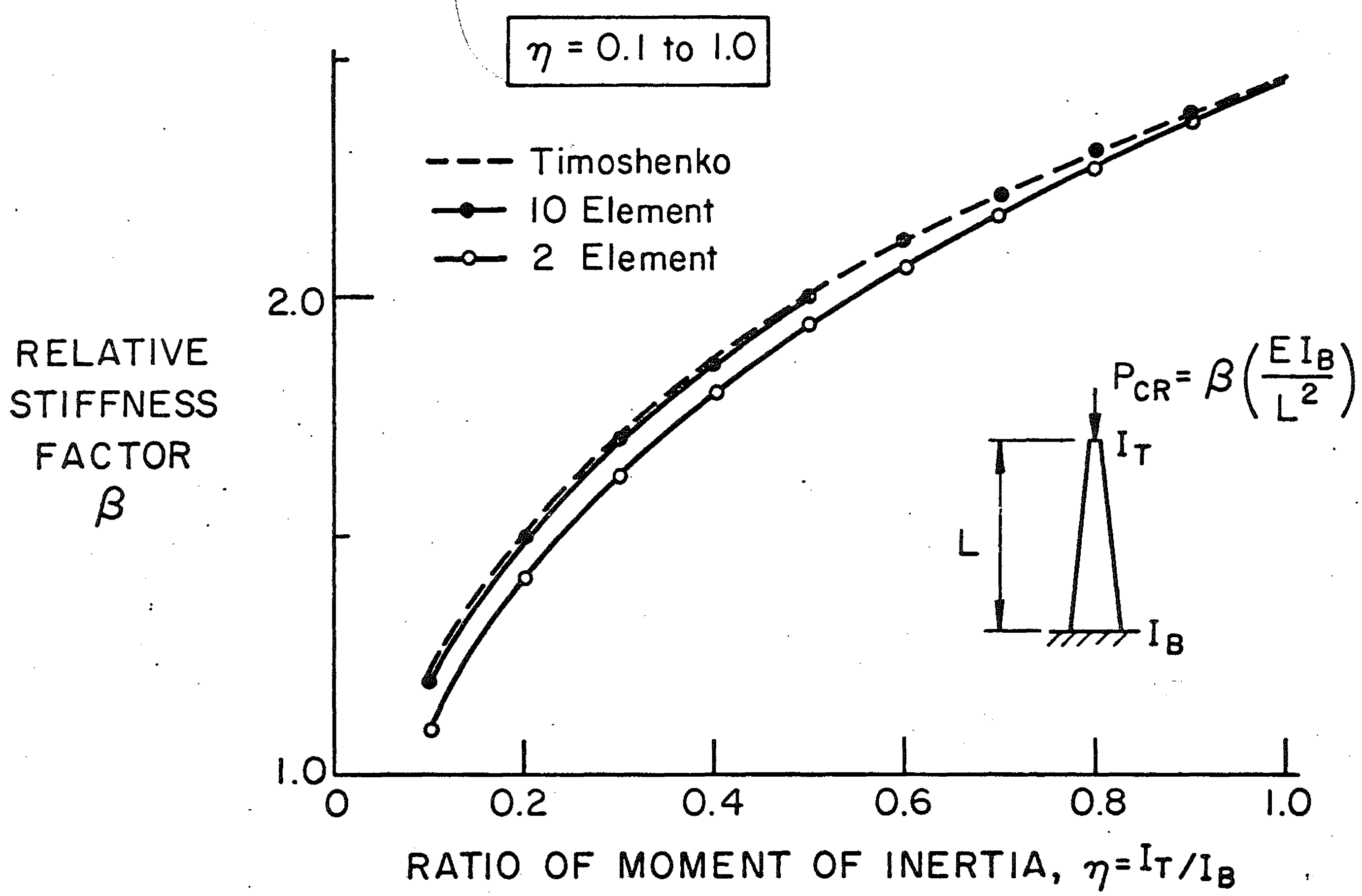

Fig. 3.9 Comparison of Finite Element and Analytical Solutions of Tapered Columns

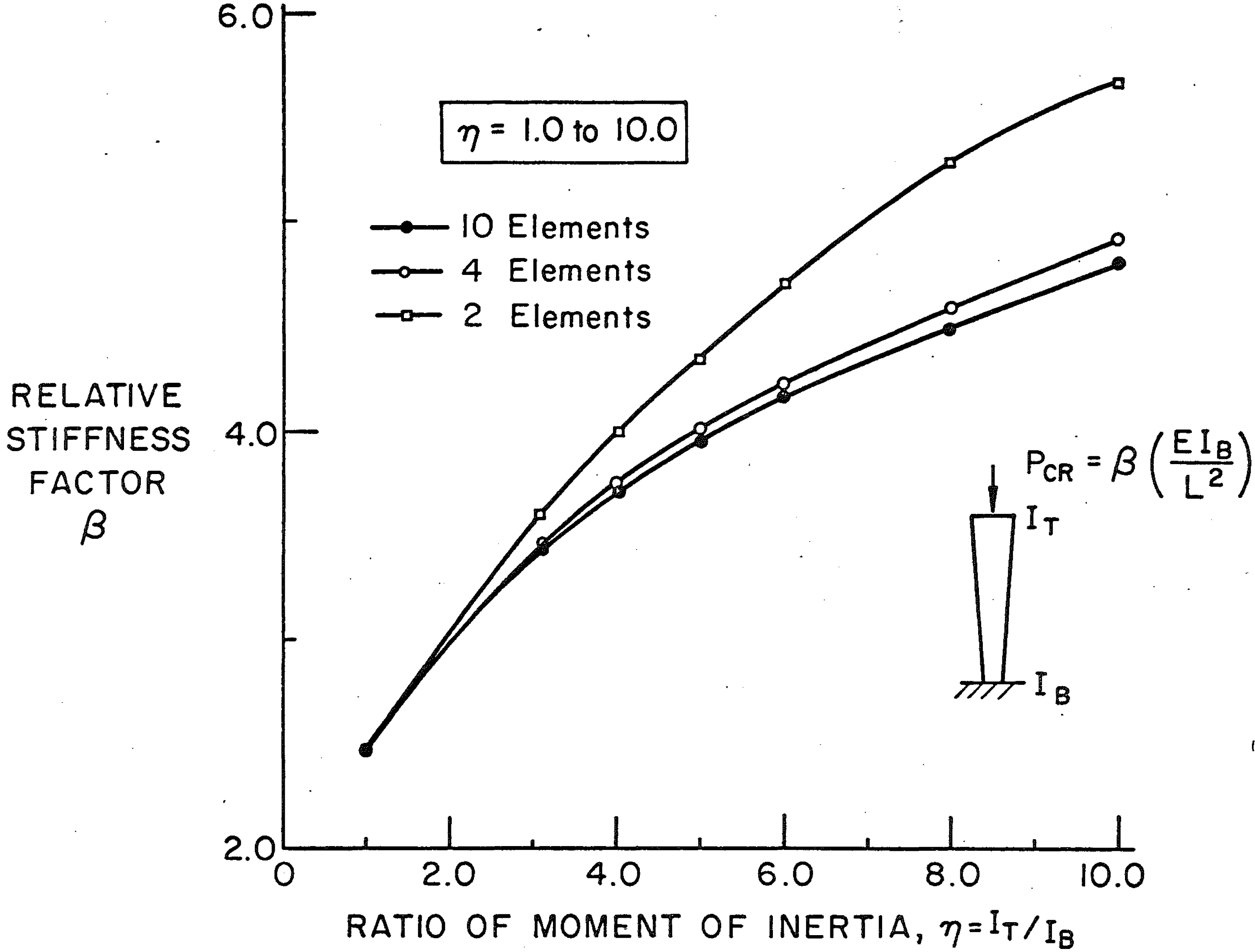

Fig. 3.10 Finite Element Solution of Critical Loads of Tapered Columns

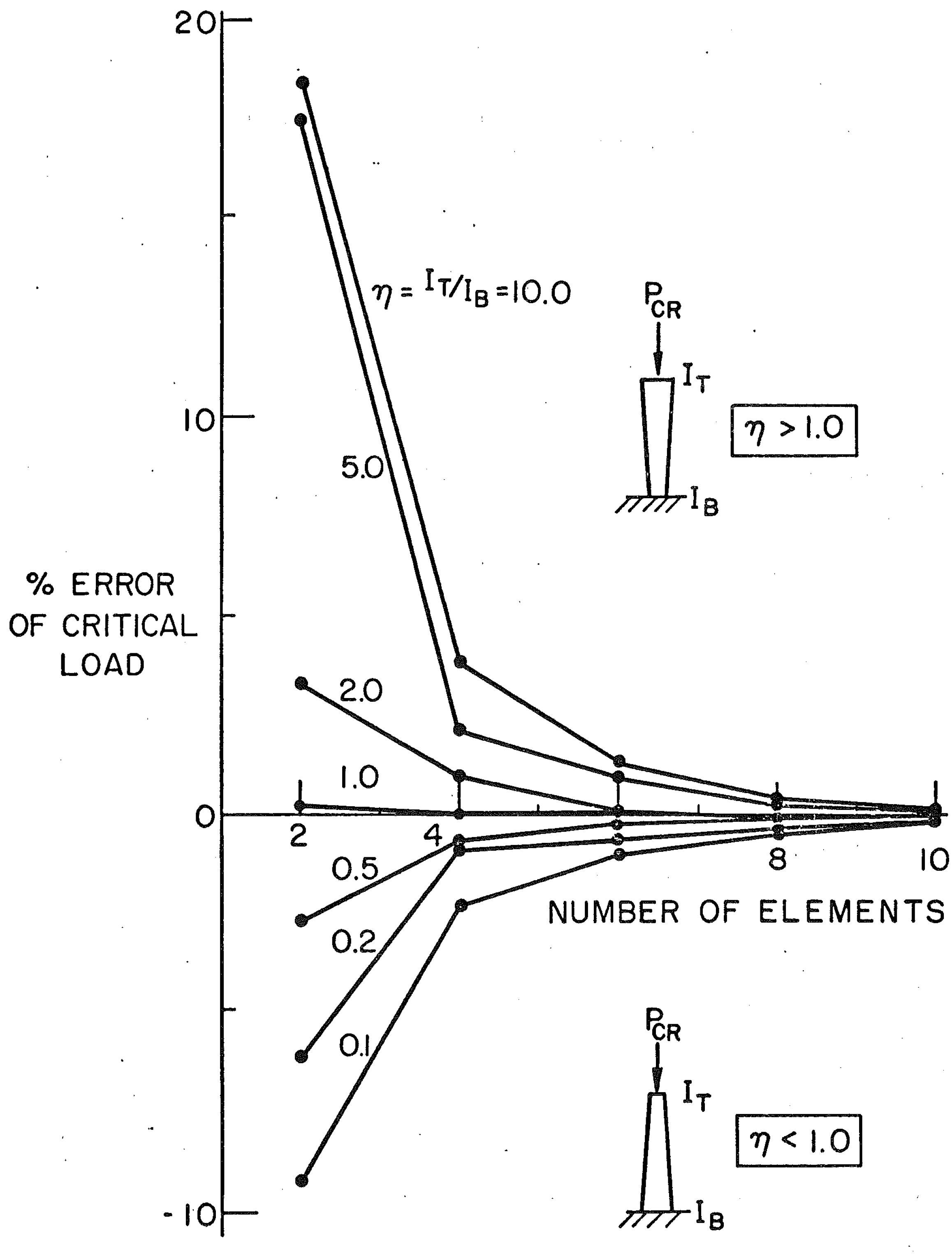

Fig. 3.11 Convergence of Finite Element Solution of Tapered Columns

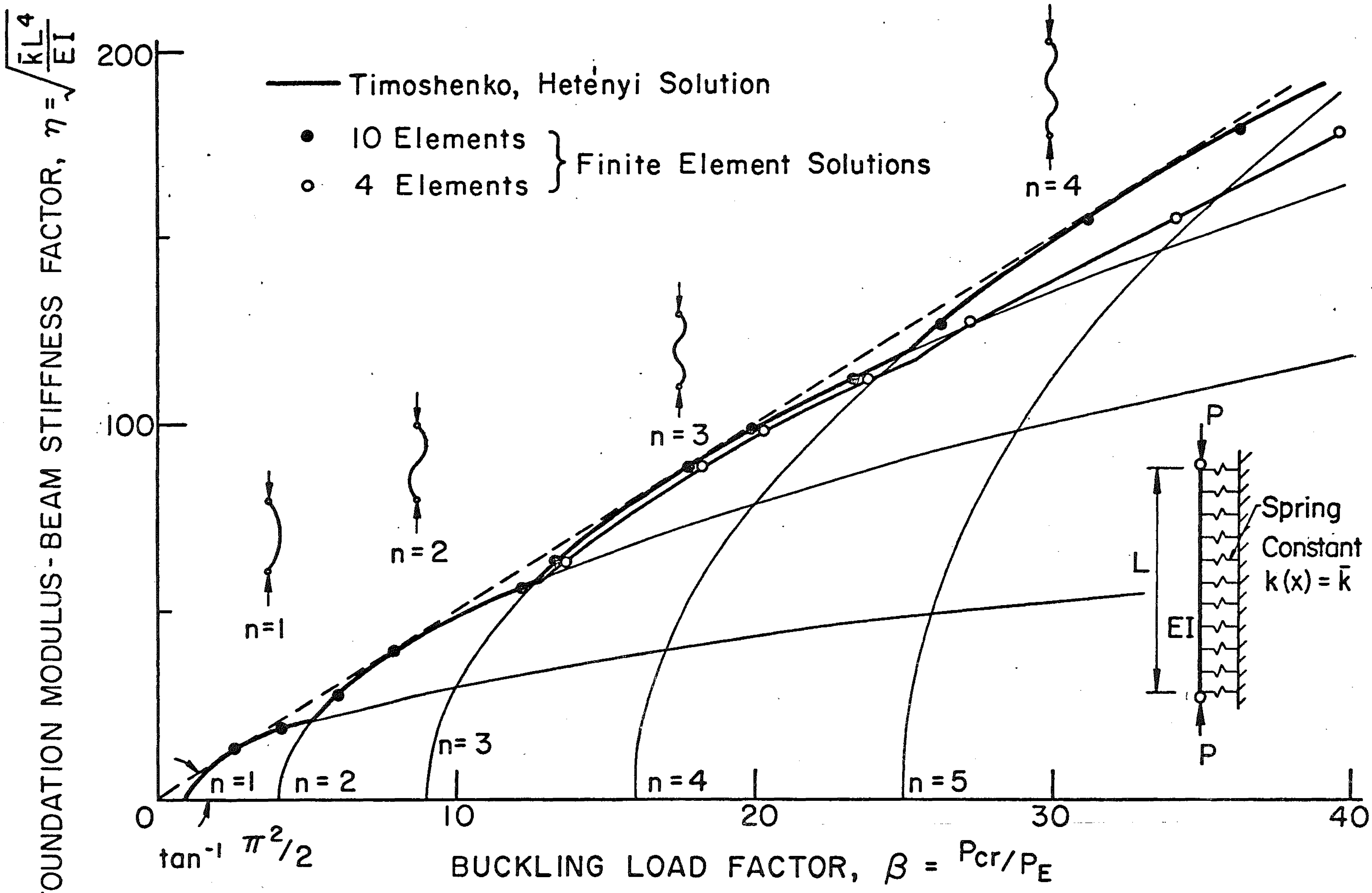

Fig. 3.12 Comparison of Finite Element and Analytical Solutions of Columns on Elastic Foundations

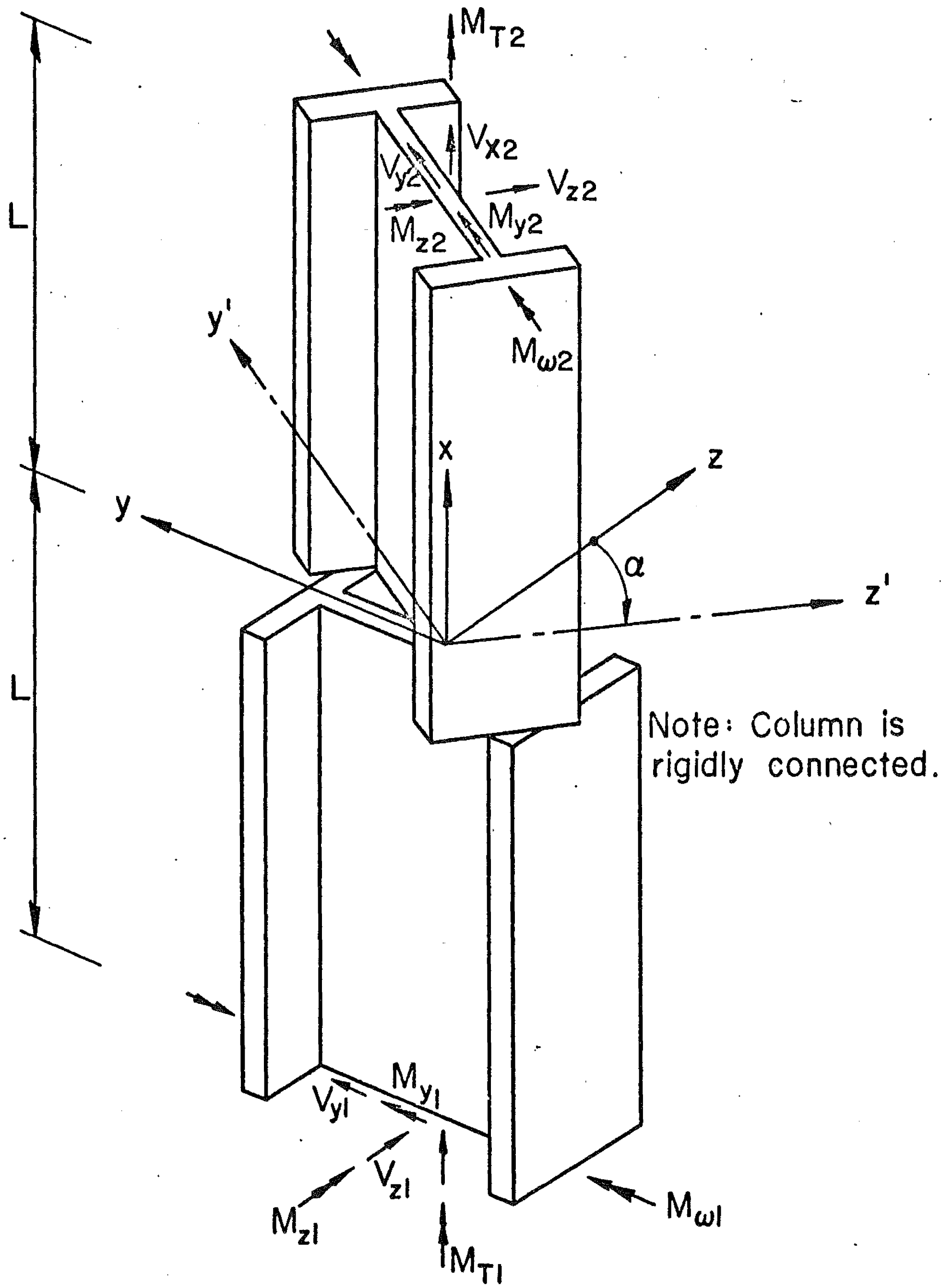

Fig. 3.13 The Generalized Forces and Displacements of a Two-Component Column

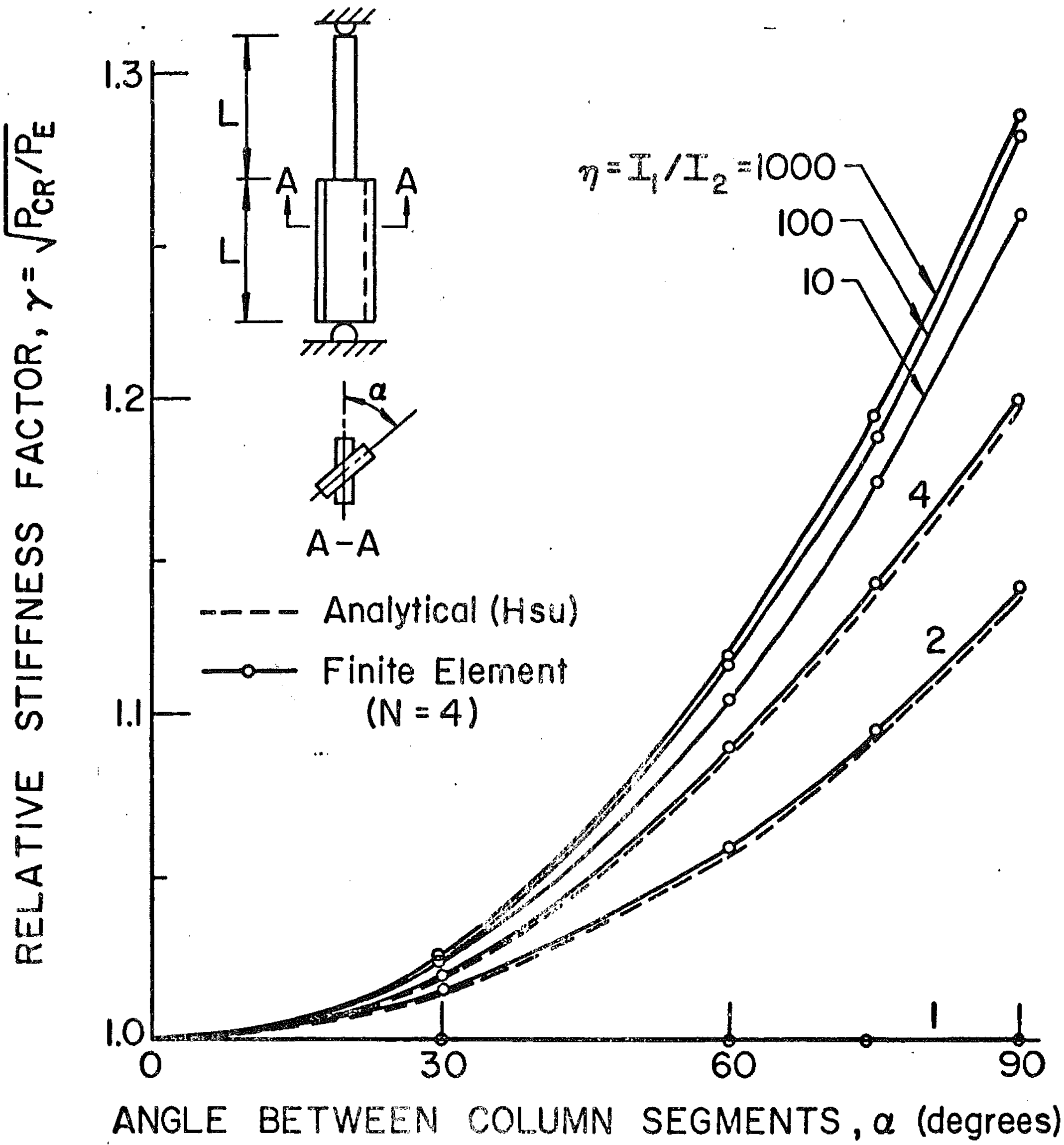

Fig. 3.14 Buckling Loads of Two-Component Columns with Pin Ends

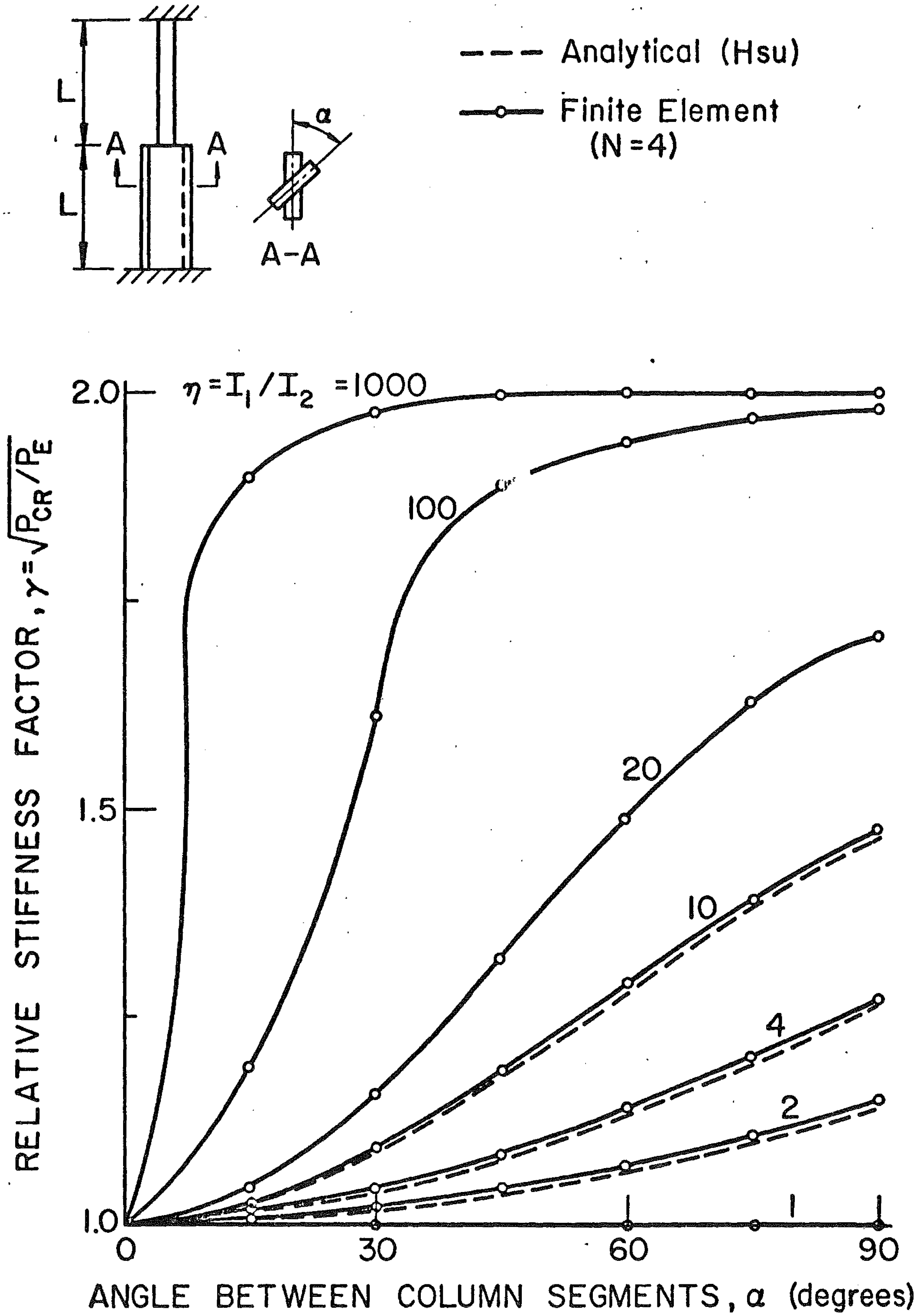

Fig. 3.15 Buckling Loads of Two-Component Columns with Fixed Ends

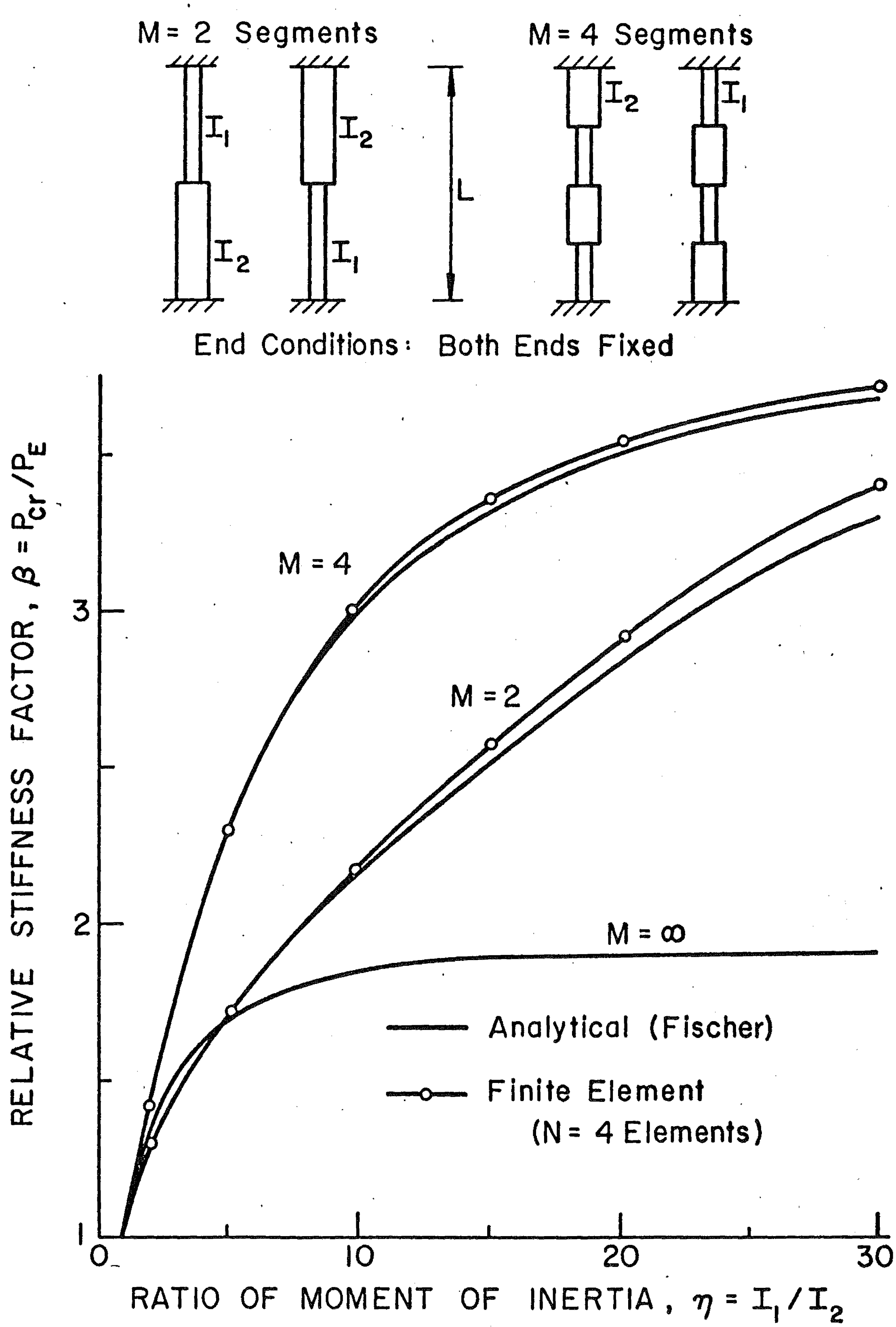

Fig. 3.16 Buckling Loads of Piecewise Prismatic Columns with Pin Ends

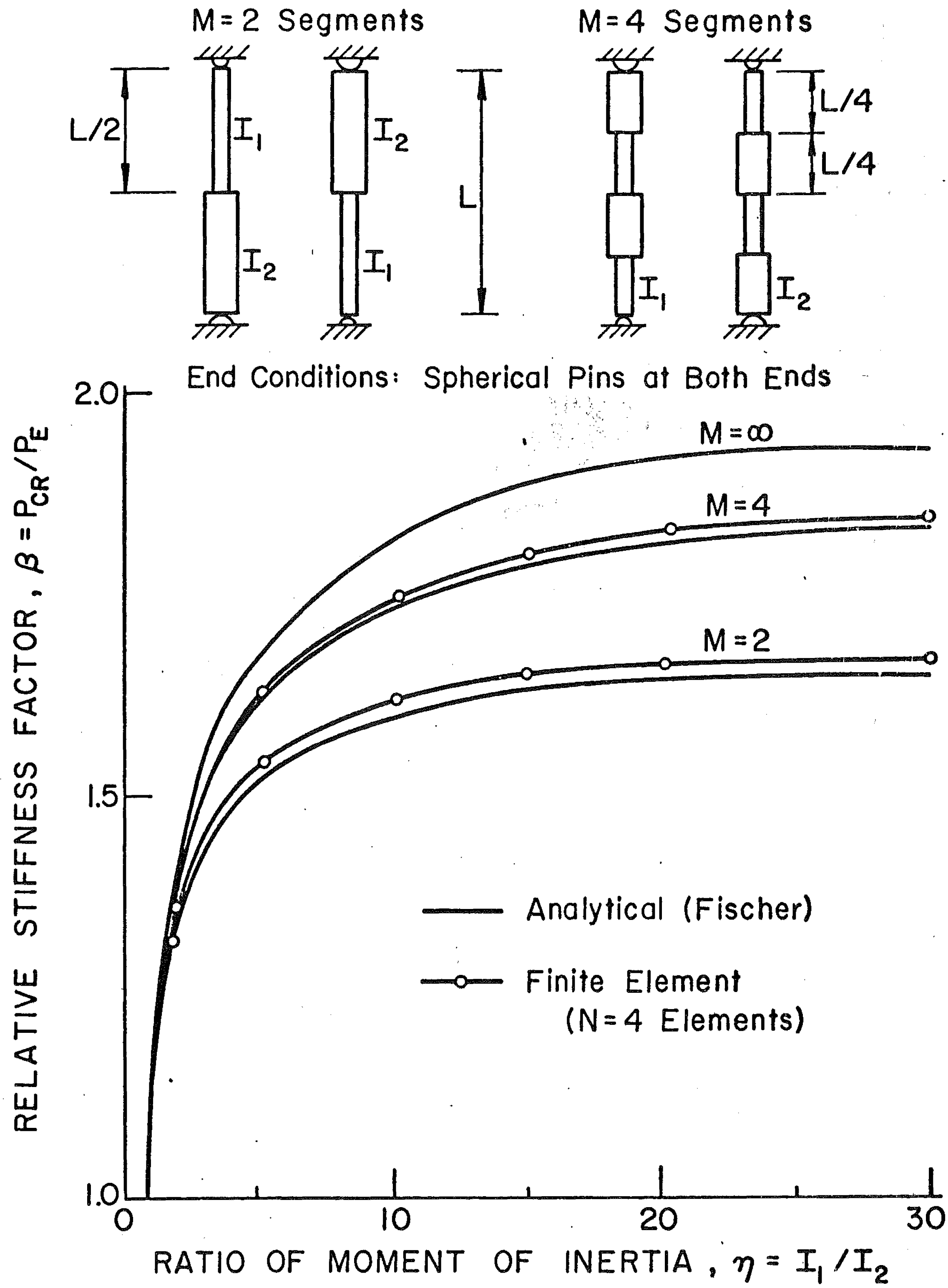

Fig. 3.17 Buckling Loads of Piecewise Prismatic Columns with Fixed Ends

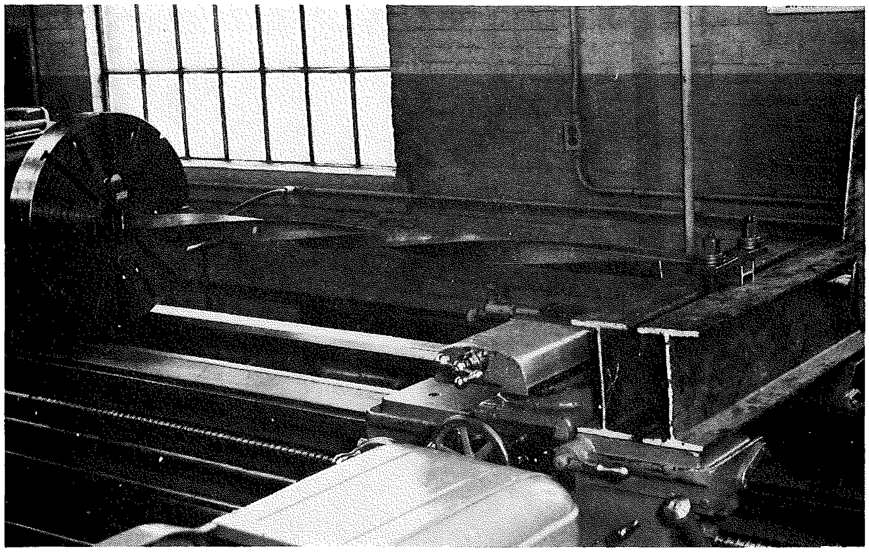

Fig. 3.18 Preparation of a Pretwisted Column

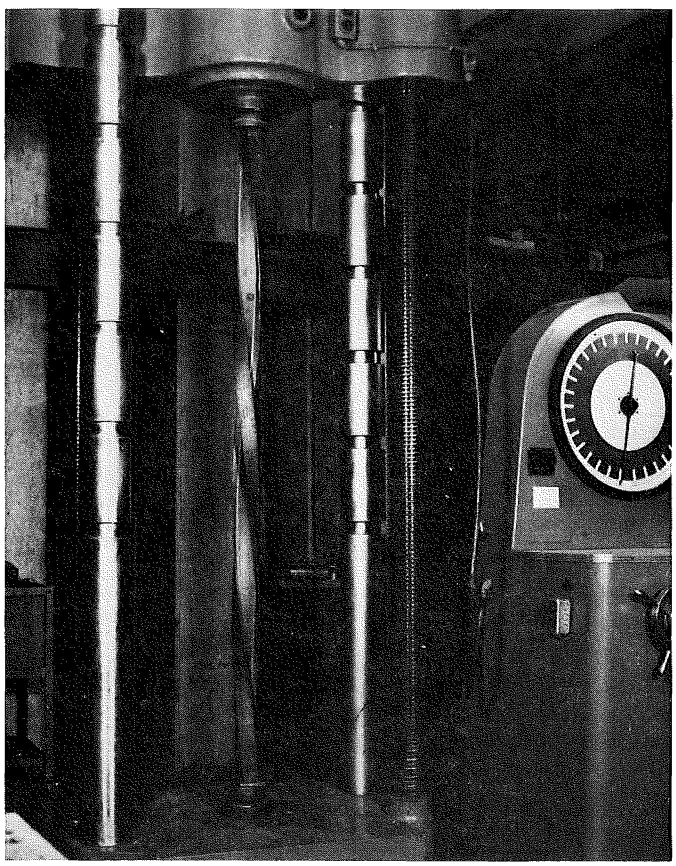

Fig. 3.19 Buckling Test of a Pretwisted Column with Knife Edge Conditions

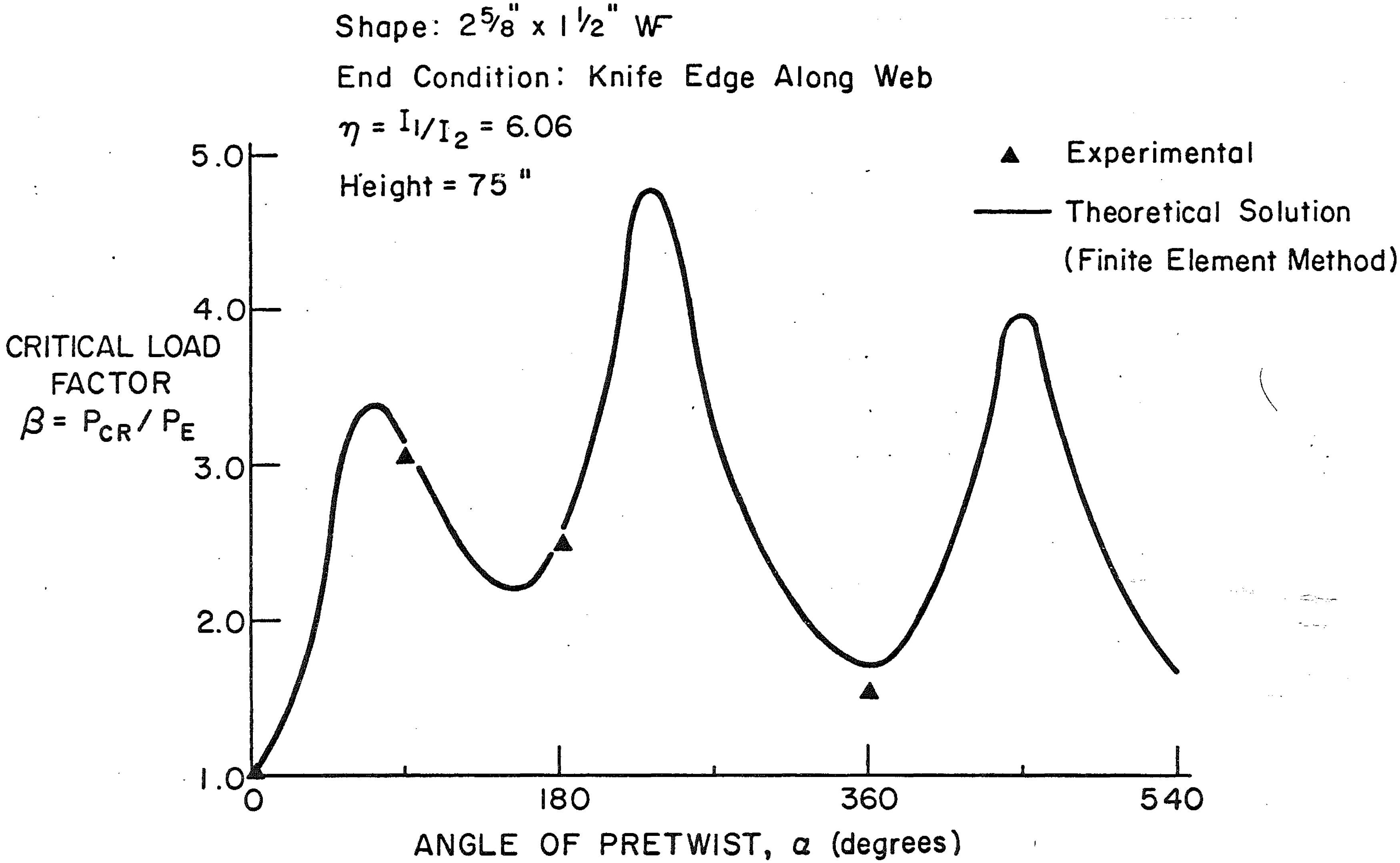

Fig. 3.20 Comparison of Finite Element Solution and Experimental Results of Pretwisted Columns

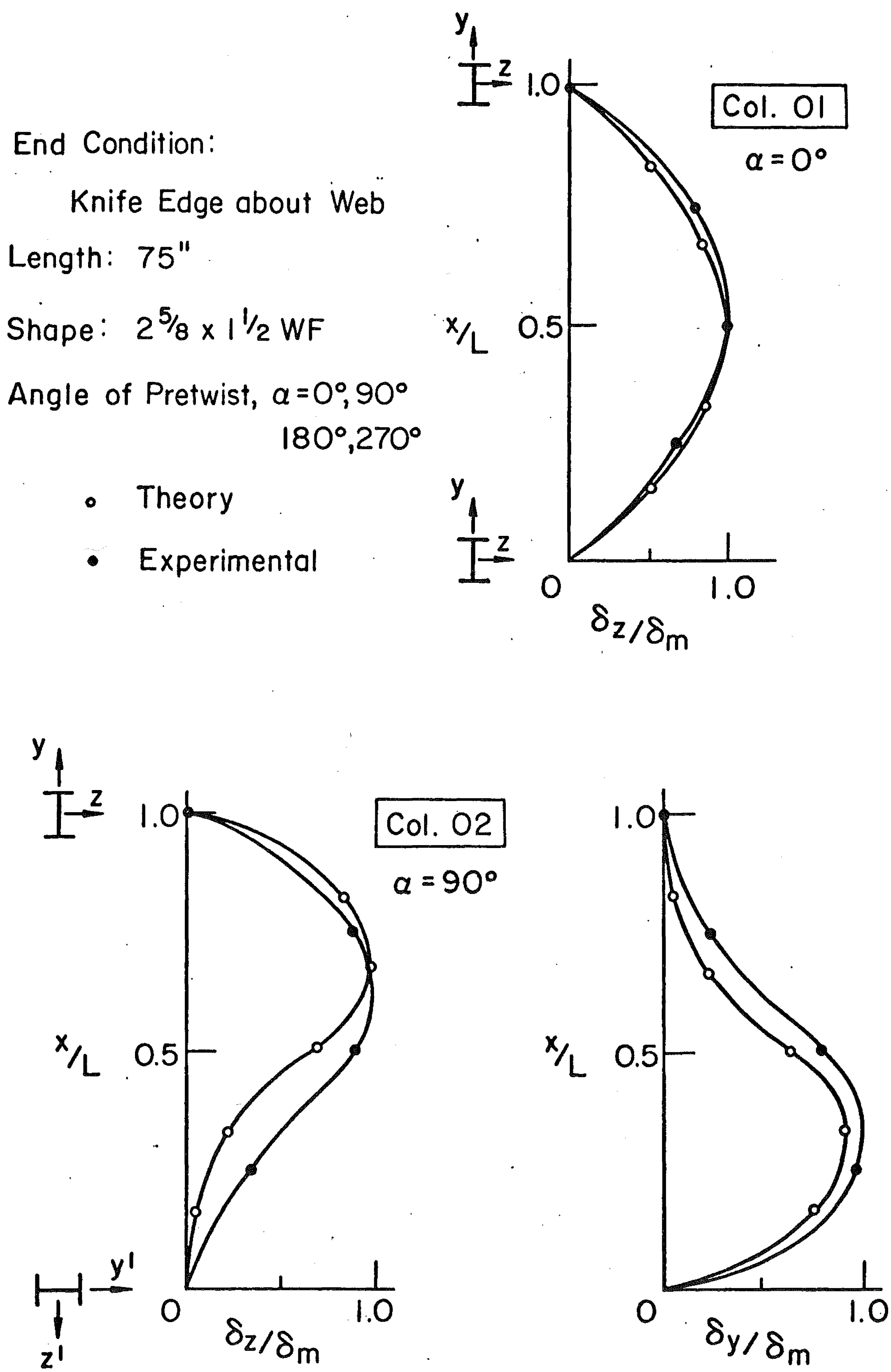

Fig. 3.21 Comparison of Theoretical and Experimental Buckling Modes of Pretwisted Columns

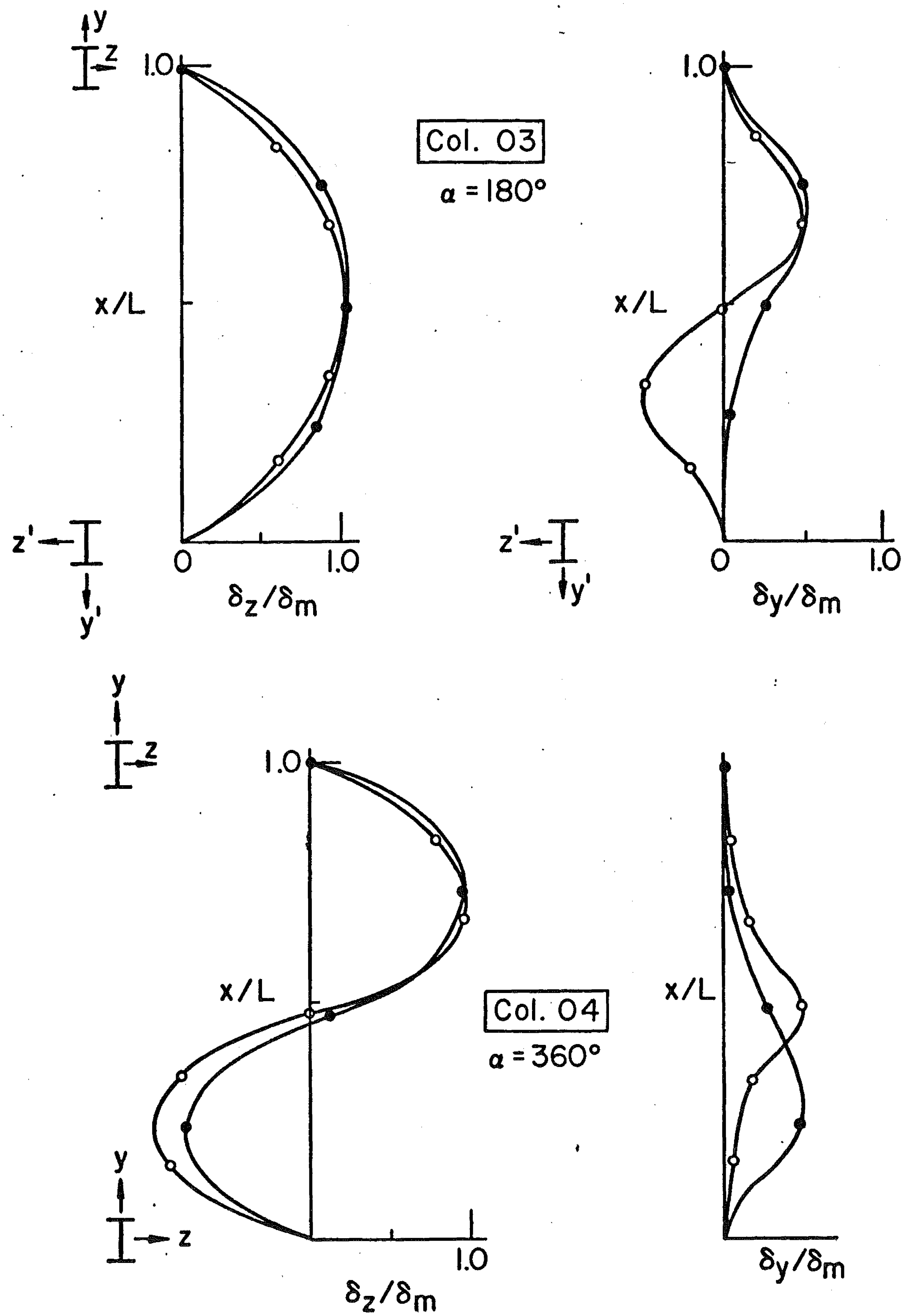

Fig. 3.21 (cont'd) Comparison of Theoretical and Experimental Buckling Modes of Pretwisted Columns

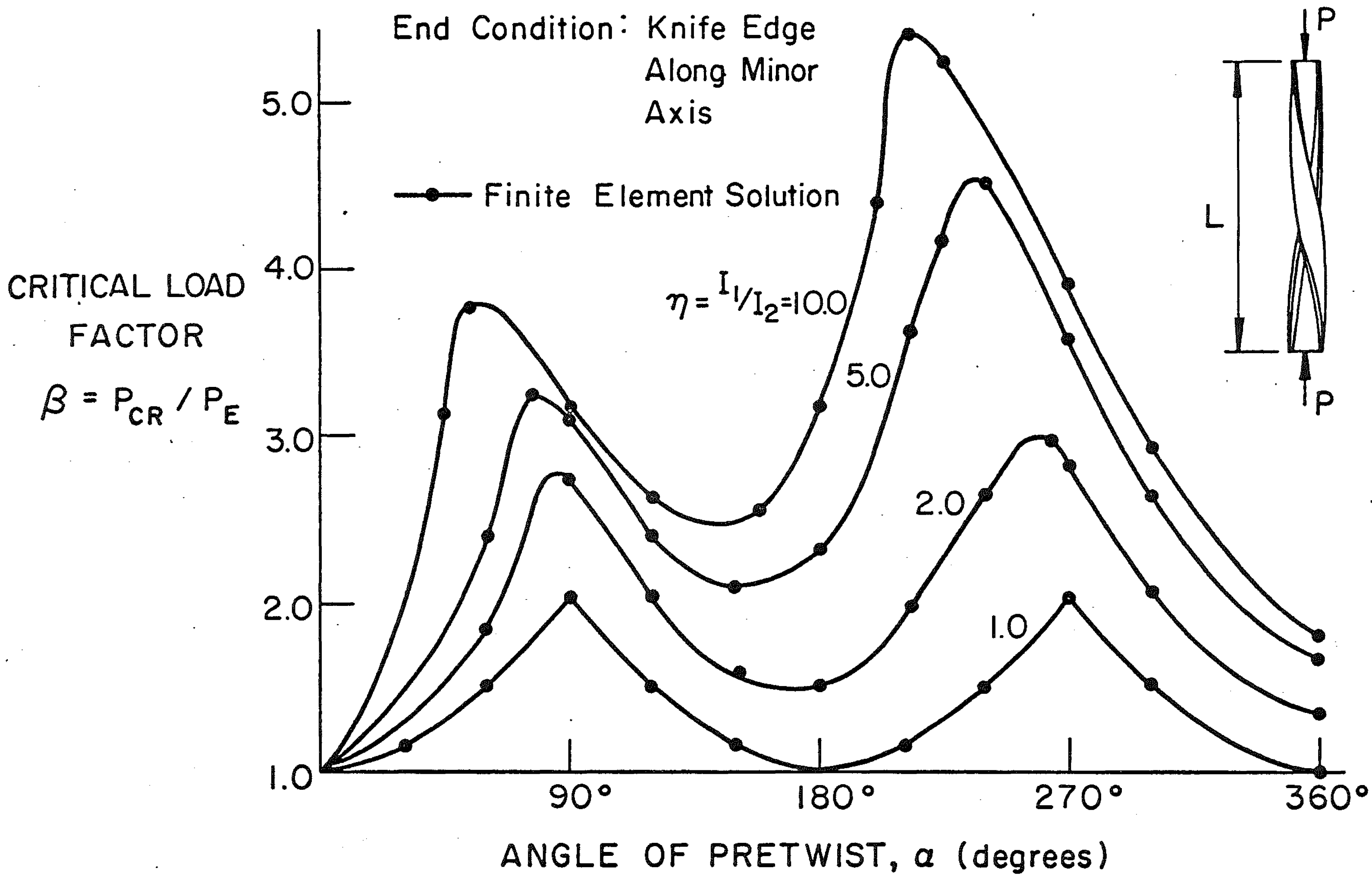

Fig. 3.22 Finite Element Solution of Pretwisted Columns with Knife Edge Conditions

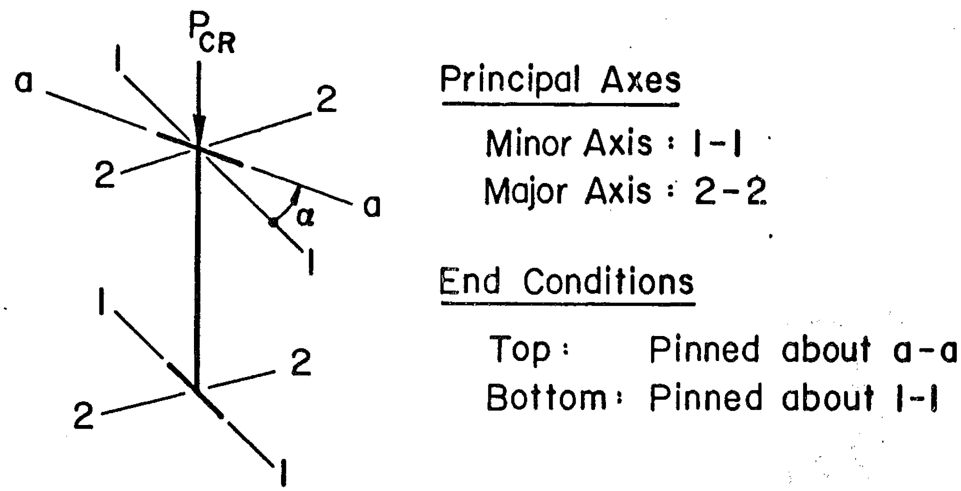

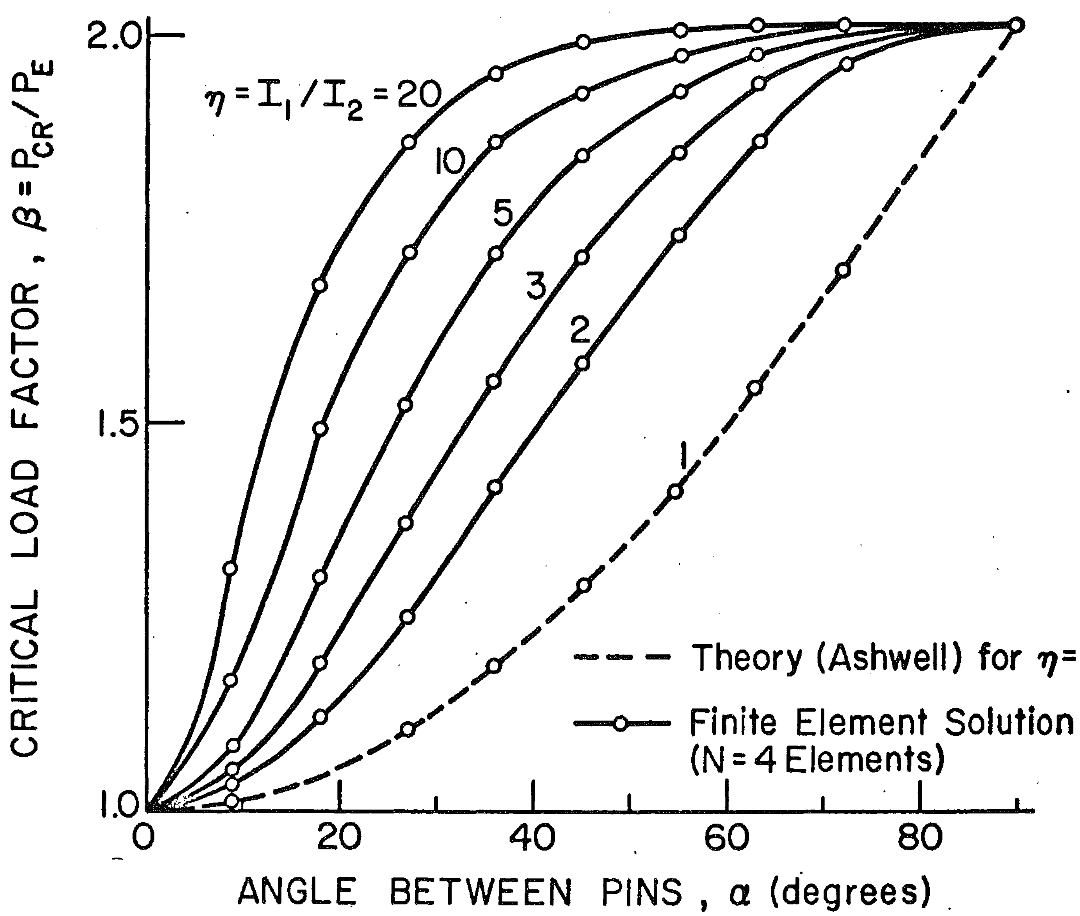

Fig. 3.23 Buckling Loads of Prismatic Columns with Crossed Pins (Pin Ends)

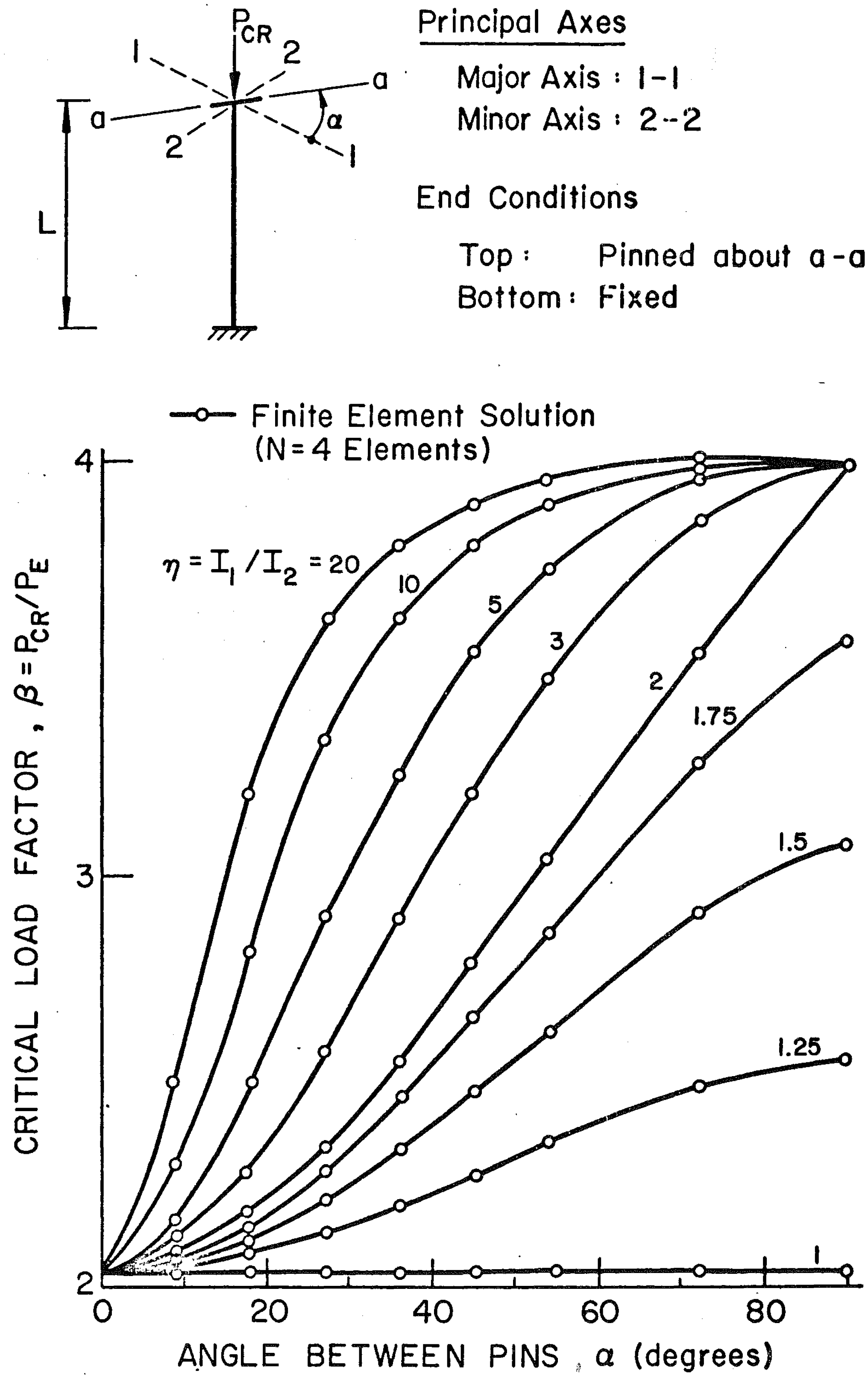

Fig. 3.24 Buckling Loads of Prismatic Columns with Crossed Pins (Fixed-Pinned Ends)

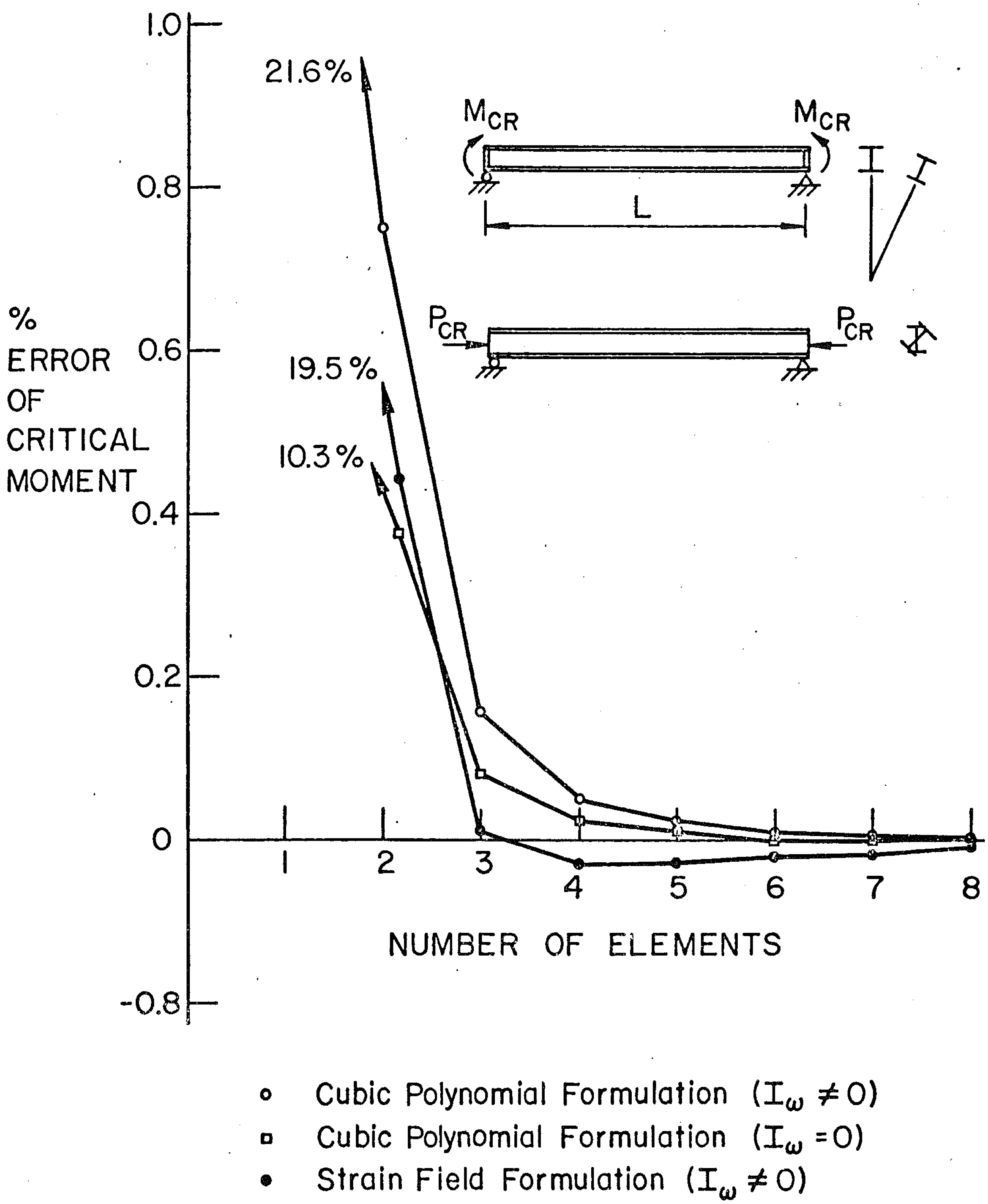

Fig. 3.25 Convergence of Finite Element Solution of Torsional and Lateral-Torsional Buckling

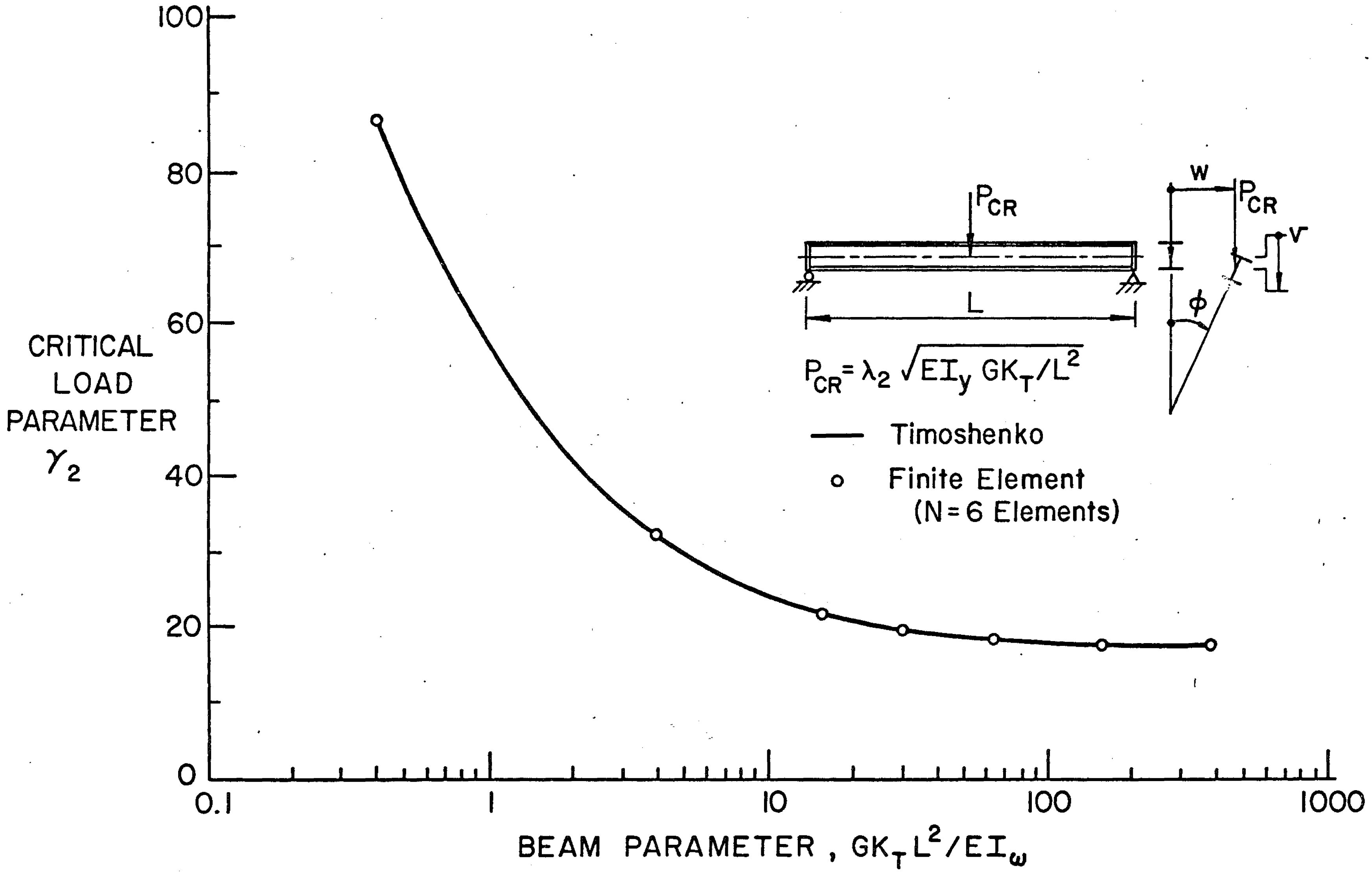

Fig. 3.26 Comparison of Finite Element and Analytical Solutions of Lateral Torsional Buckling

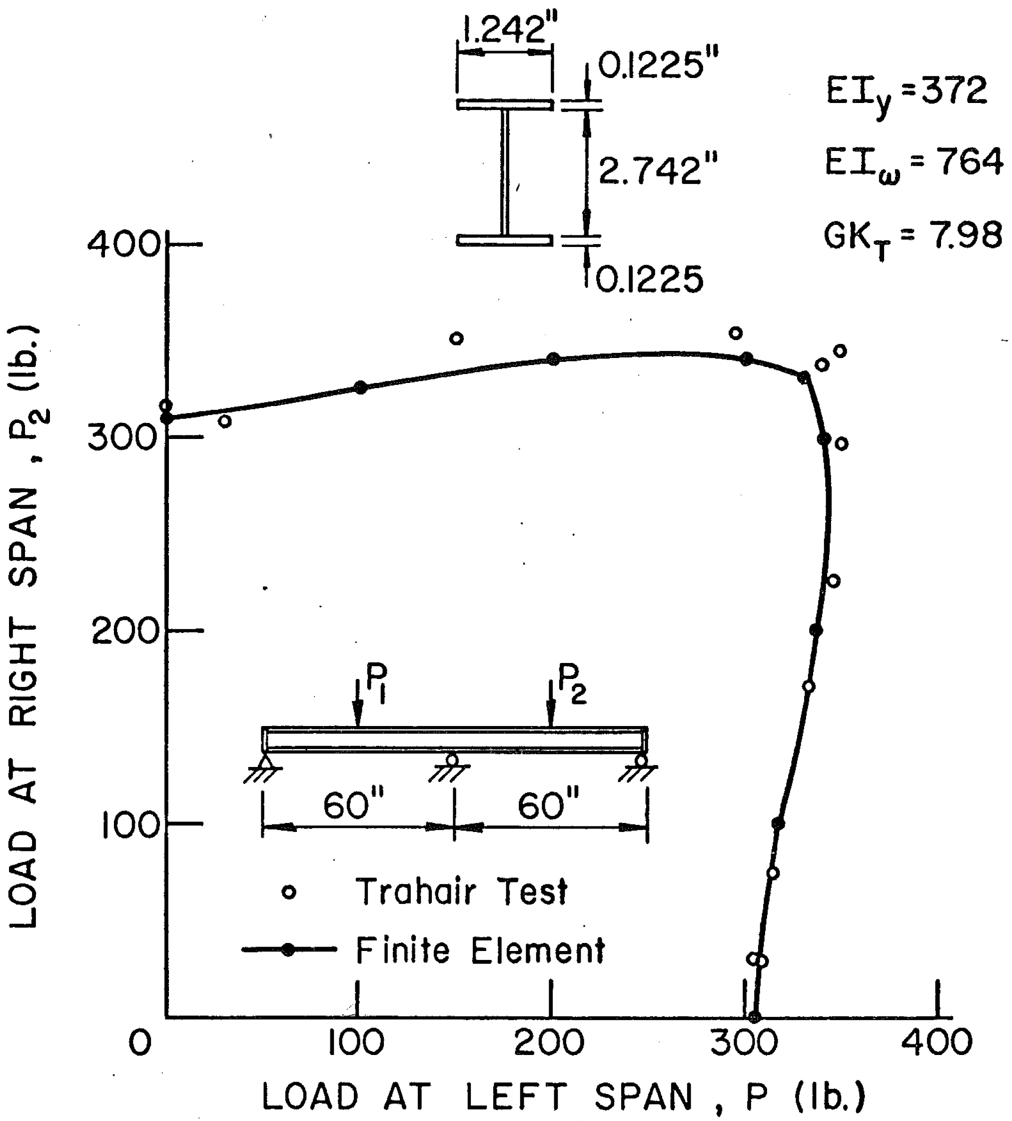

Fig. 3.27 Buckling Loads for Two-Span Continuous Beams

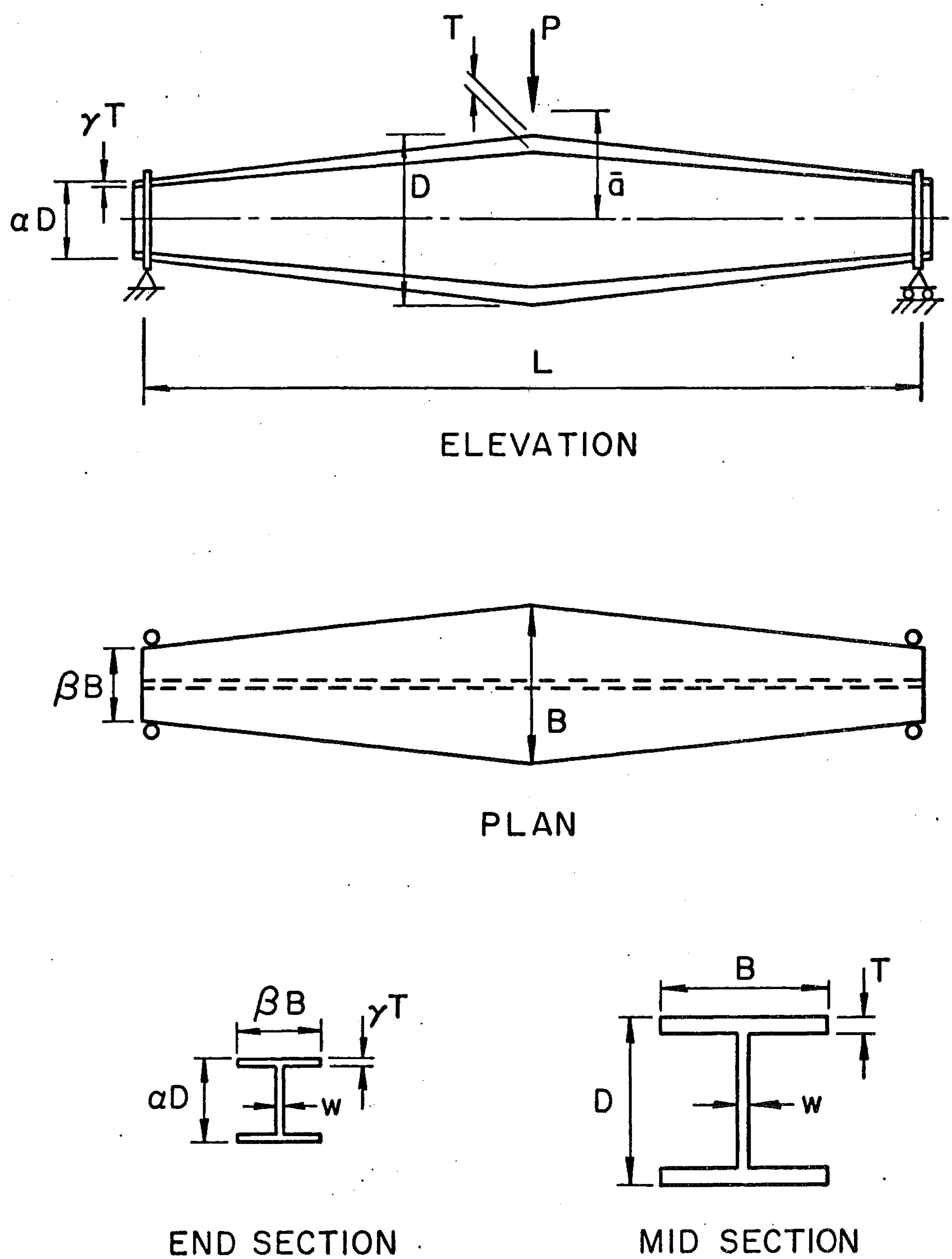

Fig. 3.28 Simply Supported Tapered I-Beam

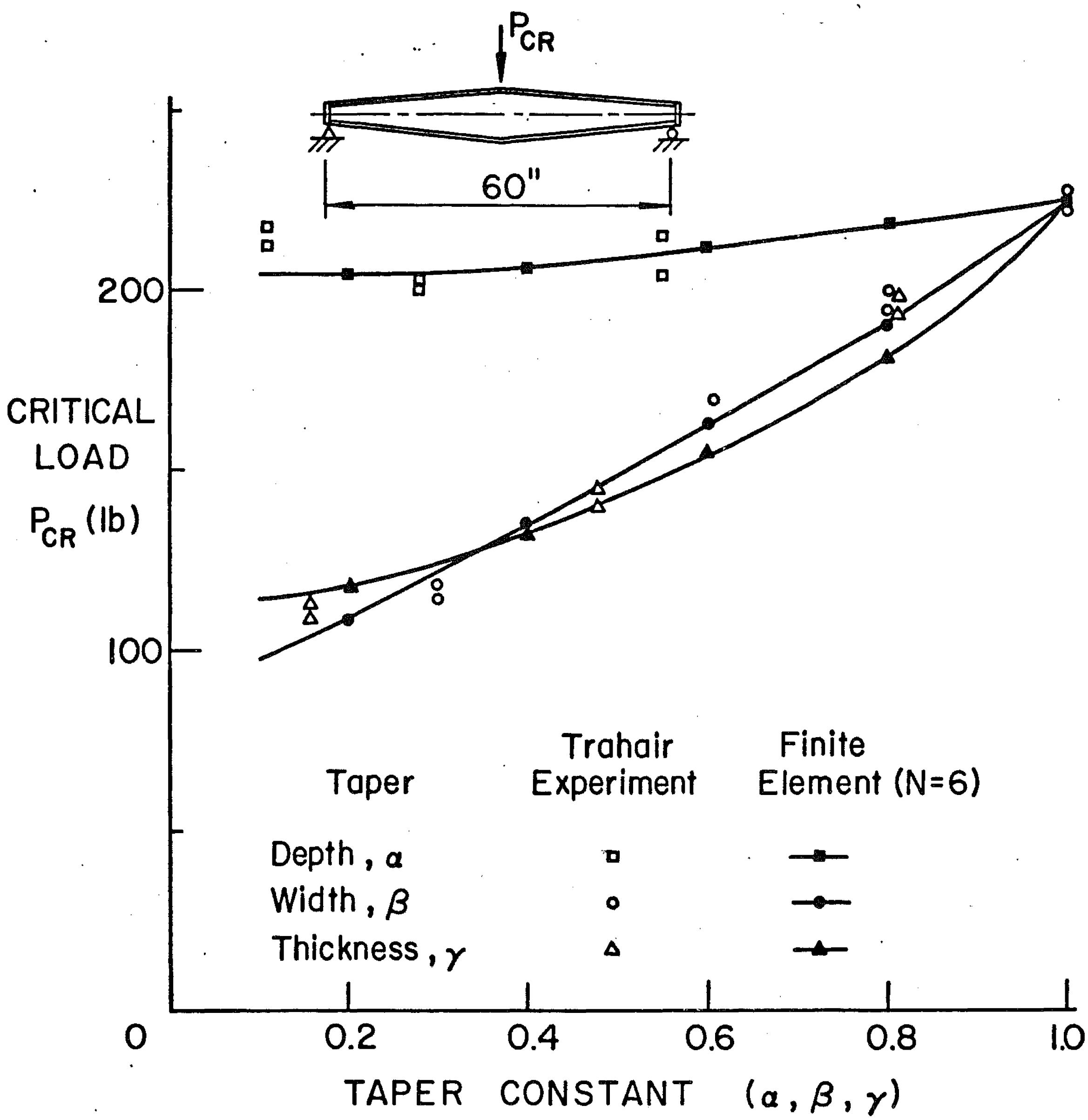

Fig. 3.29 Comparison of Finite Element Solution and Experimental Results of Lateral Torsional Buckling of Tapered Beams

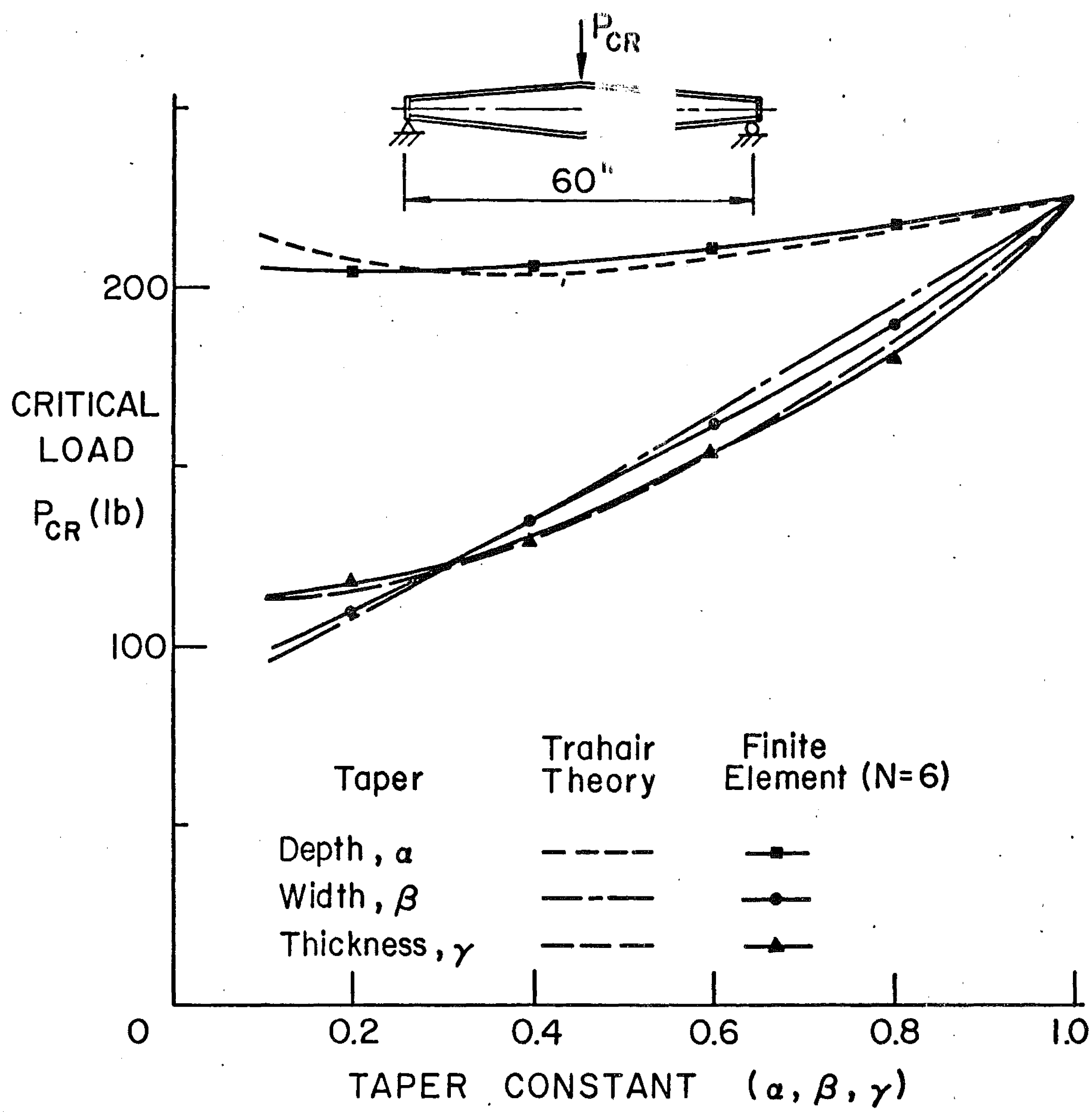

Fig. 3.30 Comparison of Finite Element Solution and Finite Integral Solution of Tapered Beams

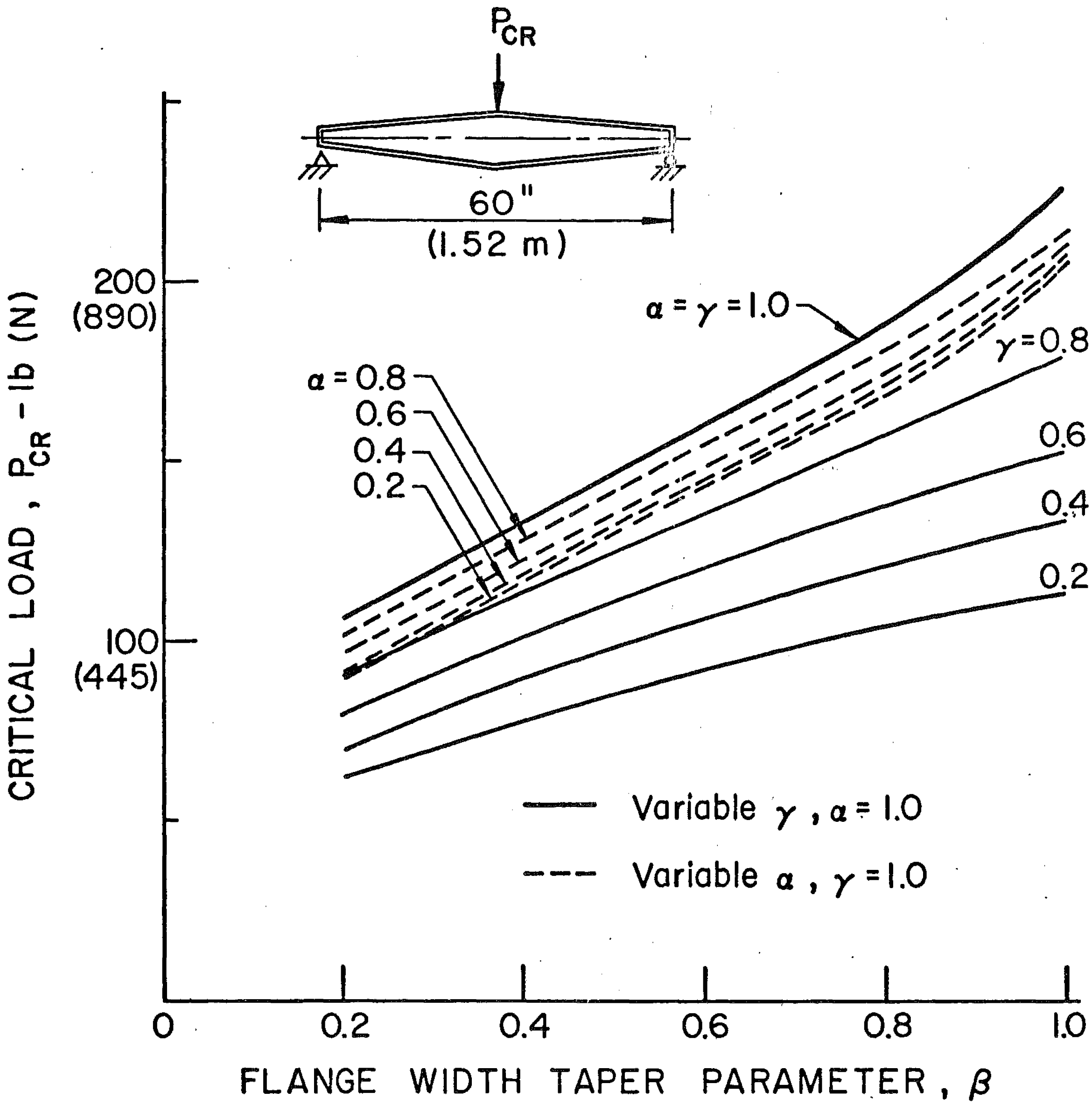

Fig. 3.31 Finite Element Solutions of Beams of Combined Tapers

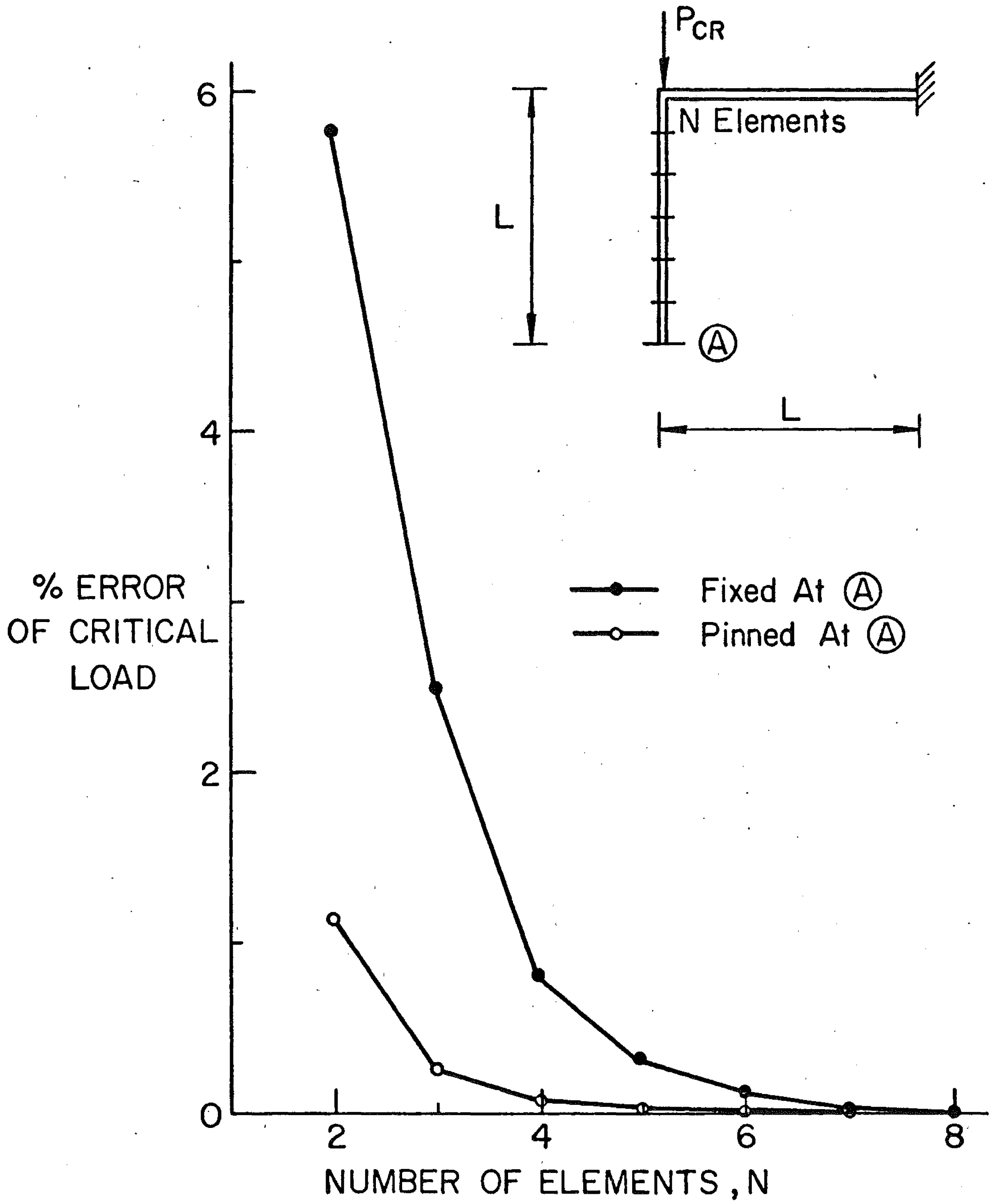

Fig. 3.32 Convergence Characteristics of Knee-Bent Frames

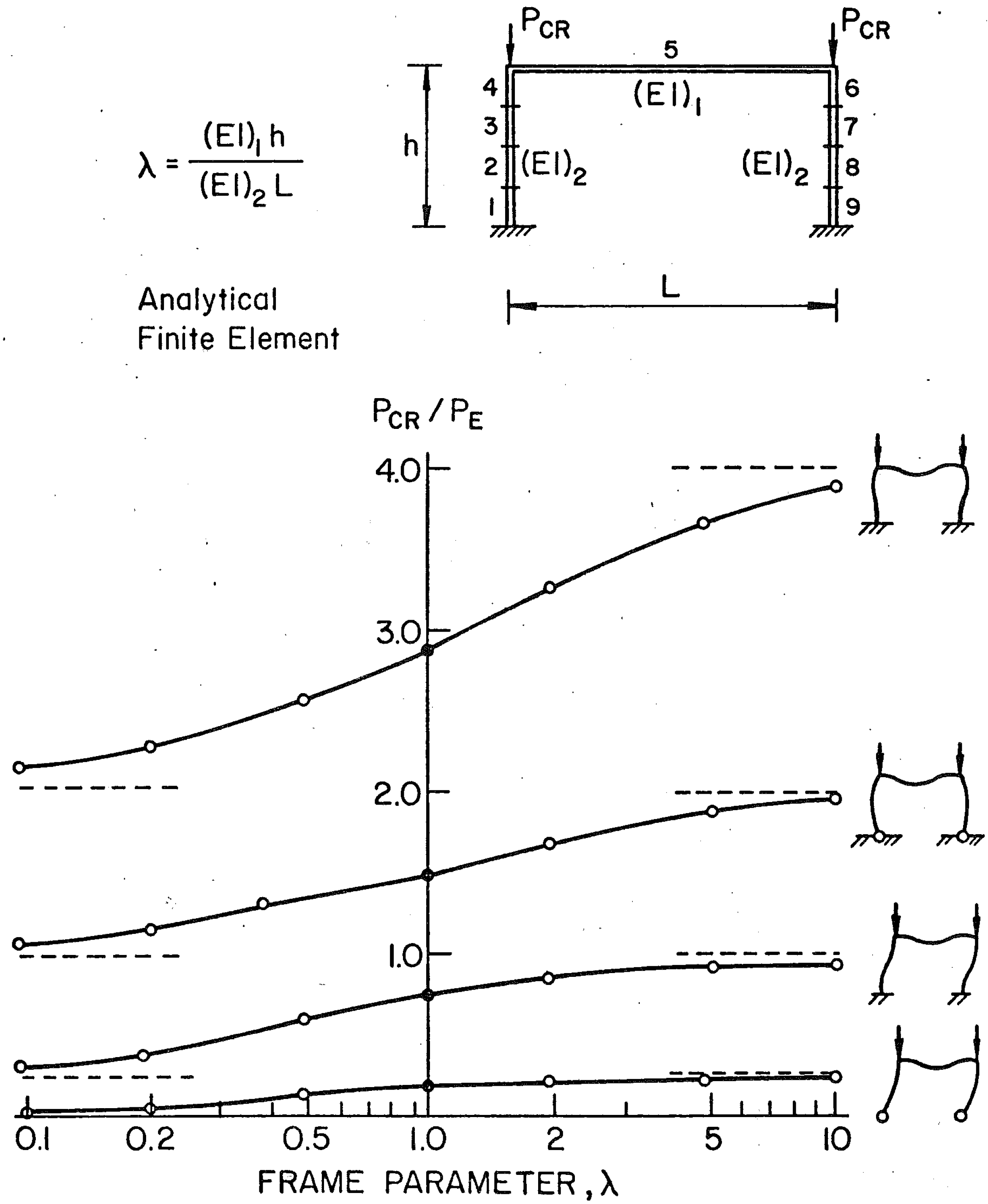

Fig. 3.33 Buckling of Single-Story Portal Frames

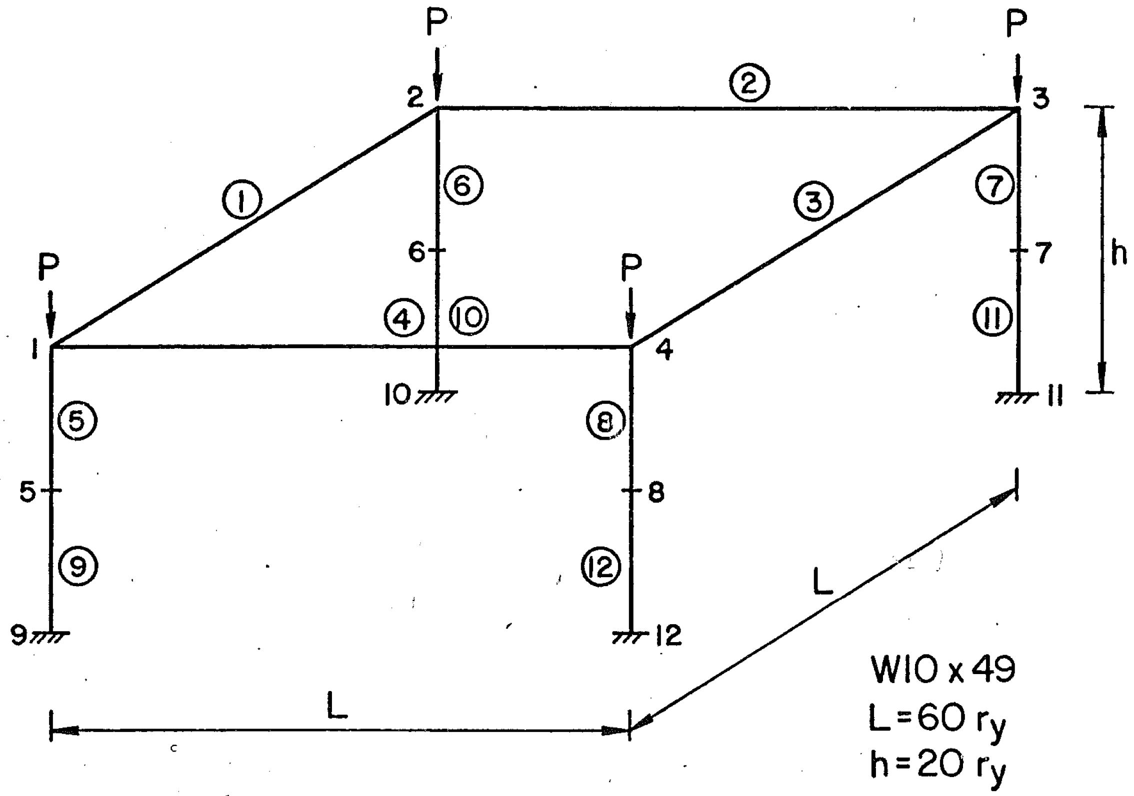

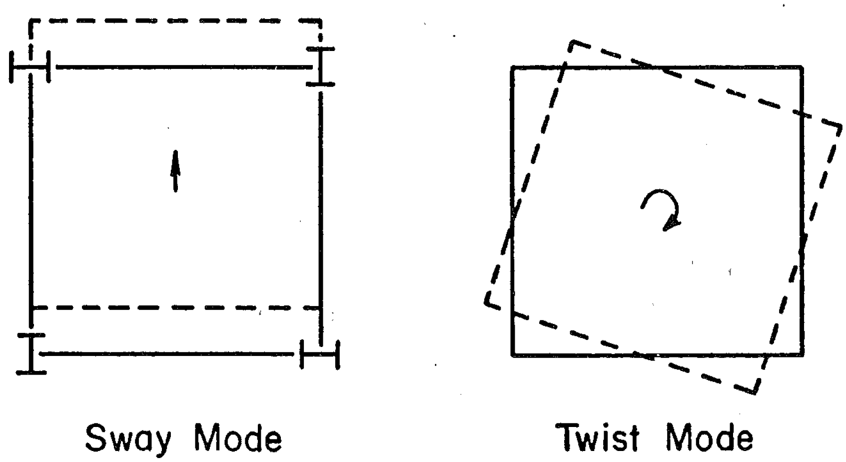

Fig. 3.34 Space Frame Buckling by Finite Element Method

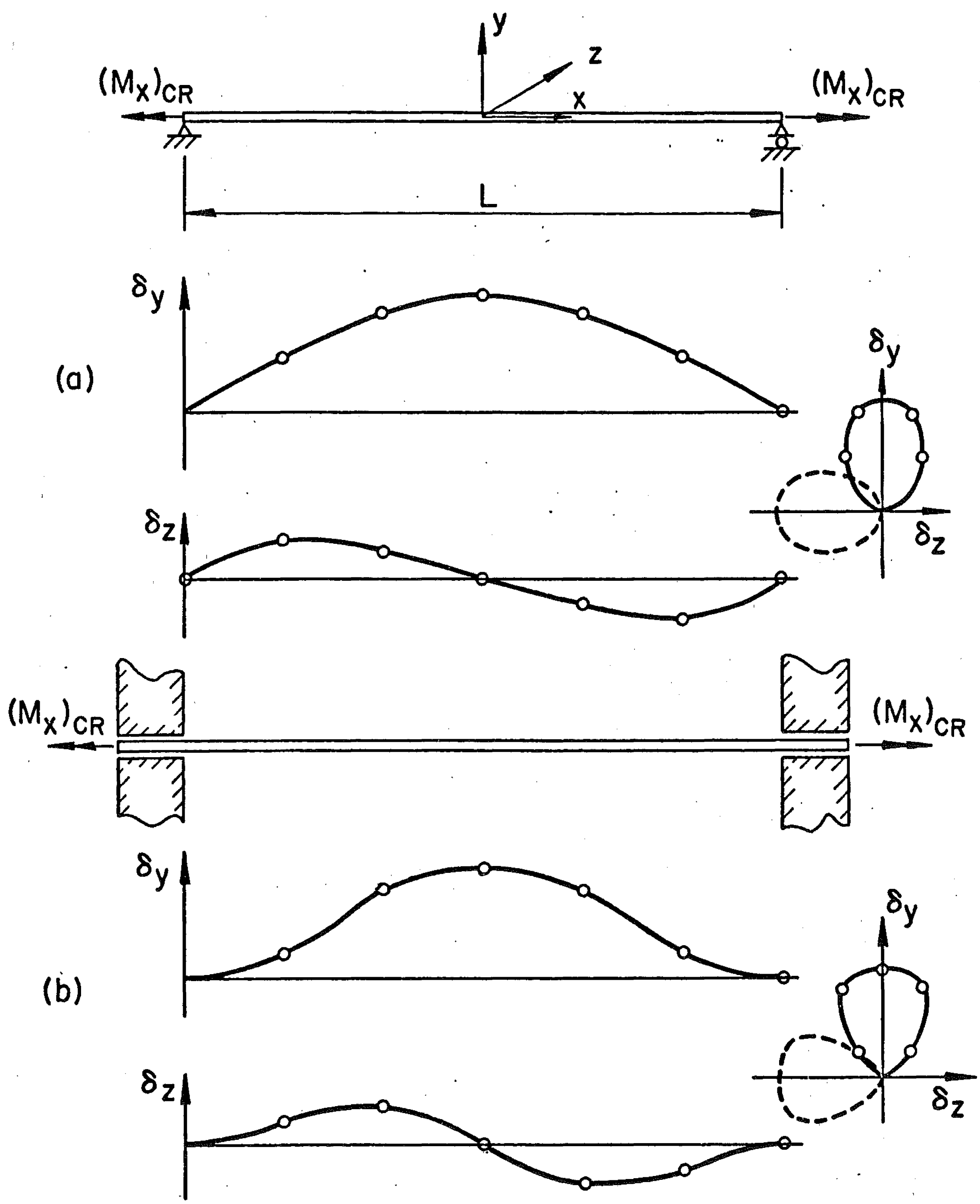

Fig. 3.35 Buckling Modes of Shafts under Pure Torsion

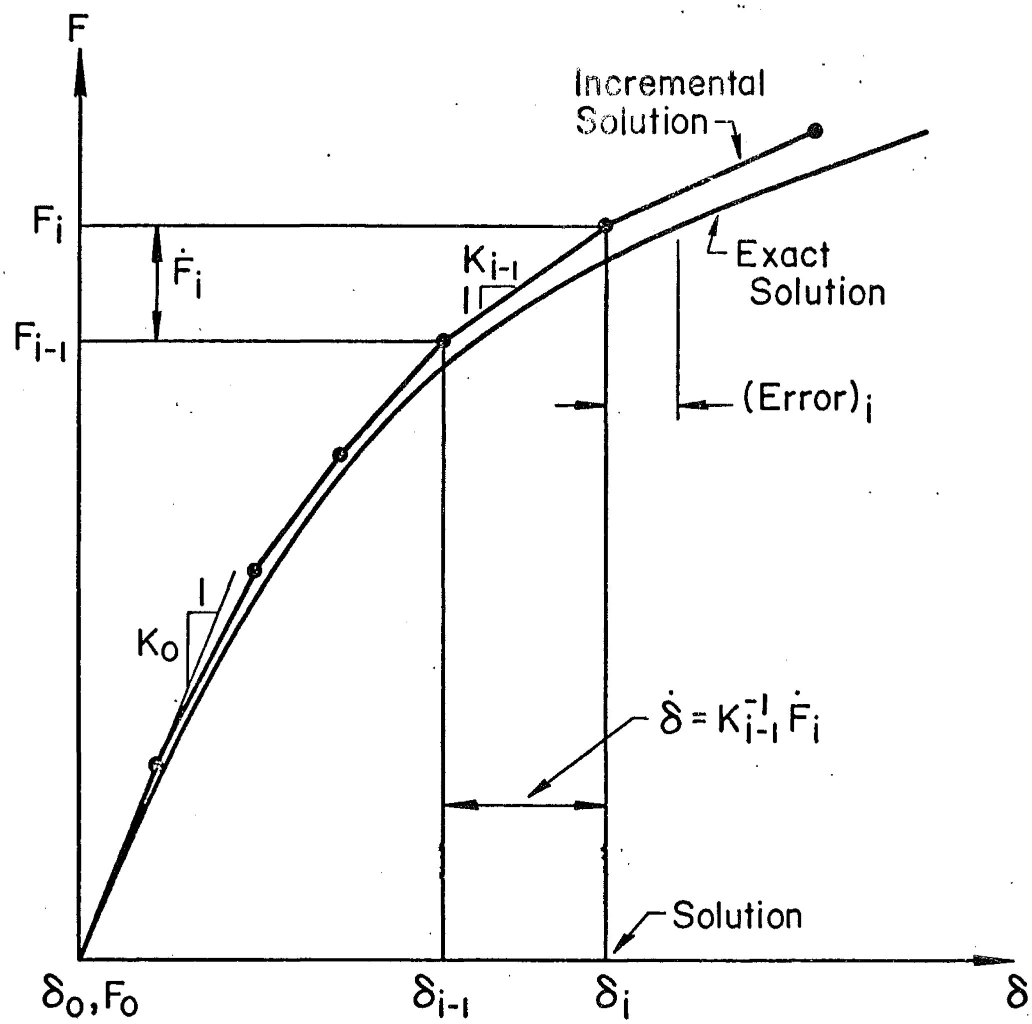

Fig. 4.1 Basic Incremental Procedure

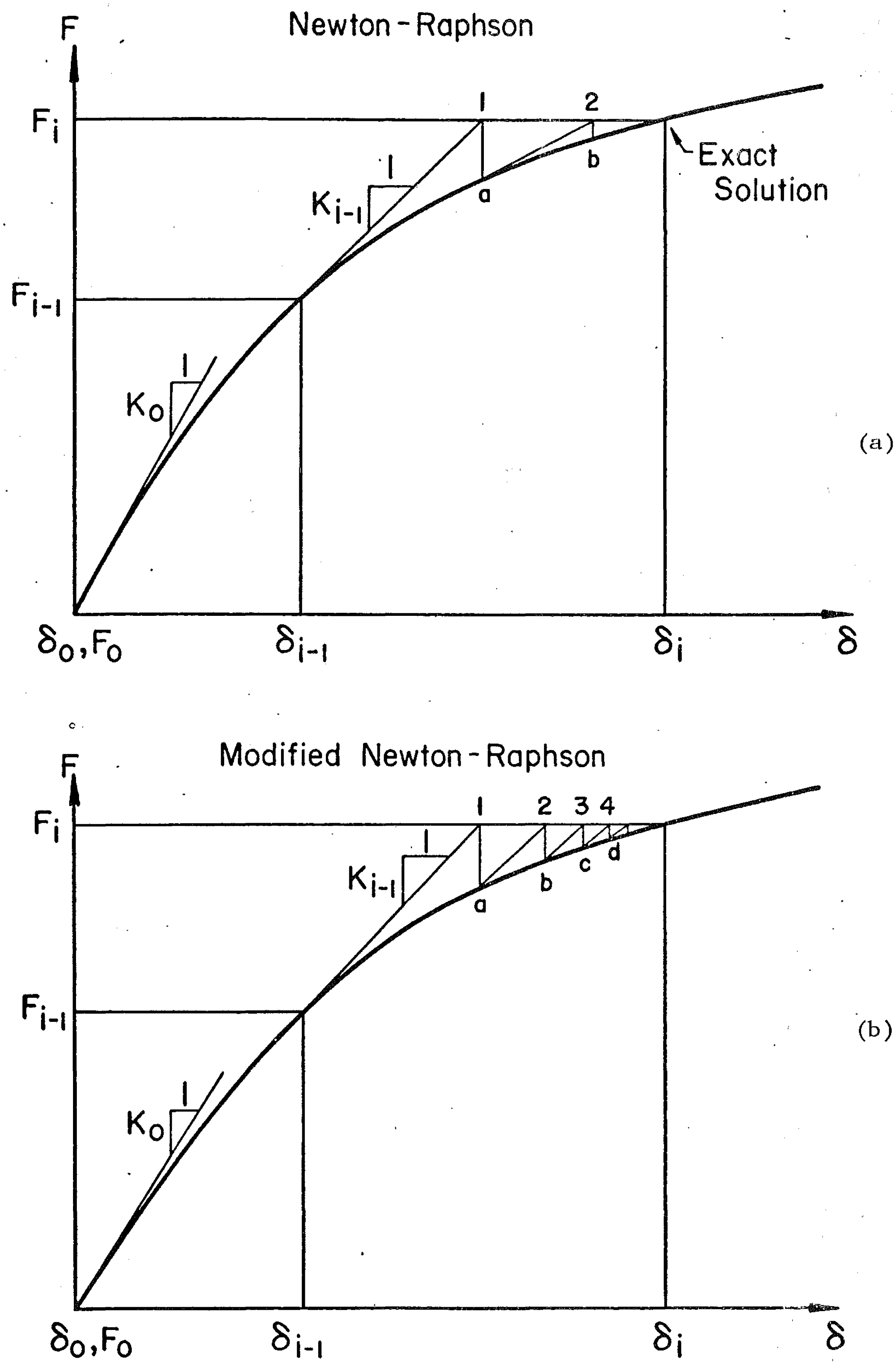

Fig. 4.2 Newton-Raphson Methods

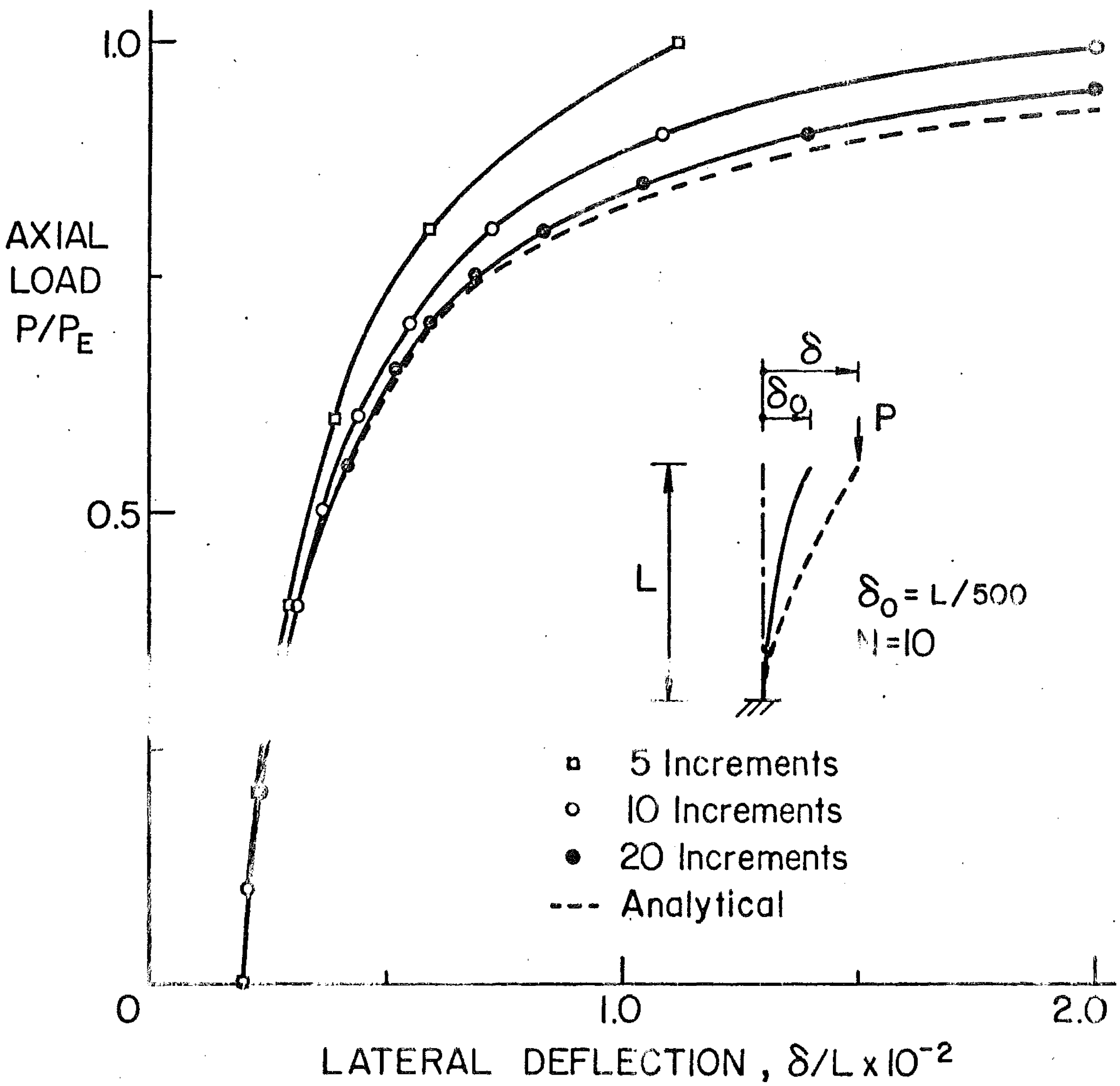

Fig. 4.3 Effect of Number of Load Increments when Using the Incremental Method

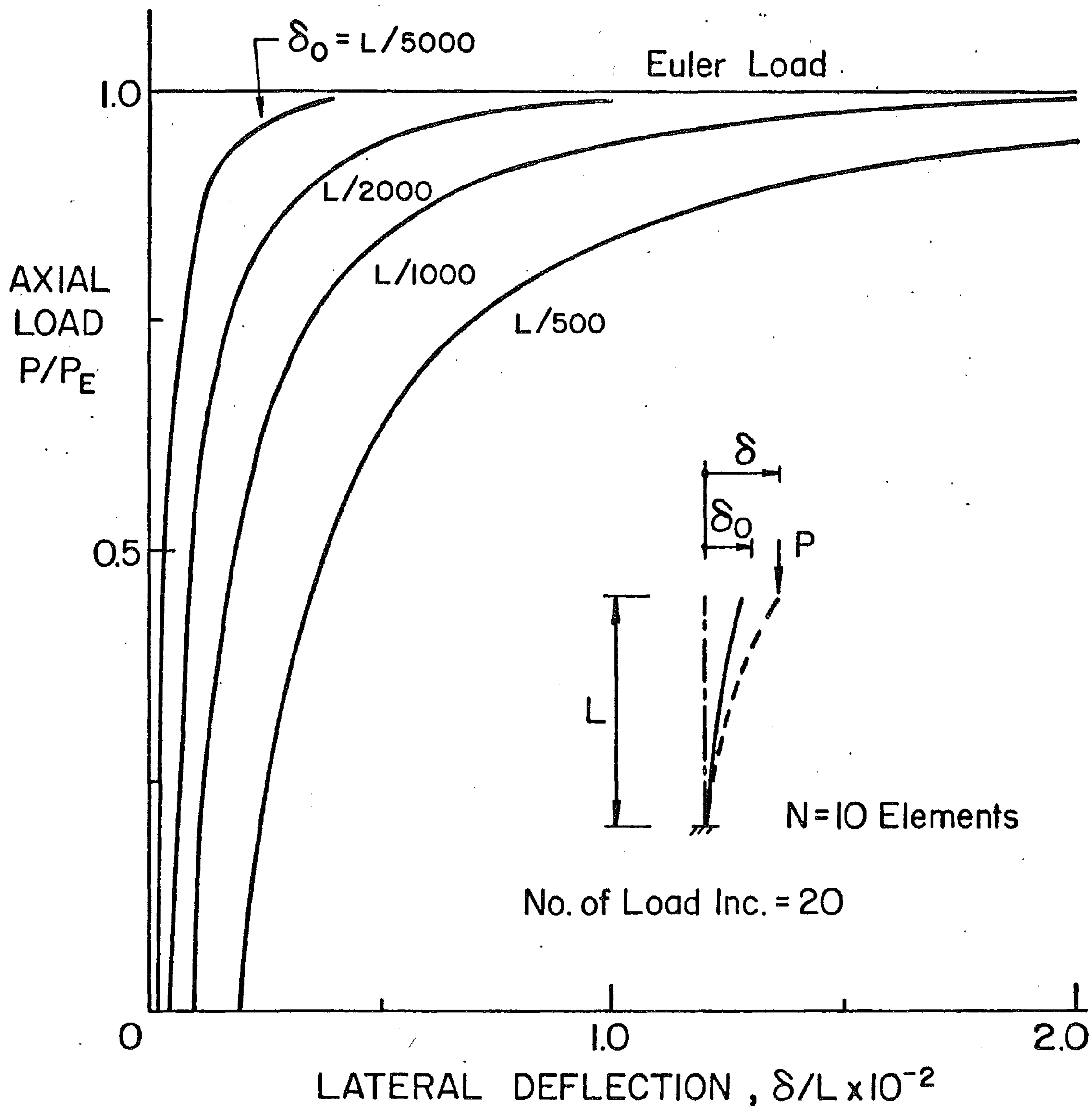

Fig. 4.4 Use of the Incremental Method to Determine Load-Deflection Curves of Columns

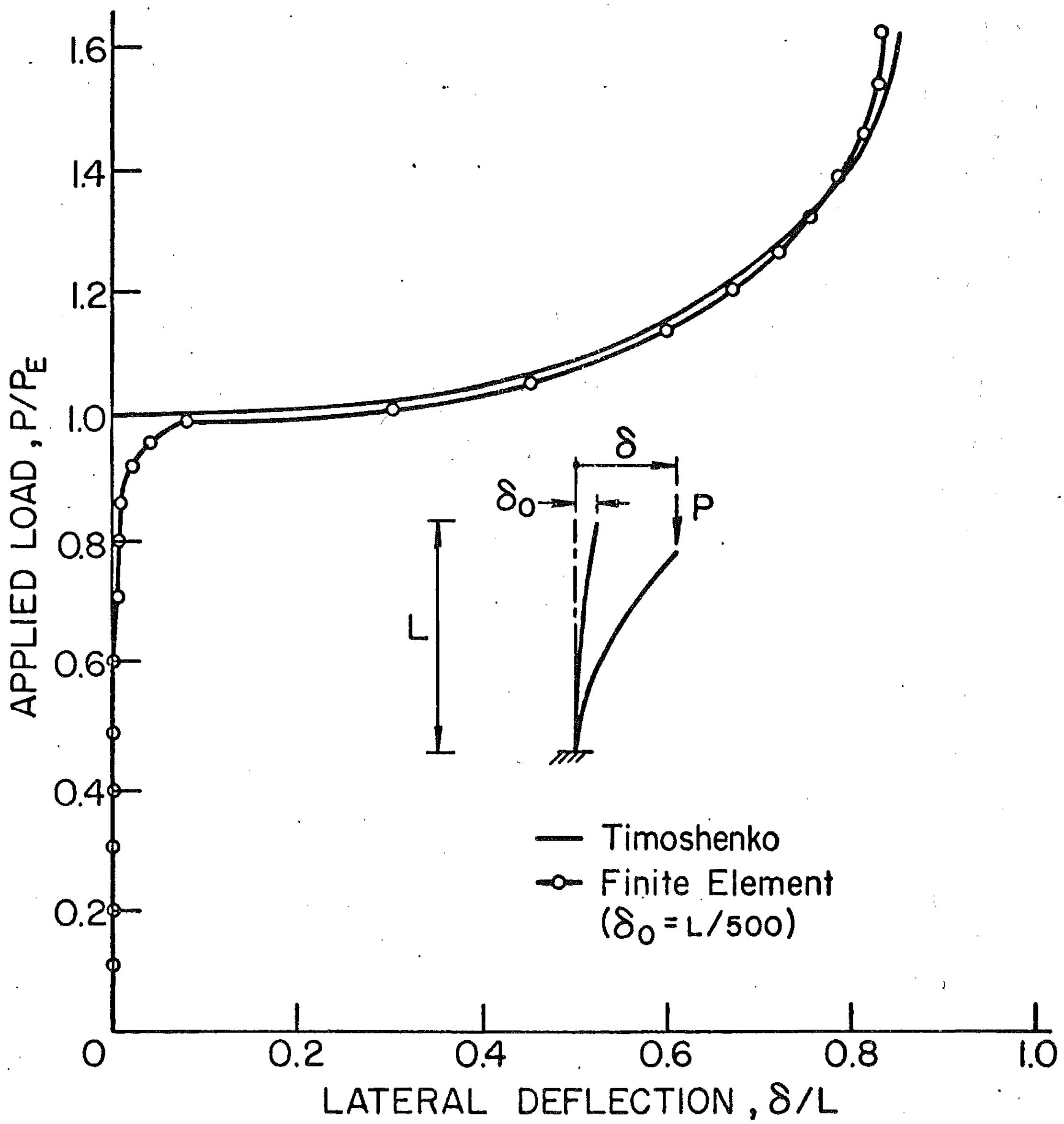

Fig. 4.5 Use of the Incremental Method for the Analysis of Large Deflections

9. REFERENCES

1. Todhunter, I. and Pearson, K.
A HISTORY FROM GALILEI TO LORD KELVIN, OF THE THEORY OF ELASTICITY AND THE STRENGTH OF MATERIALS, Dover Pub., Inc., New York, 1960.

2. Love, A. E. H.
A TREATISE ON THE MATHEMATICAL THEORY OF ELASTICITY, Dover Publications, 4th Ed., 1944.

3. Truesdell, C. and Toupin, R.
THE CLASSICAL FIELD THEORIES, Encyclopedia of Physics, Edited by S. Flügge, Springer-Verlag, 1960.

4. Medick, M. A.
ONE-DIMENSIONAL THEORIES OF WAVE PROPAGATION AND VIBRATIONS IN ELASTIC BARS OF RECTANGULAR CROSS SECTION, Journal of Applied Mechanics, Vol. 33, Sept. 1966.

5. Soler, A. I.
HIGHER-ORDER THEORIES FOR STRUCTURAL ANALYSIS USING LEGENDRE POLYNOMIAL EXPANSIONS, Journal of Applied Mechanics, Dec. 1969.

6. Hertelendy, P.
AN APPROXIMATE THEORY GOVERNING SYMMETRIC MOTIONS OF ELASTIC RODS OF RECTANGULAR OR SQUARE CROSS SECTIONS, Journal of Applied Mechanics, June 1968.

7. Timoshenko, S. P.
HISTORY OF STRENGTH OF MATERIALS, McGraw-Hill Book Company, Inc., New York, 1953.

8. Wagner, H.
TORSION AND BUCKLING OF OPEN SECTIONS, 25th Anniversary Publication, Technische Hochschule Danzig, 1904-1929, Translated in NACA TM. 807, 1936.

9. Goodier, J. N.
TORSIONAL AND FLEXURAL BUCKLING OF BARS OF THIN WALLED OPEN SECTIONS UNDER COMPRESSIVE AND BENDING LOADS, Journal of Applied Mechanics, ASME, Vol. 64, Sept. 1942.

10. Timoshenko, S.
THEORY OF BENDING, TORSION AND BUCKLING OF THIN-WALLED MEMBERS OF OPEN CROSS SECTION, Journal, Franklin Institute, Vol. 239, No. 3, March 1945.

11. Vlasov, V. Z.
THIN WALLED BEAMS, English translation published for U.S. Science Foundation by Israel Program for Scientific Translations, 1961.

12. Chen, W. F. and Santathadaporn, S.
REVIEW OF COLUMN BEHAVIOR UNDER BIAXIAL LOADING, Journal of the Structural Division, ASCE, Vol. 94, ST12, Dec. 1968.

13. Hrennikoff, A.
SOLUTION OF PROBLEMS IN ELASTICITY BY THE FRAMEWORK METHOD, Journal of Applied Mechanics, Vol. 8, 1941.

14. Ang, A. H. S. and Newmark, N. M.
A NUMERICAL PROCEDURE FOR THE ANALYSIS OF CONTINUOUS PLATES, Second Conference on Electronic Computation, ASCE, 1960.

15. Zienkiewicz, O. C.
THE FINITE ELEMENT METHOD IN ENGINEERING SCIENCE, McGraw-Hill Book Company, Inc., London, 1971.

16. Oden, J. T.
FINITE ELEMENTS OF NONLINEAR CONTINUA, McGraw-Hill Book Company, Inc., 1972.

17. Oden, J. T.
A GENERAL THEORY OF FINITE ELEMENTS, Part 1 and Part 2, Int. Journal Numerical Methods Eng., Vol. 1, No. 2 and No. 3, 1969.

18. Archer, J. S.
CONSISTENT MATRIX FORMULATIONS FOR STRUCTURAL ANALYSIS USING INFLUENCE COEFFICIENT TECHNIQUES, AIAA Journal, Vol. 3, Oct. 1965.

19. Prezemieniecki, J. S.
THEORY OF MATRIX STRUCTURAL ANALYSIS, McGraw-Hill, New York, 1968.

20. Kabaila, A. P. and Fraeijs de Veubeke, B.
STABILITY ANALYSIS BY FINITE ELEMENTS, Air Force Flight Dynamics Laboratory, Tech. Report AFFDL-TR-70-35, March 1970.

21. Thomas, J. M.
A FINITE ELEMENT APPROACH TO THE STRUCTURAL INSTABILITY OF BEAM COLUMNS, FRAMES AND ARCHES, NASA TN D-5782, May 1970.

22. Barsoum, R.
A FINITE ELEMENT FORMULATION FOR THE GENERAL STABILITY ANALYSIS OF THIN-WALLED MEMBERS, doctoral dissertation, Cornell University, 1970, University Microfilms, Ann Arbor, Michigan.

23. Gallagher, R.
A CORRELATION STUDY OF METHODS OF MATRIX STRUCTURAL ANALYSIS, Pergamon Press, Oxford, 1964.

24. Washizu, K.
SOME REMARKS ON BASIC THEORY FOR FINITE ELEMENT METHOD, Proc. Japan-U.S. Seminar on Matrix Methods in Structural Analysis and Design, Tokyo, 1969.

25. Pian, T. H. H.
FORMULATION OF FINITE ELEMENTS FOR SOLID CONTINUA, Proc. Japan-U.S. Seminar on Matrix Methods in Structuctural Analysis and Design, Tokyo, 1969.

26. Washizu, K.
MARIATIONAL METHODS IN ELASTICITY AND PLASTICITY, Pergamon Press, 1st Ed., 1968.

27. Hu, H. C.
ON SOME VARIATIONAL PRINCIPLES IN THE THEORY OF ELASTICITY AND PLASTICITY, Scintia Sinica, Vol. 4, No. 1, March 1955.

28. Prager, W.
VARIATIONAL PRINCIPLES OF LINEAR ELASTOSTATICS FOR DISCONTINUOUS DISPLACEMENTS, STRAINS, AND STRESSES, The Folke-Odquist Volume, edited by B. Brobert, J. Hult, and F. Niordson, Almquist & Wiksell, Stockholm, 1967.

29. Reissner, E.
NOTE ON THE METHOD OF COMPLEMENTARY ENERGY, Journal of Mathematics and Physics, Vol. 27, 1948.

30. Pian, T. H. H.
ELEMENT STIFFNESS MATRICES FOR BOUNDARY COMPATIBILITY AND FOR PRESCRIBED BOUNDARY STRESSES, Proc. Conf. on Matrix Methods in Structural Mechanics, AFFDL-TR-66-80, 1965.

31. Timoshenko, S. P.
ON THE CORRECTION FOR SHEAR OF THE DIFFERENTIAL EQUATION FOR TRANSVERSE VIBRATIONS OF PRISMATIC BARS, Philosophical Magazine, Vol. 41, 1921.

32. Timoshenko, S. P. and Goodier, J. N.
THEORY OF ELASTICITY, McGraw-Hill Book Company, Inc., New York, 3rd Edition, 1970.

33. Sokolnikoff, I. S.
MATHEMATICAL THEORY OF ELASTICITY, McGraw-Hill Book Company, Inc., New York, 2nd Edition, 1956.

34. Cowper, G. R.
THE SHEAR COEFFICIENT IN TIMOSHENKO'S BEAM THEORY, Journal of Applied Mechanics, Vol. 33, No. 2, June 1966.

35. Mason, W. E. and Hermann, L. R.
ELASTIC SHEAR ANALYSIS OF GENERAL PRISMATIC BEAMS, Journal of Engineering Mechanics Division, ASCE, EM4, August 1968.

36. Lauterbach, G. F., Peppin, R. J., Schapiro, S. M., and Krahula, J. L.
A FINITE ELEMENT SOLUTION FOR SAIN-VENANT BENDING, AIAA Journal, Vol. 9, No. 3, March 1971.

37. Popov, E. P.
KELVIN'S SOLUTION OF TORSION PROBLEM, Journal of Engineering Mechanics Division, ASCE, Vol. 96, EM6, Dec. 1970.

38. Krahula, J. L.
ANALYSIS OF BENT AND TWISTED BARS USING THE FINITE ELEMENT METHOD, AIAA Journal, Vol. 5, No. 6, June 1967.

39. Krajcinovic, D.
A CONSISTENT DISCRETE ELEMENTS TECHNIQUE FOR THIN WALLED ASSEMBLAGES, Int. J. Solids Structures, Vol. 5, 1969.

40. Janssen, J. D.
DE MOGELIJKHEDEN VAN DE METHODE DER EINDIGE ELEMENTEN BIJ DE BEREKENING VAN DE STERKTE EN STIJFHEID VAN DUNWANDIGE BALKEN (THE APPLICATION OF THE FINITE ELEMENT METHOD FOR THE EVALUATION OF THE STRENGTH AND STIFFNESS OF THIN-WALLED BEAMS), De Ingenieur, Vol. 82, Nr. 43, October 1970.

41. Heins, C. P., and Seaburg, P. A.
TORSION ANALYSIS OF ROLLED STEEL SECTIONS, AIA File No. 13-A-1, Bethlehem Steel, Bethlehem, Pa., 1963.

42. Basler, K. and Kollbrunner, C. F.
TORSION IN STRUCTURES, Springer-Verlag, New York, 1969.

43. Martin, H. C.
ON THE DERIVATION OF STIFFNESS MATRICES FOR THE ANALYSIS OF LARGE DEFLECTION AND STABILITY PROBLEMS, Proc. AFIT Conf. on Matrix Methods in Struct. Mech., AFFDL TR 66-80, 1965.

44. Mallett, R. and Marcal, P. V.
FINITE ELEMENT ANALYSIS ON NONLINEAR STRUCTURES, Journal of Structural Division, ASCE, Vol. 94, ST9, Sept. 1968.

45. Oden, J. T.
FINITE ELEMENT APPLICATIONS IN NONLINEAR STRUCTURAL ANALYSIS, Proc. Symposium - Application of Finite Element Methods in Civil Engineering, Vanderbilt University, 1969.

46. Martin, H. C.
FINITE ELEMENTS AND THE ANALYSIS OF GEOMETRICALLY NONLINEAR PROBLEMS, Proc. Japan-U.S. Seminar on Matrix Methods in Structural Analysis and Design, Tokyo, 1969.

47. Gallagher, R.
GEOMETRICALLY NONLINEAR FINITE ELEMENT ANALYSIS, Proc. Specialty Conf. - Finite Element Method in Civil Engineering, McGill University, 1972.

48. Novoshilov, V. V.
FOUNDATIONS OF THE NONLINEAR THEORY OF ELASTICITY, Graylock Press, Rochester, N. Y., 1953.

49. Prezemieniecki, J. S.
DISCRETE-ELEMENT METHODS FOR STABILITY ANALYSIS OF COMPLEX STRUCTURES, The Aeronautical Journal of the Royal Aeronautical Society, Vol. 72, Dec. 1968.

50. Dzhanelidze, G. Y.
ON THE THEORY OF THIN AND THIN-WALLED RODS, NACA TM 1309, Oct. 1951.

51. Golenveizer, A. L.
THEORY OF THIN-WALLED RODS, NACA TM 1322, Oct. 1951.

52. Gallagher, R. and Padlog, J.
DISCRETE ELEMENT APPROACH TO STRUCTURAL INSTABILITY ANALYSIS, AIAA Journal, Vol. 1, No. 6, June 1963.

53. Timoshenko, S. P. and Gere, J. M.
THEORY OF ELASTIC STABILITY, 2nd Edition, McGraw-Hill Book Company, Inc., New York, 1961.

54. Bleich, F.
BUCKLING STRENGTH OF METAL STRUCTURES, McGraw-Hill Book Company, Inc., New York, 1952.

55. Ziegler, H.
PRINCIPLES OF STRUCTURAL STABILITY, Blaisdell Publishing Company, London, 1968.

56. Wang, C. T.
APPLIED ELASTICITY, McGraw-Hill Book Company, Inc., New York, 1953.

57. Dalal, T. S.
COLUMNS WITH DISTRIBUTED AXIAL LOADS, The Structural Engineer, Vol. 48, No. 11, Nov. 1970.

58. Gere, J. M. and Carter, W. O.
CRITICAL BUCKLING LOADS FOR TAPERED COLUMNS, Journal of Structural Division, ASCE, Vol. 88, ST1, February 1962.

59. Wang, L. R.
PARAMETRIC MATRICES OF SOME STRUCTURAL MEMBERS, Journal of Structural Division, ASCE, Vol. 96, ST8, Aug. 1970.

60. Girijavallabhan, C. V.
BUCKLING LOADS OF NONUNIFORM COLUMNS, Journal of Structural Division, ASCE, Vol. 95, ST11, November 1969.

61. Hetenyi, H.
BEAMS ON ELASTIC FOUNDATION, The University of Michigan Press, Ann Arbor, Michigan, 1964.

62. Toakley, A. R.
BUCKLING LOADS FOR ELASTICALLY SUPPORTED STRUTS, Journal of Engineering Mechanics Division, ASCE, Vol. 91, EM3, June 1965.

63. Wieghardt, K.
UBER DEN BALKEN AUF NACHGIE-BIGER UNTERLAGE (BEAMS ON FLEXIBLE FOUNDATIONS), Zeitschrift Für Angewandte Mathematic und Physic, Vol. 2, 1922.

64. Filenko-Borodich, M. M.
SOME APPROXIMATE THEORY OF ELASTIC FOUNDATIONS, Uchenye Zapiski, MGU, No. 46, 1940.

65. Vlasov, V. Z. and Leontev, N. N.
BEAMS, PLATES AND SHELLS ON ELASTIC FOUNDATIONS (Translated from Russian), NASA and NSF, Washington, D. C., 1966.

66. Biot, M. A.
BENDING OF AN INFINITE BEAM ON ELASTIC FOUNDATION, Journal of Applied Mechanics, ASME, 36, 1937.

67. Hsu, Y.
ELASTIC BUCKLING OF TWO-COMPONENT COLUMNS, Journal of Engineering Mechanics, ASCE, Vol. 95, EM3, June 1969.

68. Fischer, W.
VERGLEICH DER IDEALEN KNICKLASTEN VERWUNDENER UND VERSETZTER STABE (Comparison of Ideal Buckling Loads of Discontinuuosly Twisted Columns), Stalbau, Vol. 39, No. 2, February 1970.

69. Ziegler, H.
DIE KNICKUNG DES VERWINDEN STABES (Buckling of Twisted Bars), Schweizerische Bauzertung, Vol. 66, 1948.

70. Zickel, J.
PRETWISTED BEAMS AND COLUMNS, Journal of Applied Mechanics, Vol. 23, 1956.

71. Fischer, W.
DIE KNICKLAST DES SCHEIDENGELAGERTEN VERWUNDENEN STABES (Buckling Load of Pretwisted Rods on Knife Edge Supports), Ingenieur-Archiv, Vol. 39, 1970.

72. Tebedge, N. and Tall, L.
PROCEDURE FOR TESTING CENTRALLY-LOADED COLUMNS, Fritz Engineering Lab Report No. 351.6, Dec. 1971.

73. Ashwell, D.
THE EULER BUCKLING LOAD OF A STRUT WITH CROSSED PINS, Engineering, 1950, pp. 709.

74. Trahair, N. S.
ELASTIC STABILITY OF CONTINUOUS BEAMS, Journal of Structural Division, ASCE, Vol. 95, ST6, June 1969.

75. Kitipornchai, S. and Trahair, N. S.
ELASTIC STABILITY OF TAPERED I-BEAMS, Journal of Structural Division, ASCE, Vol. 98, ST3, March 1972.

76. Lu, L. W.
A SURVEY OF LITERATURE ON THE INSTABILITY OF FRAMES, Welding Research Council Bulletin Series No. 81, 1962.

77. Morino, S. and Lu, L. W.
ANALYSIS OF SPACE FRAMES, Fritz Engineering Lab Report No. 331.13, March 1971.

78. Marcal, P. V. and King, I. P.
ELASTIC-PLASTIC ANALYSIS OF TWO-DIMENSIONAL STRESS SYSTEMS BY THE FINITE ELEMENT METHOD, Int. J. Mech. Science, Vol. 9, 1967.

79. Yamada, Y., Yoshimura, N. and Sakurai, T.
PLASTIC STRESS-STRAIN MATRIX AND ITS APPLICATION FOR THE SOLUTION OF ELASTIC-PLASTIC PROBLEMS BY THE FINITE ELEMENT METHOD, Int. J. Mech. Science, Vol. 10, 1968.

80. Marcal, P. V.
FINITE ELEMENT ANALYSIS WITH MATERIAL NONLINEARITIES--THEORY AND PRACTICE, Proc. Specialty Conf.--Finite Element Method in Civil Engineering, McGill University, 1972.

81. Turner, M. J., Dill, E. H., Martin, H. C. and Melosh, R. J.
LARGE DEFLECTION OF STRUCTURES SUBJECTED TO HEATING AND EXTERNAL LOADS, Journal of Aerospace Sciences, Vol. 27, 1960.

82. Haisler, W. E., Stricklin, J. A. and Stibbins, F. J.
DEVELOPMENT AND EVALUATION OF SOLUTION PROCEDURES FOR GEOMETRICALLY NONLINEAR STRUCTURAL ANALYSIS, AIAA Journal, Vol. 10, No. 3, March 1972.

83. Carnegie, W.
STATIC BENDING OF PRE-TWISTED CANTILEVER BLADING, Proceedings of the Institution of Mechanical Engineers, Vol. 171, 1957.

84. Houbolt, J. C. and Brooks, G. W.
DIFFERENTIAL EQUATIONS OF MOTION FOR COMBINED FLAPWISE BENDING, CHORDWISE BENDING, AND TORSION OF TWISTED NON-UNIFORM ROTOR BLADES, TN 1346, 1958, NACA.

85. Lawrence, K. L.
TWISTED BEAM ELEMENT MATRICES FOR BENDING, AIAA Journal, Vol. 8, No. 6, June 1970.

10. VITA

The author was born the first son of Debre Bogale and Tebedge Guddaye in Debre Tabor, Ethiopia on October 16, 1944.

He graduated from Medhane Alem High School in Addis Ababa in 1960. From September 1960 to June 1965 he studied at the College of Engineering in Haile Selassie I University. There he received the degree of Bachelor of Science in Civil Engineering with Distinction and was awarded the Haile Selassie I University Chancellor's Medal.

In June 1965 he joined the College of Engineering in H.S.I.U. as a Graduate Assistant and continued working in the same university as an Assistant Lecturer until August 1967.

In September 1967 the author received a scholarship, sponsored by the African-American Institute, to study in the Department of Civil Engineering at Lehigh University. In June 1968 he joined the staff at Fritz Engineering Laboratory as a Research Assistant. He has been associated with the research projects on Residual Stresses in Thick Welded Plates and also on European Column Studies. He was awarded the degree of Master of Science in Civil Engineering in June 1969.